Astron Astrophys Rev (2013) 21:69
DOI 10.1007/s00159-013-0069-0

REVIEW ARTICLE

Classical Be stars

Rapidly rotating B stars with viscous Keplerian decretion disks

Thomas Rivinius · Alex C. Carciofi · Christophe Martayan

Received: 6 October 2013 / Published online: 31 October 2013

Abstract In the past decade, a consensus has emerged regarding the nature of classical Be stars: They are very rapidly rotating main sequence B stars, which, through a still unknown, but increasingly constrained process, form an outwardly diffusing gaseous, dust-free Keplerian disk. In this work, first the definition of Be stars is contrasted to similar classes, and common observables obtained for Be stars are introduced and the respective formation mechanisms explained. We then review the current state of knowledge concerning the central stars as non-radially pulsating objects and non-magnetic stars, as far as it concerns large-scale, i.e., mostly dipolar, global fields. Localized, weak magnetic fields remain possible, but are as of yet unproven. The *Be-phenomenon*, linked with one or more mass-ejection processes, acts on top of a rotation rate of about 75 % of critical or above. The properties of the process can be well constrained, leaving only few options, most importantly, but not exclusively, non-radial pulsation and small-scale magnetic fields. Of these, it is well possible that *all* are realized: In different stars, different processes may be acting. Once the material has been lifted into Keplerian orbit, memory of the details of the ejection process is lost, and the material is governed by viscosity. The disks are fairly well understood in the theoretical framework of the viscous decretion disk model. This is not only true for the disk structure, but as well for its variability, both cyclic and secular. Be binaries are reviewed under the aspect of the various types of interactions a com-

T. Rivinius (✉) · C. Martayan
European Organisation for Astronomical Research in the Southern Hemisphere, Santiago 19, Casilla 19001, Chile
e-mail: triviniu@eso.org

C. Martayan
e-mail: cmartaya@eso.org

A.C. Carciofi
Instituto de Astronomia, Geofísica e Ciências Atmosféricas, Universidade de São Paulo, Rua do Matão 1226, Cidade Universitária, São Paulo, SP 05508-900, Brazil
e-mail: carciofi@usp.br

panion can have with the circumstellar disk. Finally, extragalactic Be stars, at lower metallicities, seem more common and more rapidly rotating.

Keywords Stars: emission-line, Be · Stars: rotation · Stars: oscillations · Stars: winds, outflows · Stars: circumstellar matter

1 Introduction

Be stars are enigmatic objects. They were discovered almost 150 years ago by Secchi (1866), and some of them are among the brightest stars in the sky.[1] A huge body of work has been compiled since their discovery. However, it is only in the last two to three decades that both observations and theoretical understanding of Be stars have leaped forward from taxonomical and toy-model approaches, with a plethora of mutually exclusive views, towards a general consensus on the physical properties present and processes acting in Be stars. This progress owes much to the availability of large public databases of high-precision photometry, polarimetry, and spectroscopy, including data from space missions, and the rise of new observing techniques such as interferometry. At the same time computational advances have been made, allowing the much more detailed theoretical models available today to keep pace with observations and fertilize each other.

Judging from results presented at recent conferences, a qualitative consensus has emerged, seeing Be stars as very rapidly rotating and non-radially pulsating B stars, forming a decretion disk,[2] which more precisely is an outwardly diffusing gaseous Keplerian disk. This disk if fed by mass ejected from the central star, and its further fate, after formation, is governed by viscosity. That said, our knowledge of processes is far from complete, and very important potential amendments, such as binarity or magnetic fields, are under investigation. Nevertheless, these would be additions to, rather than replacements of, the current view. While the mass-transfer mechanism between star and disk is still unclear, it is sufficiently constrained to provide a guide for further work. Research on Be stars has, finally, become a field in which quantitative properties are being investigated in detail, rather than qualitative views in general. Be stars, some decades ago considered to be peculiar and of little relevance to the main field of hot and massive stars, may turn out to be the best suited, and as well the best understood laboratories of stellar physics relevant for the upper main sequence.

The most recent summary of the field before this one was given by Porter and Rivinius (2003). Since that review a number of conferences have been held on which Be stars were either main topics or featured very prominently; an incomplete list includes: 2002 in Mmabatho (Balona et al. 2003), 2004 in Johnson City, Tennessee

[1] The brightest Be star, α Eri (B3 V), is the ninth of all stars when sorted by V-magnitude. Widely discrepant values for spectral type and temperature have been published (see SIMBAD database, and Table 4 of Kaiser 1989), emphasizing the need for further understanding.

[2] The word "decretion" is uncommon in the English language, and originally means "a decrease". However, it has become a generally accepted expression in the community as rather meaning "the act of decreasing", and it is felt that "decretion disk" properly conveys the picture of being the opposite of an accretion disk, at least in terms of the direction of mass transport (Pringle 1991, 1992).

(Ignace and Gayley 2005), 2005 in Sapporo (Štefl et al. 2007), 2009 in Viña del Mar (Rivinius and Curé 2010), 2010 in Paris (Neiner et al. 2011b), 2011 in Valencia,[3] and the same year in Madison, Wisconsin (Hoffman et al. 2012) and in Granada (Suárez et al. 2013), and 2012 in Foz do Iguaçu (Carciofi and Rivinius 2012). A review dedicated to Be/X-ray binaries was given by Reig (2011), and the IAU Working Group on Active B Stars[4] regularly publishes the "Be Star Newsletter"[5] since 1980.

Finally, highly motivated amateur astronomers have begun to contribute to the field with spectroscopic observations of increasing quality, comparable to that of small professional instruments. Spectra are made available to the community via the Be Star Spectra Database (BeSS, Neiner et al. 2011a).[6]

The sections of this work are organized as follows:

Sect. 1: The definition of Be stars and their relation to the broader field of astrophysics are discussed. Where appropriate, topics only touched upon in this Section will be discussed in detail further down.
Sect. 2: Basics on common observables most relevant to Be stars and the formation mechanisms giving rise to them are introduced.
Sect. 3: Discusses the central stars, concentrating on the rotational and pulsational properties, as well as on the magnetic field hypothesis and observations.
Sect. 4: This section deals with the actual *Be-phenomenon*, a formulation used to summarize potential mechanisms to eject the stellar matter to form the disk. First the potential agents that might be acting to eject mass and angular momentum, then the repercussions of the process on the circumstellar environment are reviewed.
Sect. 5: Summarizes the state of knowledge concerning the circumstellar disk. Disk geometry and kinematics are reviewed, then the variability. In the last subsection, the current theoretical views on Be star disks are given.
Sect. 6: Here, Be stars are considered as interacting binaries, first tidal effects are discussed, then Be stars with compact companions producing X- and γ-rays, and finally Be stars with hot subdwarf companions that have a radiative effect on the disk.
Sect. 7: Be stars are looked at as a class of stars beyond the Milky Way, as statistical samples, with special emphasis on various metallicity environments, and their potential relation to the distant universe.
Sect. 8: A summary and conclusions are presented, together with some outlook.

1.1 Definition

Father A. Secchi (1866) reported[7] an observation of γ Cas (B0.5 IV), which at the position of Hβ showed "une particularité curieuse … une ligne lumineuse très-belle

[3] No proceedings published, presentations at http://ipl.uv.es/bexrb2011/.

[4] http://activebstars.iag.usp.br/, formerly "Be star Working Group".

[5] ISSN 0296-3140.

[6] http://basebe.obspm.fr/.

[7] In the heyday of nationalism, this was communicated in French language to a German Journal by an Italian astronomer, working at *the* international organization of the time, the Vatican.

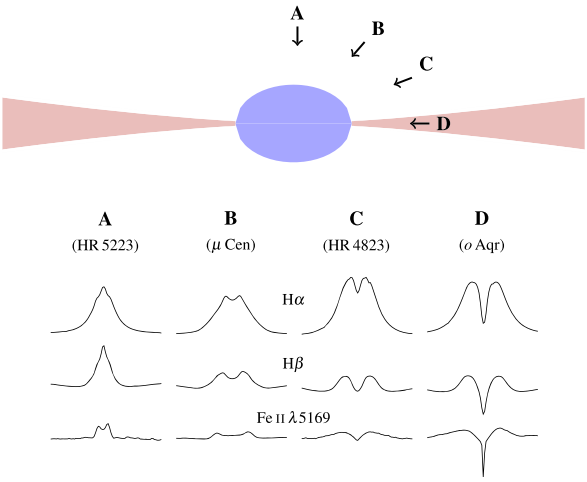

Fig. 1 Schematic view of a Be star at critical rotation and with a flared disk. The lower part shows example spectral profiles from pole-on to shell Be stars

et bien plus brillante que tout le reste du spectre." This was to become known as the first observation of a Be star. From a purely taxonomical point of view, the class of Be stars was then formed of all stars showing a B-type spectrum in combination with Balmer line emission. The variety of the class was clear early on, but still stars with P Cygni profiles and other stars were typically treated together (as for instance by Curtiss 1926). Only Struve (1931) omitted stars with P Cygni profiles, and attributed the spectra of stars like β Lyr (B8) to binarity. The remaining main sequence objects[8] he suggested to be rotationally unstable stars, namely to be "lens shaped bodies, which eject matter at the equator, thus forming a nebulous ring which revolves around the star and gives rise to emission lines." This also brought the unification of shell stars with Be stars. Shell stars are stars in which the Balmer lines have sharp absorption cores, much sharper than expected from the width of normal photospheric lines. They may or may not have double peaked emission on both sides of the absorption core. In Struve's picture, shell stars are just Be stars seen edge-on, i.e., through the disk, which gives rise to the narrow absorption lines. Figure 1 gives a schematic view of this idea. Struve's view was quite generally accepted, but came under criticism in the 1970s and 1980s, when a number of opposing models were suggested. A final breakthrough in favor of the geometric shape advocated by Struve was achieved only by interferometric observations (Quirrenbach et al. 1994). For a more detailed overview of the history of the field and ideas about Be stars, we refer to the monograph by Underhill and Doazan (1982), the reviews by Slettebak (1988) and Porter and Rivinius (2003), and the references therein.

The still widely used classical definition of Be stars was first suggested by Jaschek et al. (1981), and with the minor change of replacing the original "hydrogen lines" with "Balmer lines",[9] popularized by Collins (1987):

[8] Main sequence understood here in terms of the upper main sequence, where it comprises of the luminosity classes V to III.

[9] Infrared hydrogen lines can have purely photospheric emission in early main sequence B stars due to NLTE effects, see, e.g., Zaal et al. (1999).

> A non-supergiant B star whose spectrum has, or had at some time, one or more Balmer lines in emission.

The problem with this definition lies in its broadness. As it has to be applied to classification quality data, no better one has been formulated yet. There is some ambiguity in this definition, since it basically includes all main sequence B-type stars with circumstellar material above densities of about 10^{-13} g cm^{-3}. This is regardless of the physical mechanism by which this material was transported into, and is eventually kept in, the circumstellar environment: it is actually unavoidable that circumstellar gas at and above such density will form Balmer line emission around a B-type star.

1.1.1 Taxonomically similar objects

It is quite common for a B star to have circumstellar emission. According to the original definition above, all luminosity class V–III objects with emission would qualify as Be stars, even if they are physically different. However, there are distinctions that can be used to distinguish the objects commonly termed classical Be stars from those emission-line objects of other provenance, even if these, laid out below, are not easily applied for the purpose of bulk classification.

Supergiants Particular for early B stars with high $v \sin i$ one sometimes finds misclassifications of evolved objects as main sequence stars. For instance, HD 64760 and κ Aql have virtually identical spectra both in the visual and UV-region,[10] including weak Hα emission, yet the former is classified B0.5 Ib, the latter B0.5 III. Their weak emission does not come from a disk, even if it is found on both sides of the line, similarly to Be stars, but rather originates in an angular momentum conserving stellar wind type outflow (see, e.g., Kaufer et al. 2006 for HD 64760 and Puls et al. 2008 for a general review of hot star winds, and the typically much stronger winds of supergiants).

Herbig stars Among the B stars with emission lines situated closer to the main sequence in the Hertzsprung–Russell diagram, Herbig Ae/Be stars are easiest to confuse with classical Be stars. These are young stellar objects in the final stages of accretion, generally with fossil gaseous disks (Waters and Waelkens 1998). The more active earlier types are quite distinct in emission morphology and variability, often showing P Cygni and inverse P Cygni profiles, making it easy to tell them apart (Alecian 2011). More quiet objects, however, can be (and have been) mistaken for classical Be stars, like 51 Oph (B9.5 V), which was counted as a classical Be star until a strong infrared excess due to dust was discovered (Waters et al. 1988). Such an excess has never been seen in a classical Be star, so that infrared or mm observations well distinguish the two classes.

[10] Spectra are available from the ESO (http://archive.eso.org/) and IUE (http://archive.stsci.edu/iue/) archives.

Mass transferring binaries Several types of systems with B-type primary components[11] are known. Obvious cases include Algol and W UMa type variables, i.e., eclipsing contact or semi-detached systems in which the secondary fills the Roche lobe and the accretion onto the primary gives rise to the line emission. The systems of β Lyr and a few similar stars are more complex, nevertheless the circumstellar emission comes from material being transferred from one star to another (or ejected out of the system). None of them was ever considered to be a classical Be star in Struve's sense, but the mechanism of Roche lobe overflow has been proposed to be responsible for Be stars in general (Kříž and Harmanec 1975). As the quality of radial velocity measurements from spectroscopic data increased (Baade 1992), companions were indeed found, but these were not filling their Roche lobes (see, e.g., references in Harmanec et al. 2002a), although some have been in the past and underwent spin-up (see, e.g., de Mink et al. 2013, for the physics involved). No classical Be star has yet been found to have a Roche lobe filling companion, and given Sects. 3 to 5, any such star would have to be discussed in a different framework of physics.

B[e] stars This is an inhomogeneous group of B stars showing Balmer line emission plus forbidden emission lines (Lamers et al. 1998). The latter are not observed in classical Be stars. Four of five subgroups are supergiant stars, young stellar objects, symbiotic binaries, and compact planetary nebulae, partly discussed above. The nature of the fifth group, sometimes dubbed "unclassified B[e]" type stars, is not quite clear as of now, but in any case the forbidden lines and the dust-type infrared excess make them quite distinct from the classical Be stars, i.e., this is clearly a different population with likely a different mechanism responsible for the filling of the circumstellar environment (which may nevertheless be disk-shaped).

Star with emission line magnetospheres Magnetic B stars do not typically show line emission, but depending on the field strength, wind, mass loss and rotation, they can have Balmer line emission forming in the magnetosphere (Petit et al. 2013). Not long ago, this was a class of objects where only a single member had been well investigated, namely σ Ori E (B2 V, Landstreet and Borra 1978). Meanwhile several other stars have been found and analyzed, including the rapid rotators HR 7355 and HR 5907, both B2 V (Rivinius et al. 2010; Grunhut et al. 2012). They have in common that the circumstellar environment shows variability with strictly the same period as the photosphere, namely the rotational one, and little to no secular variation, which clearly distinguishes them from classical Be stars.

1.1.2 Oe and A–F shell stars

Another important question is whether the border drawn by restricting Be stars to B-type stars reflects any physical reality or is artificially created by the classification scheme. Oe stars are classified equivalently to Be stars as being of luminosity class V to III and have a morphologically similar emission spectrum. Most are of late O subtype, i.e., close to the B star range (Conti and Leep 1974; Negueruela et al.

[11] We use "primary" to designate the star that dominates the photospheric spectrum in the visible range.

2004) and have been assumed to be a blueward extension of the Be class. However, spectropolarimetric observations by Vink et al. (2009) and the original experience of Be stars as a fairly inhomogeneous class suggest caution in ascribing such a nature to all of them, in particular for the earlier subtypes.

The situation is similar with A- and F-type shells stars (Slettebak 1986; Waters et al. 1988). Some of them, mostly those of earlier subtype, show weak Hα emission as well, but due to the weakness of the ionizing radiation this vanishes quickly towards later types. From the spectral appearance, it is quite conceivable to ascribe those shell lines to disks, and thus regard them as the late-type extension of Be stars. As the example of 51 Oph has shown, however, there is quite some probability that at least part of these objects would rather be β Pictoris like objects, i.e., a subtype of Herbig stars in which the disk is primordial with a dust-component and not, like in classical Be stars, only formed during the main sequence lifetime.

This suggests that, although Be-like objects exist outside the spectral class B, restricting the analysis to actual B-type stars will likely not restrict their understanding, but on the contrary may avoid problems by excluding doubtful cases. Hence "classical Be stars" as discussed in this review are those objects that remain if all the above cases are discounted from the population of B stars with emission lines at large.

Other definitions, based on derived physical properties, have been proposed (e.g., by Martayan et al. 2011), but lack applicability for taxonomical purpose, unless each individual star could be thoroughly analyzed. Properties such as rapid rotation or the presence of a viscous decretion disk should therefore not be used for definition purposes. However, as will be seen, such properties are indeed corollaries to the definition of a "classical Be star".

1.1.3 Dynamic behavior and variability

The most striking observational property of Be stars is their variability on basically all time scales longwards of a few minutes, offering insight to a great number of astrophysical phenomena and their interplay.

Already the emission itself in Be stars is transient. The definitions by Jaschek et al. and Collins explicitly include this. Emission can come and go over the time scale of several decades. When present, it can reach some tens of Ångströms in Hα equivalent width (*EW*), swaying between higher and lower values, and then decay over several years to a normal B-type photospheric absorption spectrum. These changes can be observed photometrically and gave rise to the γ Cas class of variable stars defined in, e.g., the General Catalogue of Variable Stars as eruptive variables.

Variability in the emission-line profile is also quite common. An example is the "violet-to-red cycles" (V/R variations), in which the two peaks of the emission lines vary in height against each other. Cycle lengths range from weeks to decades, but while the shorter ones are usually binarity driven, the longer ones are due to a more or less stable one-armed density wave pattern in the disk (Sect. 5.3). In general, variations on intermediate time scales either reside in the disk or are due to binarity.

Phenomena in the close circumstellar environment or on the stellar surface cause variability on time scales of a few days. Not only are the stellar rotational and typical pulsation periods very similar (Sects. 3.1 and 3.2), but as well the Keplerian orbital

period close to the star (e.g., seen for localized mass ejections) falls in that range, as do the viscous transport times through the inner disk (Sect. 5.3), taking a few days to weeks at most. While most photospheric variations are pulsational, the circumstellar environment contributes with cyclic phenomena, e.g., from non-circularized material in orbit, and with more secular variations in which the orbiting material is distributed radially. Stars in which such short-term periodic processes dominate the photometric variations are termed "λ Eri variables".

Time scales shorter than about half a day are often due to β-Cephei type pulsational modes when periodic, in particular in earlier type Be stars, but in later type stars it is more common that the associated phenomena are transient. Examples have been observed in X-ray and characterized as "shot"-type activity, and in the visual wavelength region as "dimples" in line profiles (Sects. 3.3 and 4).

1.2 Astrophysical context

Be stars show a unique combination of properties at a very nearby distance and at convenient brightness, and are therefore well accessible to detailed study. What is learned from Be stars in terms of fundamental astrophysical processes can then be applied to more distant or less accessible objects.

1.2.1 Stellar rotation

Be stars, and possibly their non-emission line equivalents, the Bn stars, are the most rapidly rotating classes of non-degenerate stars, certainly so in terms of $v \sin i$, and possibly in terms of fractional critical rotation, where the championship might have to be shared with S Dor variables (also known as Luminous Blue Variables, or LBVs), which are proposed to be rapid rotators as well (Groh et al. 2009).

This makes them excellent objects to study the effects of rapid rotation and test the respective theories at their extreme. Concerning the stellar wind, for instance, it was discussed whether fast rotation should enhance the wind density at polar or equatorial latitudes, which has important repercussions on, e.g., the mass loss of S Dor variables (Puls et al. 2008). The pulsational properties of rapidly rotating stars differ from the non-rotating cases, opening a window into the interior structure under the effect of rotation (Reese et al. 2009, 2013; Lee 2012).

Finally, Be stars rotate sufficiently fast to investigate the validity of traditional approximations, such as the Roche approximation for the stellar stability or the gravity darkening for the latitude-dependent temperature and flux distribution of rapidly rotating stars (Sect. 2.3.1).

1.2.2 Evolutionary context

How do Be stars connect to the pre- and post-main evolution of the stars within the B star mass range? Be stars exist already at the zero-age main sequence, even though they are less common than in later stages (Sect. 7.1). Their rapid rotation poses constraints on the ubiquity of angular momentum loss mechanisms. Rotational mixing alters the chemical enrichment pattern of core and surface, consequentially

the evolutionary paths throughout the main sequence differ from non-rotating stars (Maeder and Meynet 2010, and references therein). In turn also the evolution of the surface angular momentum across the main sequence lifetime poses constraints on internal processes. Having left the main sequence, the earliest B stars are counted among the "massive stars", i.e., they have masses above 8 $M_{\odot}$ and will evolve into core-collapse supernovae. It has been suggested that their rapid rotation has some connection to long gamma ray bursts (see, e.g., Woosley and Bloom 2006; Martayan et al. 2010b; Maeder and Meynet 2012). It is also important to recognize that Be stars are not rare objects, they are a large subgroup of B stars (about 15–20 % in the local environment, see Sect. 7.2.2), and at low and extremely low metallicity, such as Population III stars, they might even be the overwhelming majority of B stars (Sects. 7.2 and 7.3).

1.2.3 Disk physics

In several astrophysical systems the interface regions between a comparatively compact object and its more extended environment are often marked by a gaseous disk. Although the evolutionary contexts and absolute dimensions differ widely, e.g., from proto-planetary disks and protostars to active galactic nuclei, the elementary physical processes of gravity, radiative transfer, and radiative pressure have much in common (Woosley 1993; Balbus and Hawley 1998; Hartmann et al. 1998; Lubow et al. 1999; Nelson et al. 2000; King et al. 2007, just to name a few works on disks in various contexts). In particular, Be disks share exactly the same physics with the well-studied accretion disks around protostars but are called instead "decretion disks" in reference to the fact that in Be disks mass is usually flowing away from the star whereas in protostars disk matter flows towards it. The existence of global waves has been evoked to explain cyclic asymmetries in emission-line profiles (Sect. 5.3). A detailed understanding of these phenomena will have applicability in other systems, such as planetary rings, proto-planetary systems, close binary stars and galactic nuclei. In particular, these phenomena may play an important role in planet formation. Be disks in binary systems (Sect. 6) are subject to important and complex processes, namely, precession, warping, tidal deformation and truncation. Be/X-ray binaries (Sect. 6.2), in addition, offer the possibility to study the interaction between the relativistic wind of the compact object and the disk. Finally, viscosity is a key process governing the fate of these disks (Sects. 5.2 and 5.3). Since viscous transport of both matter and angular momentum occurs in relatively small volumes (and, therefore, in short time scales), temporal studies of viscosity-related variability offer the opportunity to measure the kinematic viscosity of the material, which in turn will serve as a constraint to any theory of viscosity.

2 Be star observables

This section discusses the quantities observed in Be stars in terms of the mechanisms contributing to their values and, for some of them, the observing/analysis techniques used. The examples presented below, concerning the disk, were computed for a reference model based on the one introduced by Faes et al. (2013, their Table 1). Keeping

all other parameters equal, we increased the disk radius to 100 $R_\star$, and present results for two base densities (10^{-11} g cm^{-3} and 10^{-10} g cm^{-3}) and a number of different inclinations. Computations were done with the HDUST code (Carciofi and Bjorkman 2006), based on the viscous decretion disk model. See Sect. 5.4 for the details and observational support of this model.

2.1 Flux in the continuum

The observed spectral energy distribution (SED) of a Be star results from an interplay of photospheric emission, disk emission of reprocessed radiation and disk absorption. Thomson scattering by free electrons can also change the SED. The relative importance of these processes varies greatly with wavelength and viewing angle. For instance, the ultraviolet, which can be highly depleted for edge-on stars, will be enhanced in pole-on stars owing to light scattered off the disk. The photospheric flux is more naturally discussed together with the photospheric lines, for which we refer to Sect. 2.3.1, and restrict this section to the influence of the disk, treating the photospheric flux as a given source of photons.

The role of the disk is best understood in terms of a *pseudo-photosphere*, which is a region of the disk that is radially opaque to radiation of the continuum. The dimension of the pseudo-photosphere is wavelength dependent. For an isothermal, viscous Keplerian disk (see Sect. 5), seen pole-on, the size of the pseudo-photosphere grows with wavelength approximately as (Carciofi and Bjorkman 2006)

$$R_\lambda^{\rm eff} = \overline{R}\lambda^{0.41}, \tag{1}$$

where $\overline{R}$ depends on the disk temperature, density and geometry. For a given disk, i.e., a given value of $\overline{R}$, there is a wavelength shortwards of which there will be no pseudo-photosphere ($R_\lambda^{\rm eff} \leq R_\star$). In this case, the disk emits as a diffuse, optically thin gas. If a pseudo-photosphere exists emission can conceptually be seen as a combination of optically thick inner ($r < R_\lambda^{\rm eff}$) and thin outer ($r > R_\lambda^{\rm eff}$) contributions. The effect will depend on the disk viewing angle

- *Pole-on.* Since the disk is colder than the photosphere (Sect. 5) the SED will be simply the superposition of the stellar continuum with a redder disk (excess) continuum. The relative weight of stellar vs. disk emission depends on the size of the pseudo-photosphere: At visual wavelengths the excess hardly reaches half a magnitude, but may dominate the total flux in the near-infrared, and certainly does so from the mid-infrared onwards (see Haubois et al. 2012; Sigut and Patel 2013, and references therein).
- *Edge-on*. Here the disk may absorb and scatter part of the stellar flux. If the pseudo-photosphere is small, this will result in a net dimming of the system, such as observed in shell stars. If the pseudo-photosphere is large, however, the large emitting area will counterbalance the decrease in photospheric flux, causing a net brightening. For instance in ζ Tau (B2 IV), a shell star, this causes a dimming bluewards of $\approx$1.4 μm and a brightening longwards (see Fig. 14e).

Figure 2 illustrates the formation region of the continuum disk emission for several bands and two disk densities. What is plotted is the integrated flux as a function of

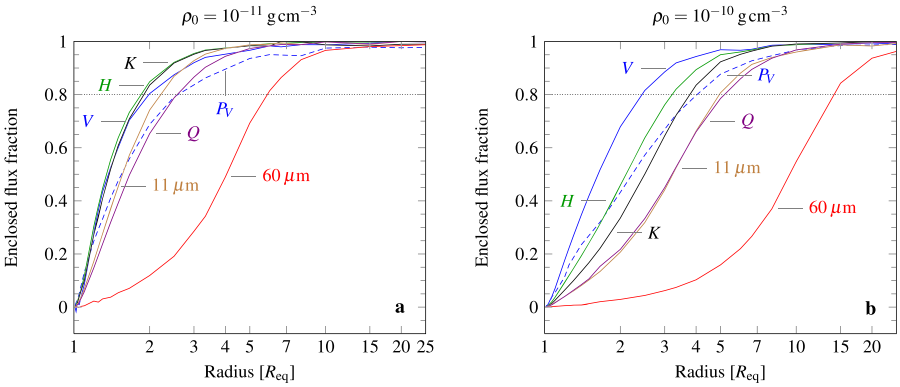

Fig. 2 The formation loci of continuum emission for various wavelength bands and V-band polarized flux P_V, expressed in accumulated disk contribution as function of increasing radius for two different densities. The stellar flux $F_\star$ was subtracted so that each curve starts at zero. The *dotted limit* marks 80 % of the total flux, which corresponds to the integrated flux inside the FWHM for a Gaussian shaped emission profile. Data were computed with HDUST for the reference model of Faes et al. (2013), for a disk seen at $i = 30°$

radial distance from the star, normalized to the total flux for a disk with a radius of 100 $R_\star$. This shows that different bands have different formation loci. For instance, 80 % of the V-band flux comes from inside 1.8–2.5 $R_\star$, depending on the disk density, while the same fraction, at 60 µm, originates from a much larger volume (inside 5–15 $R_\star$). In the dense case, all bands shown have a pseudo-photosphere, from ∼2 $R_\star$ in V to about 11 $R_\star$ at 60 µm. In the low-density case the clustering of the curves for V, H and K bands indicates that a significant pseudo-photosphere starts only between the K band and 11 µm.

2.2 Polarization of the continuum

After the realization in the 1960s and 1970s that the non-zero intrinsic polarization of some stars originated in their circumstellar envelopes, polarimetry became a standard tool to study these systems. For Be stars, in particular, polarimetry provided key insights as to the nature of their disks. When light from the central star is scattered by free electrons in the ionized disk, it becomes polarized perpendicular to the scattering plane, formed by incident and scattered direction, resulting in a non-zero polarization for an asymmetric scattering region. For a geometrically thin disk, the polarization direction, measured as its position angle, will be perpendicular to the disk plane (see Sect. 5.1.4).[12]

Brown and McLean (1977) derived an analytical approximation for the optically thin transfer of polarized light in electron envelopes with axial symmetry. Optically thin is a key approximation to avoid having to deal with multiple scattering. Brown and McLean found that the net polarization depends on three envelope parameters:

[12] A strongly distorted and thermally inhomogeneous star, i.e. a rapidly rotating one will show intrinsic polarization, too. However, the effect is completely negligible compared to the one caused by the disk.

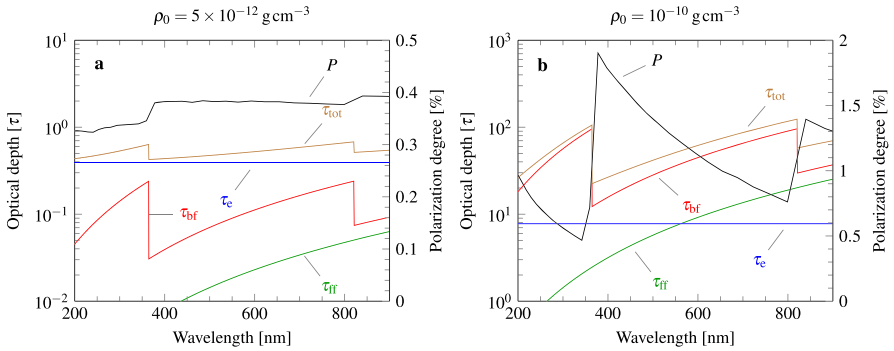

Fig. 3 Polarized spectrum P and radial optical depth contributions along the midplane of a Be disk. The total optical depth τ_{tot} is the sum of the optical depth for each continuum opacity source (free-free τ_{ff}, bound-free τ_{bf}, and Thomson scattering τ_e). *Left*: Low-density case ($\rho_0 = 5 \times 10^{-12}$ g cm^{-3}). *Right*: High-density case ($\rho_0 = 10^{-10}$ g cm^{-3}). Data were computed with HDUST for the reference model of Faes et al. (2013), for a disk seen at $i = 70°$

an average electron optical depth, $\bar{\tau}$, a shape factor, γ, describing the degree of asymmetry, and the inclination between the axis of symmetry and the line of sight, as

$$P = \bar{\tau}(1 - 3\gamma)\sin^2 i. \tag{2}$$

This approximation produces an increase from zero to maximum polarization with the inclination i in the form of $\sin^2 i$. On the one hand, the inclusion of an absorptive opacity significantly reduces the polarization (e.g., Fox 1991). On the other hand, multiple scattering (i.e., a diffuse radiation field, e.g., Wood et al. 1996b) was found to be able to *increase* the polarization. Then, the simple relation $P \propto \sin^2 i$ no longer holds: light scattered parallel to the disk can be absorbed or scattered again, which reduces the polarization, and the maximum P is reached for $i \approx 70$–$80°$ (Wood et al. 1996b; Halonen and Jones 2013). Neither does the polarization level grow linearly with density, as multiple scattering and attenuation set an upper limit. Observations and models agree that the maximum polarization of Be disks is about 2 %. In Fig. 2 the region whence the V-band polarized flux originates is shown for two disk densities.

A typical example of the continuum polarization of a Be star is shown in Fig. 14f. The Paschen and Brackett continua are nearly linear with a negative slope, with abrupt changes at the H I ionization thresholds. The Balmer continuum (e.g., Bjorkman et al. 1991) is much more complex due to metal line opacities. Several processes such as multiple scattering, disk absorption and emission, occultation by the central star, etc., as well as the details of the geometry of the disk and the physical state of the gas, all concur to define the shape of the polarized continuum.

Figure 3 shows theoretical polarized spectra of Be disks, together with the optical depth for the three main continuum opacities, namely, electron scattering, H I photoionization, and bremsstrahlung (free-free). The low-density model (panel a) illustrates the optically thin case. The polarization is small (≈0.4 %) and the main opacity source is electron scattering, so the polarized continuum is nearly "gray". As

density increases (panel b), the electron optical depth increases $\propto\rho$, but H I and free-free opacities are approximately proportional to ρ^2 (e.g., Bjorkman and Bjorkman 1994). Since the *pre-scattering absorption* of starlight reduces the polarized flux, the polarized continuum becomes inversely correlated to the H I opacity.

In the visual regime the H I opacity always dominates over the free-free opacity. In the near-infrared this relation reverts, the disk opacity becomes entirely free-free dominated, and, thus, the polarization levels will be rather small.

2.3 Spectral lines

Most of the current knowledge about Be stars was derived spectroscopically. The spectral lines intrinsic to Be stars can come from three regions: the star itself, the actual disk, and the circumstellar environment above the disk up the to polar regions.

2.3.1 Photospheric lines

The appearance of the photospheric lines is governed by the rapid rotation not only through rotational broadening. In addition, the near-critical rotation alters the photospheric properties of the star itself.

As misunderstandings may arise from the various definitions used when discussing critical rotation, it is important to clarify them: A star rotates critically, when the rotational velocity at the equator, $v_{\rm rot}$, equals the Keplerian circular orbital velocity[13] at the equator, $v_{\rm orb}$. In the case of a critically rotating star, because of the increasing equatorial radius $R_{\rm eq}$, while $R_{\rm pole}$ remains roughly the same (see below), the actual orbital velocity at the equator is increased towards the critical one, but remains under that limit until criticality is reached. For a non-critically rotating star one has, therefore, to distinguish between $v_{\rm crit}$ and $v_{\rm orb}$. Associated with the linear velocity $v_{\rm crit}$ is the angular velocity $\Omega_{\rm crit}$.

Rotational velocities can be expressed in angular and linear velocities. Thus, for a given stellar mass $M_\star$, one can define four quantities:

$$v_{\rm crit} = \sqrt{\frac{2}{3}\frac{GM_\star}{R_{\rm pole}}} \quad \text{and} \quad \Omega_{\rm crit} = \sqrt{\frac{8}{27}\frac{GM_\star}{R^3_{\rm pole}}} \tag{3}$$

and

$$v_{\rm orb}(R_{\rm eq}) = \sqrt{\frac{GM_\star}{R_{\rm eq}}} \quad \text{and} \quad \Omega_{\rm orb}(R_{\rm eq}) = \sqrt{\frac{GM_\star}{R^3_{\rm eq}}}. \tag{4}$$

The 2/3 factor above comes from the oblateness of $R_{\rm eq} = 2/3\ R_{\rm pole}$ for critical solid body rotation (see Chap. 2 of Maeder 2009, for the derivation of this factor). The first two equations are traditionally used for rotational statistics, and are only meaningful in the Roche approximation.[14]

[13] Often just "Keplerian orbit" is said, but we note non-circular Keplerian orbits are common in Be star disks as well, see Sect. 5.3.

[14] Named in honor of E.A. Roche (1820–1883) for his work on equipotential surfaces.

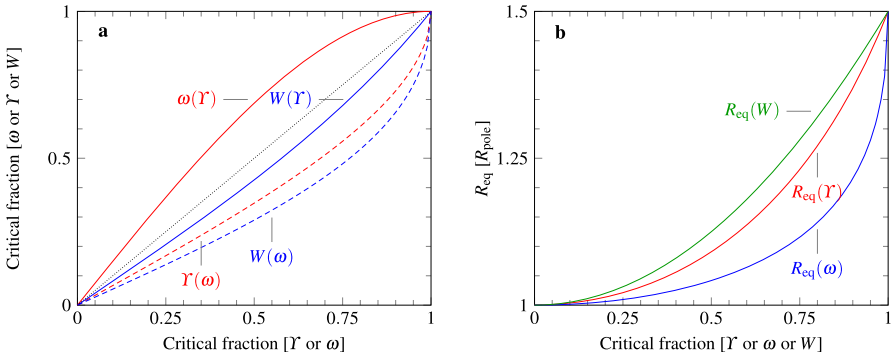

Fig. 4 *Left*: Conversions of Υ, ω, and W as functions of ω and Υ. The *dotted line* marks the identity relation. *Right*: $R_{\rm eq}$ as function of ω, Υ and W. Figure based on Owocki, priv. comm, see text for definitions

The latter two are independent of the rotation type (solid or differential), and are more useful to set the scale of disk rotation. The use of both angular and linear velocities then gives several possible definitions of the critical fraction for the purpose of rotation statistics

$$\omega = \frac{\Omega_{\rm rot}}{\Omega_{\rm crit}} \quad \text{and} \quad \Upsilon = \frac{v_{\rm rot}}{v_{\rm crit}}. \tag{5}$$

There is no convention how to designate the critical fraction in linear velocities; apart from Υ other symbols are used as well, including ω and W. A third definition, unfortunately so far not very widespread in Be star publications, is the physically most meaningful

$$W = \frac{v_{\rm rot}}{v_{\rm orb}}, \tag{6}$$

as it defines what velocity boost is required for a given star to launch material into the closest possible orbit, i.e., just above the photosphere at the equator.

Based on the relations for oblateness given by Collins and Harrington (1966), one can derive conversions between Υ, ω, W and their relation to $R_{\rm eq}$, keeping $R_{\rm pole}$ fixed (Owocki, priv. comm.)

$$\Upsilon(\omega) = 2\cos\left(\frac{\pi + \arccos(\omega)}{3}\right), \tag{7}$$

and

$$\omega(\Upsilon) = \cos\left(3\left[\arccos\left(\frac{\Upsilon}{2}\right) - \pi\right]\right). \tag{8}$$

These relations are illustrated in Fig. 4a. The equatorial radius as a function of Υ or ω (see Fig. 4b) then is

$$R_{\rm eq}(\Upsilon) = \frac{3}{2}\frac{\Upsilon}{\omega(\Upsilon)} R_{\rm pole} \quad \text{or} \quad R_{\rm eq}(\omega) = \frac{3}{2}\frac{\Upsilon(\omega)}{\omega} R_{\rm pole}. \tag{9}$$

Using Eqs. (3), (4) and (9)

$$\frac{v_{\rm crit}}{v_{\rm orb}} = \sqrt{\frac{2}{3}\frac{R_{\rm eq}}{R_{\rm pole}}} = \sqrt{\frac{\Upsilon}{\omega}}, \tag{10}$$

so that one can expand

$$W = \frac{v_{\rm rot}}{v_{\rm orb}} = \frac{v_{\rm rot}v_{\rm crit}}{v_{\rm crit}v_{\rm orb}} = \sqrt{\frac{\Upsilon^3}{\omega}}. \tag{11}$$

The functions $W(\Upsilon)$ and $W(\omega)$ are shown in Fig. 4a. We note that this expression for W still relies on the Roche approximation, which, however, is far more robust for values below unity than at the critical limit: Towards the critical limit the Roche approximation is not observationally tested, and deviations may occur for a non-rigidly rotation pattern (e.g., Jackson et al. 2004). We refer to Chap. 4 of Cranmer (1996), Meynet et al. (2010), and van Belle (2012) for a more thorough discussion of the relation of these quantities. Above, a fixed $R_{\rm pole}$ was assumed. It should be noted that $R_{\rm pole}$ actually shrinks with $\Omega_{\rm rot}$, but only by about 1.5 % between no rotation and the critical value in the Be star mass range (see Fig. 2 of Ekström et al. 2008).

Since, as pointed out, W is the physically most meaningful quantity for the discussion of Be stars, and has also come to be used in the context of magnetospheres (Petit et al. 2013), we would like to discourage the further use of ω or Υ, in particular since the conversion using Eqs. (7), (8), and (11) is fairly trivial. This will be done for the remainder of this work.

A slightly different definition for the critical fraction is sometimes found in asteroseismology

$$\omega_{\rm seism} = \Omega_{\rm rot}\left(\frac{GM_\star}{R_\star^3}\right)^{-1/2}, \tag{12}$$

where for $R_\star$ the *mean* radius of the rotationally deformed star is used. Since this is smaller than the actual equatorial radius, critical rotation occurs around $\omega \approx 0.75$ in this notation.

von Zeipel (1924) noted that in a rotating star in radiative equilibrium the local flux is proportional to the local surface gravity and remarked that "the effective temperature has its maximum at the poles and its minimum at the equator".[15] This effect has become known as gravity darkening, and is nowadays well known in the form of $T_{\rm eff} \propto g_{\rm eff}^{1/4}$ (Collins 1963). The exponent 1/4 can be generalized to a parameter, often called von Zeipel's β (see left panel of Fig. 5 for the consequences of this effect on $v \sin i$ determination).

Figure 6 illustrates the effect of gravity darkening and rotational distortion on the stellar surface for two values of $W = 0.62$ (upper row) and 0.90 (lower two rows). The total flux emitted by a surface element is $\propto T_{\rm eff}^4$ (panels 6a and 6e), but the

[15] Often called the von Zeipel theorem, this is actually only a facet; in its complete form the theorem is about the unattainability of radiative equilibrium in a rotating body of gas.

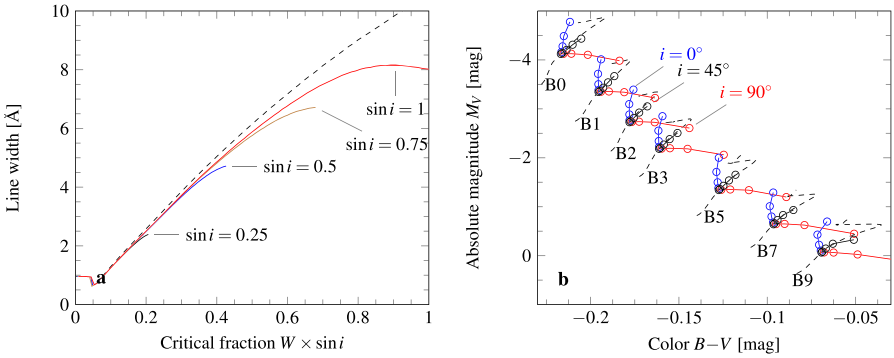

Fig. 5 The gravity darkening effects of rapid rotation on the photospheric appearance of a B star. *Left*: As W (for the relation to Υ see the text or Fig. 4) approaches unity, the observable line width becomes degenerate. Shown are four values of inclination, labeled with their $\sin i$. *Right*: The increasingly different appearance of rapidly rotating B stars from the non-rotating case in the photometric Hertzsprung–Russell diagram, for $W = [0.00, 0.20, 0.41, 0.64, 0.93]$ and three different inclinations 0° (*blue*), 45° (*black*) and 90° (*red*). Note the points for $W = 0.00$ and 0.20 fall almost onto each other, significant differences start only at about $W \approx 0.4$. Figures adapted from Townsend et al. (2004)

chromatic flux is strongly wavelength dependent. The effect is much more severe for UV or visual wavelengths than in the infrared (panels 6b to 6d and 6f to 6h). Apart from this, also different transitions will be affected differently.

For lines like Si III and He I in an early type B star, for instance, the polar regions will contribute much more strongly to the total equivalent width of the line than the equatorial region. In turn, Si II and Fe II lines will be formed more equatorially (panels 6i to 6l).

Gravity darkening has been interferometrically observed in a number of stars. In some objects the results are compatible with $\beta = 0.25$, in others, however, a lower β was found (e.g. $\beta = 0.20$ was assumed for α Eri by Domiciano de Souza et al. 2012a; see also van Belle 2012, for a review). The value of $\beta = 0.25$ relies on a radiative atmosphere in rigid rotation, while in a convective atmosphere the exponent is lower (around $\beta \approx 0.08$ according to Lucy 1967). In particular for later type Be stars the equator may become cool enough to be convective at high W. An alternative to a fixed β, better reproducing the observed distribution of values, has been proposed by Espinosa Lara and Rieutord (2011), where β itself becomes a function of W. This also moves the problem of the equatorial temperature becoming very small, and even zero for critical rotation (when $g_{\rm eff}$ becomes zero), to a value of W much closer to 1.

Due to gravity darkening, the spectrum of a rapidly rotating star cannot any longer be characterized like that of a non-rotating star, by only two parameters (typically chosen to be $T_{\rm eff}$ and $\log g$). In turn, it requires four physical parameters (for instance $T_{\rm eff,pole}$, $R_{\rm pole}$, $M_\star$, and W) and a fifth, the inclination i, to determine the appearance of a rapid rotator to an observer (see right panel of Fig. 5 for the effect if i).

The other important process affecting the photospheric line profiles is pulsation. For a discussion of stellar pulsation physics, however, we refer to more general works in that field, such as Aerts et al. (2010) or Saio (2013).

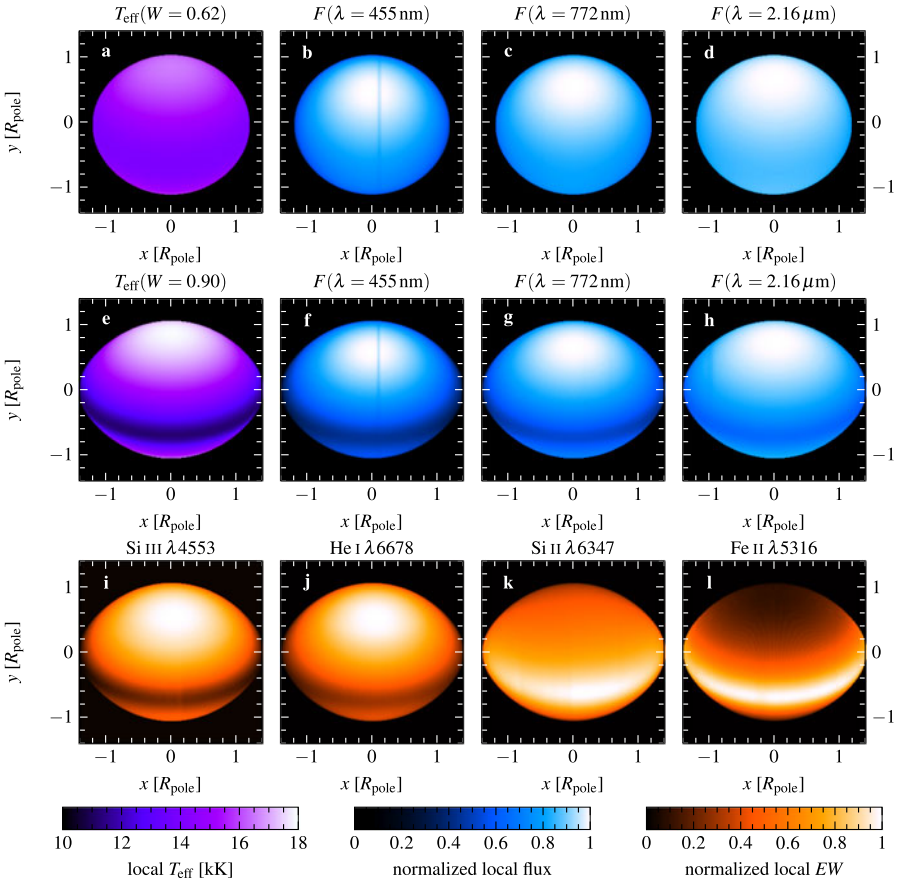

Fig. 6 Appearance of a gravity darkened star. *Upper row*: Surface appearance of a star rotating at $W = 0.62$. From *left* to *right*: Temperature and flux distributions in line free regions at $\lambda = 455$ nm, $\lambda = 772$ nm, and $\lambda = 2.16$ µm (or nearly so: the dark vertical strip in the flux panel for 455 nm is, actually, due to a spectral line). *Middle row*: Same as upper row, but for $W = 0.90$. *Lower row*: The equivalent width in the locally emergent spectrum as a function of position on the stellar surface for Si III λ4553, He I λ6678, Si II λ6347 and Fe II λ5169. In order to estimate the actual contribution to the spectral line, they further have to be multiplied with the local flux. Images computed by A. Domiciano de Souza with the spectral synthesis code CHARRON (Domiciano de Souza et al. 2012b), based on the physical parameters found for α Eri, but seen at $i = 60°$ for illustration (Domiciano de Souza et al. 2012a, for details, note in particular that $\beta = 0.20$)

2.3.2 Disk emission and absorption

The typical emission-line appearance of Be stars is shown in the lower part of Fig. 1. The two important cases are the optically thick and optically thin limits. The hydrogen lines are optically thick and the dominant formation process is recombination, while many metal lines are optically thin, in particular if they arise from NLTE effects, such as optical pumping. While hydrogen lines form in a large part of the disk, from the kinematic properties of the line emission (mainly the full width at the base

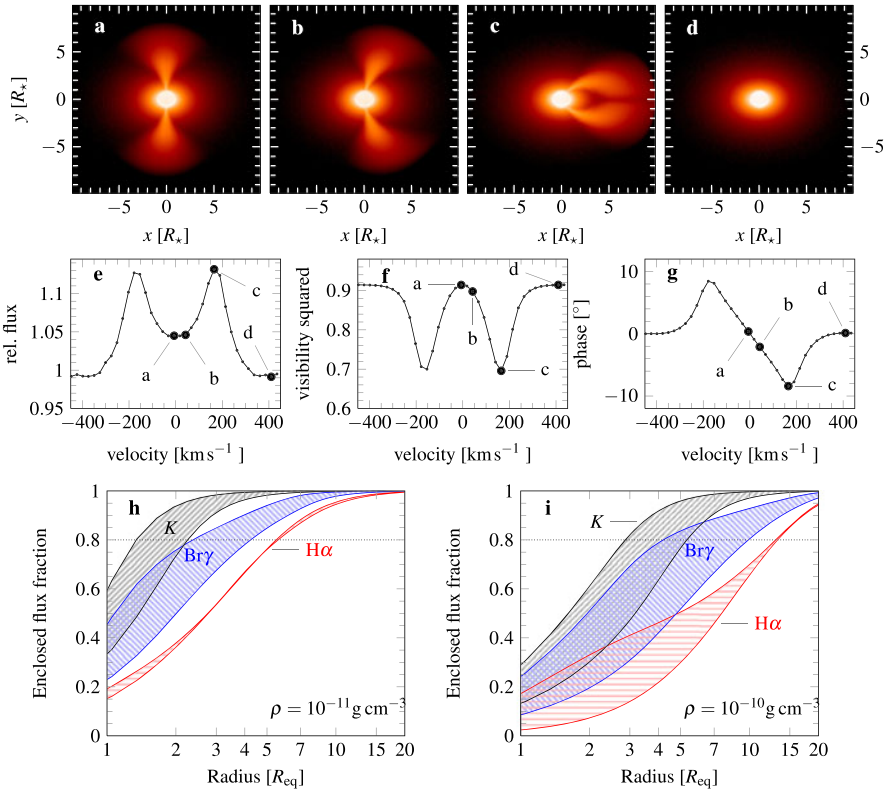

Fig. 7 *Upper row*: The formation regions of an emission line (here Brγ) as a function of Doppler velocity (see, e.g., Stee et al. 1995; Kraus et al. 2012, for similar figures). The brightness contrast between star and faintest parts shown is 10^5. Gravity darkening is not very pronounced at this wavelength (see Fig. 6), and as well the equator is "back-illuminated" by the disk in this model. *Middle row*: The resulting spectral profile and the interferometric squared visibility and phase for a baseline along the major axis (x-direction), computed for a spectral resolution of $R = 12\,000$. *Lower row*: Percentage of integrated circumstellar flux as a function of distance from the center along the major axis, i.e., as seen by an interferometric instrument, for K-band, Hα, and Brγ. The hatched regions indicate the range from the (smaller) pole-on to (larger) edge-on cases. The *dotted limit* marks 80 % of the total flux, corresponding to the FWHM for a Gaussian shaped emission profile. Figure adapted from Fig. 1 of Faes et al. (2013, computed with HDUST), using their reference model data for Brγ. The inclination angle for panels (**a**)–(**g**) is 45°, for (**h**) and (**i**) 0° to 90°

of the emission) one can tell that helium emission forms very close to the star only, as do doubly ionized metals, while singly ionized metal emission forms relatively far from the star.

Figure 7 shows the regions where line emission originates for Brγ, as a function of projected radial velocity across an optically thick emission line. At zero radial velocity the emission formation region "flips" over the star from the approaching to the receding side of the disk (Fig. 7a). The central depression in the profile is thus caused already by the smaller emitting area at low velocities, and closer to edge-on viewing self-absorption becomes important. The separation of the two emission peaks correlates with the $v \sin i$ of the star and with the size of the emission region

(Hanuschik 1996), but one has to be aware that optical thickness effects, particularly for Hα, affect the correlation parameters (Hummel 1994).

At polar and equatorial inclinations additional effects are seen. For optically thick lines, non-coherent scattering broadening shifts the peaks at polar inclinations and creates a "wine bottle" profile (Hummel 1994), as seen in Hα and Hβ of row A of Fig. 1. At equator-on inclinations, the disk is not only self-absorbing, but veils the star, and narrow and deep absorption lines are formed (row D of Fig. 1). Since the disk is cooler than the star, these are typically lines of hydrogen and singly ionized metals, but in early type Be stars He I can show shell characteristics as well. Because of the detailed characteristics of the "flipping over" of the formation region across the stellar disk, a "central quasi emission" (dubbed QEM or CQE in the literature) can arise in shell lines (Hanuschik 1995; Rivinius et al. 1999; Faes et al. 2013). The usual observables for emission lines include the equivalent width (EW), the peak height above the continuum in units of the continuum (E/C), the full width at half maximum and radial velocity, as well as the height ratio of the two peaks (V/R).

Violet-to-red variations The double-peak emission structure is not always symmetrical. In this case the ratio between the two peaks, V/R, usually varies cyclically. Historically not always the same definition of V/R has been used (e.g., whether the continuum flux should be subtracted, before taking the ratio or not) and, even worse, the definition was sometimes omitted, making a quantitative comparison with more recent data impossible. For new publications, we recommend not only the definition should be clarified, but best the peak heights V and R should be given separately.

2.3.3 Wind emission and absorption

The regions above and below the disk, i.e., viewed at polar latitudes, are more or less equivalent to those surrounding a normal B-type star (see Sect. 5.1.5). The governing processes in this part of a Be star wind are the same as in any radiatively driven stellar wind. At more equatorial latitudes, winds are found at later spectral types than in B stars. This might be due to disk itself, producing shell lines also in the UV, or a possible transition between disk and wind, where disk material might be entrained by the wind. At the densities encountered, the only observable ones are usually ultraviolet resonance lines observed as P Cygni profiles and accessible from space only, most typically C IV and Si IV. From these, wind expansion kinematics and column densities can be derived. The mere presence of these ions in a B-type wind is due to a phenomenon called "superionization", and comes from the intrinsic instability of radiatively driven winds giving rise to shock-induced X-ray emission, which then creates these high ionization levels. For a review, see Puls et al. (2008), and, concerning Be stars in particular, their Sect. 2.2.1 about rotational effects on the wind's latitudinal structure, leading to a polar enhancement of the wind for rapidly rotating B stars.

2.4 Polarization of spectral lines

The most important process for the polarimetry of spectral lines is the depolarization of the continuum polarization (see Sect. 2.2) due to line emission. Emitted line pho-

tons may usually be considered unpolarized,[16] and if line emission rises significantly above the continuum the polarization of the continuum is diluted. The respective path in a Stokes (Q, U) diagram is a linear excursion towards zero intrinsic polarization (Vink et al. 2005; Harrington and Kuhn 2009a). However, observed spectral line signatures of rotating disks are more complicated than that and often show loops in the (Q, U) diagram. This is thought to be partly due to scattering of line photons in the disk, partly due to selective absorption (Wood et al. 1993; Vink et al. 2005), and possibly other effects play a role as well (of which many exist, see for instance Harrington and Kuhn 2009b, and references therein). Obviously, modeling the signature requires a well-understood and complete physical treatment of the radiative line transfer. For this reason, even though the spectropolarimetric signature harbors great diagnostic potential, it has only been little explored beyond toy-models, so far.

Magnetic fields are measured using the circular polarimetric signal, observed in the Stokes V parameter, in spectral lines produced as a consequence of the Zeeman effect.[17] For rapid rotators or weak fields the two most suitable detection methods rely on combining the signal from multiple spectral lines to derive the averaged longitudinal field strength $\langle B_z \rangle$. The Least Squares Deconvolution (LSD) procedure by Donati et al. (1997) bins together selected spectral lines into a single profile and is used with high spectral resolution data. Magnetic configurations with $\langle B_z \rangle = 0$ can be detected with this technique, including, in principle, localized magnetic features (Kochukhov and Sudnik 2013). For instruments with medium resolution (Bagnulo et al. 2002) gave a linear correlation between Stokes V/I and a function of λ, I, and $\mathrm{d}I$, valid under the weak field approximation

$$\frac{V}{I} = \left[-\mathrm{g_{eff}} \mathrm{C}_z \lambda^2 \frac{\mathrm{d}I}{I\,\mathrm{d}\lambda} \right] \times \langle B_z \rangle, \tag{13}$$

where C_z summarizes the physical constants

$$\mathrm{C}_z = \frac{\mathrm{e}}{4\pi\,\mathrm{m_e c^2}} \sim 4.67\,10^{-13}\ \text{Å}^{-1}\,\mathrm{G}^{-1}. \tag{14}$$

Typically an effective Landé factor $\mathrm{g_{eff}} = 1$ is used (Casini and Landi Degl'Innocenti 1994). Since $\langle B_z \rangle$ is measured from the slope of all points $V(\lambda)/I(\lambda)$ when plotted vs. the right-hand side of Eq. (13), this will be referred to as "slope method".

2.5 Quantities observed with high-angular resolution techniques

Interferometrically, Be stars have mainly been investigated with optical long baseline interferometry (OLBI, sometimes the acronym LBOI is used as well), i.e., at wavelengths between about 0.5 and 2.2 μm and with baselines between a few tens and a few 100 meters. Interferometric observations are taken either in integrated light, or spectrally resolved across a spectral line. Technically, the presence of an embedded point source (the star) with significant flux contribution in the continuum at the

[16] Some line processes, such as resonant scattering, will result in polarized line emission.

[17] Magnetic fields produce Stokes Q and U signatures as well, but typically one or two orders of magnitude smaller than Stokes V.

above mentioned wavelengths is a great asset for calibration purposes, and in high-resolution observations allows the use of relative quantities (i.e., with respect to the local continuum). The basic interferometric observables are visibility (fringe contrast) and phase (fringe position). Since the absolute value of the latter is garbled by the atmosphere even in the most favorable conditions, it is either combined to an invariant closure phase over three baselines, or in spectrally resolved observations of spectral lines measured relative to the adjacent continuum. The observables related to the intensity distribution on sky are derived from the Fourier series reproducing this distribution (see, e.g., Petrov et al. 1996, for the principles of differential interferometry). The series can be written as a function of the baseline vector in such a way that even terms contribute to visibility and odd terms to phase (see Appendix B of Lachaume 2003), i.e., the symmetric shape information is in the visibility, the skewness in the phase. The respective first terms in these series, dominating for marginally resolved targets, are representative of overall size and position of the photocenter.

A detailed interferometric study of the central Be star itself has so far only been possible for α Eri. Domiciano de Souza et al. (2012a) demonstrate the power of differential phases across a photospheric line (Brγ) as being more sensitive and going beyond the spatial scales probed by the visibility when determining photocenter shifts. However, in all but the most nearby Be stars the central star is not or only marginally resolved. This means that even if the disk is fully resolved the visibility will not drop below a certain value, given by the flux ratio between disk and star. One has to be careful to make sure whether the assumption of only marginally resolving the target is true for all components of the Be star, when interpreting phases.

Figure 8 illustrates this for the Brγ-line. The data are from Meilland et al.'s (2012) observations of α Ara (B2 V). Panels e and f of Fig. 8 (the latter taken with a baseline parallel to the major axis of the disk) are well comparable to panels f and g of Fig. 7, which were computed for the so-called "astrometric regime" (Lachaume 2003). The data in panels g and h of Fig. 8 were taken only at slightly longer baselines, but the effects of starting to resolve the envelope are clearly visible in the phase signature. In panel a, finally, the circumstellar envelope is strongly resolved in the Brγ line (see, e.g., Faes et al. 2013, for theoretical profiles of resolved Be star disks).

A baseline along the minor disk axis does not produce any phase signature as long as the disk emission is symmetric (for a well resolved disk this requires that it must not be significantly obscured by the star). This is seen in panels b, c, and d of Fig. 8, where the visibility is "U" or "V"-shaped, instead of having a "W"-shape as along the major axis. The phases show a zero phase signature in panel c, where the baseline was almost perfectly aligned with the minor axis, and mirror each other on panels b and d.

Panels h and i of Fig. 7 show the percentage of integrated flux (line + continuum) as a function of distance from the center along the major axis of the disk. This is appropriate for comparison with interferometric measurements using a two-component model (disk + star). The 80 % level corresponds to the flux encircled within the FWHM of a Gaussian disk component. Because the disk is geometrically thin (see Sect. 5.1.5), a dense disk seen edge-on will appear larger (i.e., have larger Gaussian FWHM) to a baseline vector oriented parallel to the equator than the same disk seen pole-on. The hatched areas in the panels h and i bracket these two cases. Such a trend,

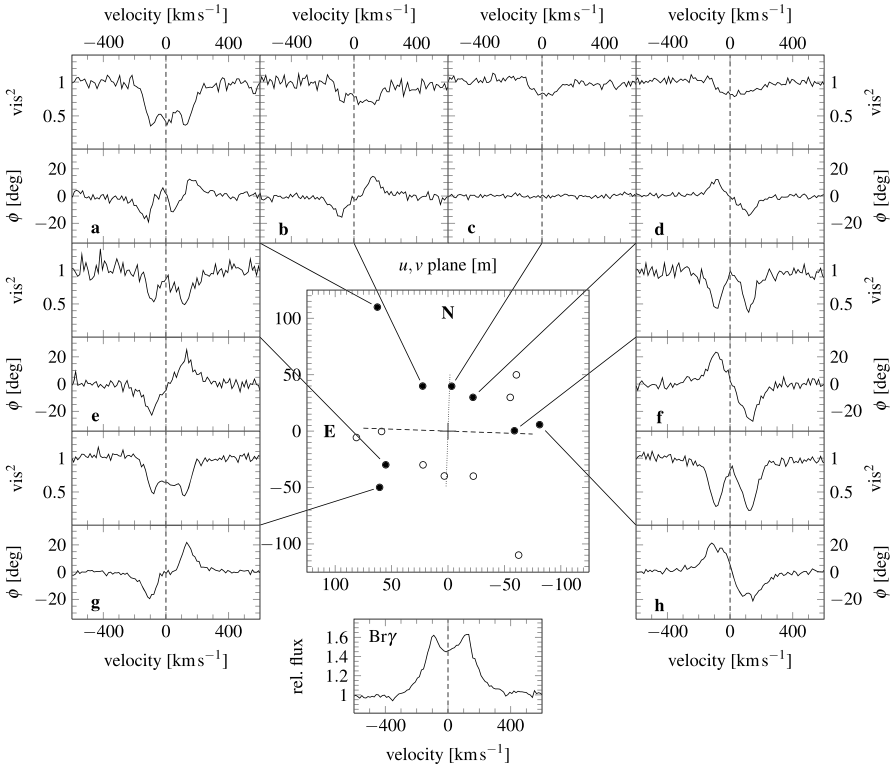

Fig. 8 Spectrointerferometric data of α Ara by Meilland et al. (2012), all taken with AMBER at the VLTI within a few days. The *central panel* shows where in the u, v-plane each dataset is located. Conjugated points, which only differ by an inverted sign of the phase, are shown as *open circles*. The major and minor disk axis orientation according to Meilland et al. (2012) are indicated with a *dashed* and a *dotted line*, respectively. In *all panels* the continuum visibility was normalized to unity, and the continuum phase to zero

shell stars seemingly having larger disks, is indeed seen in Table 2, though not at a statistically significant level with the current data.

Unless many measurements were taken at different baseline lengths and angles, the so-called u, v-coverage, any interpretation of interferometric data strongly relies on assumptions, usually provided by modeling the system (and, therefore, interpretation relies as well on the choice of the model). The most simple, purely geometrical approach without regard of kinematics or radiative transfer is provided by LITpro[18] (Tallon-Bosc et al. 2008). Notable physical models of Be disks are SIMECA (Stee and de Araujo 1994, time-independent, parameterized structure and radiative transfer) and its successor by Delaa et al. (2011), BEDISK (Sigut and Jones 2007, time-independent, partly self-consistent structure, parameterized radiative transfer), and

[18]Strictly speaking LITpro is a tool to reconstruct interferometric observables out of geometric building blocks to reconstruct the on-sky intensity map. Other, similar tools exist, but only LITpro has so far been used for Be stars, to our knowledge.

HDUST (Carciofi and Bjorkman 2006, time-dependent partly self-consistent structure, time-independent self-consistent radiative transfer) and the model developed by Gies et al. (2007) for infrared data.

The photocenter offset in a spectral line, e.g., the disk emission with respect to the adjacent continuum can also be measured by *spectroastrometry*, tracing the position of the spectrum perpendicular to the dispersion. This was done for nearby Be stars with large disks to investigate the disk rotation law (Wheelwright et al. 2012). With a precision of about 0.2 mas this method is reaching a similar range as OLBI proper.

3 Central stars

3.1 Be stars as rapid rotators

Gravity darkening, introduced in Sect. 2.3, affects the determination of the rotational velocity $v \sin i$, and hence W, because the most rapidly rotating part of the star is becoming inconspicuous as $W \gtrsim 0.75$ (see, e.g., Stoeckley 1968; Townsend et al. 2004, as well as the left panel of Fig. 5). Recent interferometric results corroborate this effect, see Fig. 13 of van Belle (2012), who notes that "actual oblateness values are always well in excess of the simple predictions from $v \sin i$". This has effectively reopened the discussion of how close Be stars rotate to the critical limit, and given rise to codes explicitly taking it into account, like BRUCE/KYLIE by Townsend et al. (op. cit.), FASTROT by Frémat et al. (2005), or CHARRON by Domiciano de Souza et al. (2012b).

Further complications in deriving $v \sin i$ are posed by the Be nature itself. In stars with more massive disks additional line absorption in shell stars, as well as possible line emission in Be stars, let the observed profiles attain a narrower appearance. Unfortunately, lines typically used, such as the stronger helium lines or Mg II λ4481, are among the more easily affected. This will bias the derived statistics to slower rotation. A further bias will come from undetected binaries, where the photospheric absorption does not originate in the same component as the Balmer emission. This will not only bias the derived statistics to slower rotation, because an arbitrary companion is more likely to be a slower rotator, but as well to earlier spectral subtypes, which a companion dominating the photospheric flux (i.e., this is actually the primary of such a system) is expected to have for an non-evolved binary.

On the level of individual stars, intrinsically slow rotation has been claimed for some objects. Moujtahid et al. (1998) suggest six such stars; however, Rivinius et al. (2006) discuss these and find the available evidence unconvincing. The slowly rotating star β Cep (B2 III) was for some time thought to be a Be star (Henrichs et al. 2000), but it turned out to be a binary where the observed photospheric spectrum does not originate from the Be star (Schnerr et al. 2006), illustrating an extreme case of the earlier mentioned bias mechanism. Furthermore, based on medium spectral resolution interferometric data, Meilland et al. (2007a) obtained only $W = 0.47$ for

κ CMa (B1.5 IV). Later, however, using high resolution data, Meilland et al. (2012) concluded for $W = 0.75$.[19]

On the other hand, there is evidence for several Be stars to be rotating very close to, maybe even at the critical limit. Most enigmatically, there is α Eri, for which the photospheric flattening was observed to be 1:1.56, i.e., even more than predicted by the Roche approximation for critical rotation (Domiciano de Souza et al. 2003). Considering a pseudo-photosphere contribution from a weak disk (which makes a star look more flattened than it actually is), present at the time of observing, Carciofi et al. (2008) derive a rotation of $W \geq 0.90$, and more recently Domiciano de Souza et al. (2012a) obtained $W = 0.94 \pm 0.04$. This is the most direct measurement of the rotational properties of a Be star to date. More indirect evidence for rotation close to the critical limit comes from several stars which are binaries with evolved companions (see Sect. 6.3). Due to their mass-transfer history, they must have been spun up. Asteroseismic (see, e.g., Cameron et al. 2008) as well as some interferometric (Stee et al. 2012, 2013) results also indicate a very close to critical rotation.

However, it must be kept in mind that rapidly rotating B stars exist that are not Be stars. α Leo (B8 IV) has been observed interferometrically to rotate at $W = 0.81$ (McAlister et al. 2005), and the entire spectral class of Bn stars, about as numerous as the Be stars in a magnitude limited sample, such as the Bright Star Catalog (Hoffleit and Jaschek 1991), is defined as rapidly rotating B stars (seen equatorially, hence the "*n*", signifying shallow, very broadened lines) but not showing Balmer emission. A close investigation of the class properties of Bn stars has not yet been undertaken, unfortunately.

Statistical studies of the rotation, relying on deconvolving of $\sin i$ from the measured $v \sin i$, such as Chauville et al. (2001), point quite homogeneously to a mean value of $\overline{W} = 0.75$ with a rather small intrinsic scatter of the same order as the observational uncertainty. Townsend et al. (2004) pointed out that this might not be the true average, however; it could as well indicate an upper detection threshold for $v \sin i$ at about 75 to 80 % critical rotation. This has prompted a number of new studies on the matter. Cranmer (2005) undertook a thorough statistical analysis. At variance with most other studies, Cranmer derived a very strong dependence of $\overline{W}$ on spectral type, increasing from $\overline{W} = 0.46$ for the earliest to $\overline{W} = 0.93$ for the latest Be stars. However, Cranmer used, as input data, the catalog data of 462 Be stars tabulated by Yudin (2001), and as discussed by Howarth (2007), this catalog shows systematic differences in $v \sin i$ vs. other sources, and neither is it homogeneous in itself. McSwain et al. (2008) investigated 16 Be stars in NGC 3766, all of intermediate $T_{\rm eff}$ for B stars, and derive that the rotational velocities in their sample is consistent with $0.63 < W < 0.74$.

Frémat et al. (2005) used the input spectra of Chauville et al. (2001) for 130 stars, and applied their own code, FASTROT, fitting all five parameters to determine a rapidly rotating star simultaneously. Finding $W = 0.68$ as the "most likely value" of W for a Be star (i.e., the median of W, not $\overline{W}$), their conclusions do not differ

[19] Here and below we make use of Eqs. (7), (8), and (11) to convert the literature values, typically listed as ω or Υ, to W. The uncertainties in estimating $v_{\rm crit}$ and $v_{\rm orb}$ are equivalent to each other, as long as the Roche approximation is used.

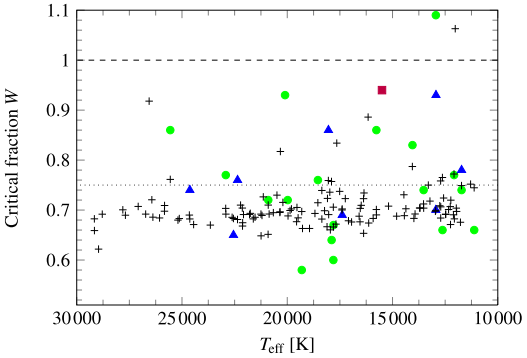

Fig. 9 Rotational rates W for Be stars derived with FASTROT modeling (Frémat et al. 2005, + signs), direct interferometric imaging (Domiciano de Souza et al. 2012a, α Eri, purple square), by determining the inclination angle interferometrically (Meilland et al. 2012, blue triangles), and by assuming $\sin i = 1$ for shell stars (Rivinius et al. 2006, green disks)

very much from Chauville et al., not finding any trend with either $T_{\rm eff}$ or $\log g$. Unfortunately, a close inspection of the data reveals some potential problems, e.g., in a histogram of the derived inclination the bin $i > 80°$ is almost empty, even known shell stars being assigned partly much lower inclinations. Given the fairly subtle effects in the spectrum to distinguish between a star rotating intrinsically at $W = 0.75$ and a star rotating at $W > 0.75$, it is unlikely that such a method would be able to determine inclinations with a typical uncertainty of less than 3°, as quoted by Frémat et al. (op. cit.). Since, however, all five parameters are derived in one simultaneous step, this may cast some doubt on the other four. The very small scatter of W computed from Table 9 of Frémat et al. (2005, see + signs in Fig. 9), being smaller than the average uncertainty by a factor of about 2, is somewhat surprising indeed.

Rivinius et al. (2006) restricted themselves to 26 shell stars, thereby avoiding the problem of $\sin i$, since $\sin i \approx 1$ for shell stars. Without considering gravity darkening, they get $\overline{W} = 0.75 \pm 0.14$ and consider it as a lower limit, well in agreement with Townsend et al. (2004), and no significant trend with $T_{\rm eff}$. Meilland et al. (2012) use a similar approach, in that they determine the inclination interferometrically (using the disk as proxy), and then use $v \sin i$ and $v_{\rm crit}$ from Frémat et al. (2005) to derive W. They obtain $\overline{W} = 0.76$, also without a trend over $T_{\rm eff}$ (see Fig. 9).

The method applied by Ekström et al. (2008) differs, as they compare the actual incidence of Be stars with rotational evolution of a synthetic sample. According to this test, which discards any contribution to rotation by spin-up through binary evolution, in order to explain the observed number of Be stars, B stars must be able to become Be stars if they rotate at and above $W = 0.62$.

Huang et al. (2010), using observational data from open clusters, approach the problem from the B star side, and identify the highest W observed in the distribution of non-Be stars. They obtain $W \leq 0.93$ for late-type B stars ($M_\star < 4$ M$_\odot$), dropping to $W \leq 0.56$ for $M_\star > 8.6$ M$_\odot$. This does not exclude Be stars at lower W, but non-Be stars at higher values.

Not including the study by Cranmer (2005) due to problems with the input data, as discussed above, the key properties of Be star rotation can be summarized as follows.

1. The measured $\overline{W}$ for Be stars is around 0.8. The distribution is quite narrow, of the order of the observational uncertainty, and does not depend on temperature or effective gravity.
2. Given the effect pointed out by Townsend et al. (2004), some of these must rotate more rapidly. How many Be stars are affected by this bias is unknown, but likely not all, as, for instance, it would be difficult to explain the incidence of Be stars with only critical rotators (Ekström et al. 2008).
3. The minimum W for a B star to become a Be star is around 0.7. As $\overline{W}$ is invariant with $T_{\rm eff}$, this minimum cannot strongly depend on temperature, either.
4. At least for Be stars observed in open clusters, there is a value of W above which all B stars become Be stars, which *does* depend on temperature, and that increases from about 0.64 to about 0.95 as the $T_{\rm eff}$ of the star decreases.

Combining points 3 and 4 suggests that the mechanism forming Be stars in early B subtypes must be close to 100 % efficiency already at low W, since an early B star at and above the minimum W in almost all cases becomes a Be star, so that there cannot be many "failed attempts". In late subtypes, however, such "failures" are more common, as otherwise no, or almost no, plain B stars could be observed at such high W as 0.93. Indeed many of the Bn stars are late-type B stars; for instance α Leo, discussed above, is of type B8 IVn. The processes contributing to the Be-phenomenon (see Sect. 4) are possibly stronger, and/or more numerous for early-type Be stars than they are for late-type ones.

The works by Ekström et al. (2008) and Granada et al. (2013) investigated the angular momentum evolution of B stars and their link to Be stars. In particular, a B star that starts its life with an already high W will inevitably hit the critical limit later during its main sequence life, and from then on, at the latest, must get rid of the excess angular momentum. This provides predictions for the minimum mass- and angular momentum loss rates and, as discussed above, constraints on Be star statistics.

3.2 Pulsating Be stars

A major question debated in the last three decades has been whether the variability with periods between 0.5 and 2 d is due to pulsation, or due to rotation (see Porter and Rivinius 2003, and references therein). Rivinius et al. (2003) argued that in most early-type Be stars the observed variability is due to low non-radial order g-mode pulsation, with grouped multiperiodicity including modes with higher mode number ℓ observed in some stars.

A breakthrough was brought about by photometric satellite missions, fueling recent advances in asteroseismology in general (Aerts et al. 2010). Multiperiodicity of Be stars is now routinely observed. Walker et al. (2005) were the first to report multiperiodicity from space observations, in the Oe star ζ Oph (O9.5 V). Some of the periods could as well be identified in spectroscopy. Walker et al. (2005) suggested the designation SPBe stars for such pulsators; however, as it is becoming increasingly clear that all Be stars fit into that class, a separate designation is probably not necessary. Saio et al. (2007) were the first to discover low amplitude (≈1 mmag) pulsation in a late-type Be star, the B8 Ve star β CMi. See Table 1 for an overview of the stars

Table 1 Multiperiodic Be stars found by space-based photometry

Star	Sp. type	Frequencies [c/d]	Mode types	References
ζ Oph	O9.5 Ve	1.2 to 19.1	high-ℓ p-modes	a
HD 51452	B0 IVe	≈1.5 to 4.5	p-modes & g-modes	b
		0 to ≈1.5	gi-modes	b
HD 49330	B0.5 IVe	0.87, 1.47, 2, 2.94	low-ℓ g-modes	c
		11.86, 16.89	high-ℓ p-modes	c
HD 127756	B1/2 Vne	0.03	retrograde r-modes?	d
		1, 2	prograde g-modes	d
HD 51193	B1.5 IV	0.72, 1.4, 2.6	pulsation	e
CoRoT 102719279	B2.5 e	0.9, 1.1, 2.3	pulsation	f
HD 217543	B3 Vpe	0.03	unexplained	c
		1.7, 3.7	prograde g-modes	c
α Eri	B3 Vpe	0.775	pulsation	g
		0.725	orbital variation	g
HD 163868	B5 Ve	≈0.01	retrograde r-modes?	h, i
		1.6, 3.3	low-ℓ prograde g-modes	h
		1.6, 3.3	retrograde g-modes	i
HD 181231	B5 IVe	0.62, 0.7, 1.25	low-ℓ g-modes	j
CoRoT 102761769	B5–6 IV–Ve	2.45	pulsation	k
β CMi	B8 Ve	3.3	low-ℓ g-modes	l
HD 50209	B8 IVe	0.1, 0.8, 1.5, 2.2	low-ℓ g-modes	m
HD 175869	B8 IIIe	0.64	rotational?	m
		1.3	g-mode	n
KIC 6954726	–	0.1, 0.9, 1.027, 1.7	inconclusive	o

[a]Walker et al. (2005), [b]Neiner et al. (2012a), [c]Huat et al. (2009), [d]Cameron et al. (2008), [e]Gutiérrez-Soto et al. (2011), [f]Gutiérrez-Soto et al. (2010), [g]Goss et al. (2011), [h]Walker et al. (2005), [i]Savonije (2007), [j]Neiner et al. (2009), [k]Emilio et al. (2010), [l]Saio et al. (2007), [m]Diago et al. (2009a), [n]Gutiérrez-Soto et al. (2009), [o]Balona et al. (2011)

analyzed so far. New ground-based results point in the same direction (e.g., Uytterhoeven et al. 2007; Gutiérrez-Soto et al. 2007; Levenhagen et al. 2011, for V2104 Cyg, B6 V, NW Ser, B2.5 III, and V1446 Aql, B2 IV and λ Pav, B1 V, respectively). Analyzing 18 Be stars in the first CoRoT exoplanet field, Semaan et al. (2011) find that "generally the frequency spectrum shows a forest of frequencies around one or two main frequencies as well as several isolated frequencies." Semaan (2012) gives a detailed light-curve analysis of 15 Be stars observed with CoRoT, all of which are reported as multiperiodic pulsators.

Be star light curves have sometimes been reported as of double- or even triple-wave (Cuypers et al. 1989; Balona et al. 1992), which was often interpreted as supporting evidence of a rotational nature. The light curves of HD 50209 (B8 IV, Fig. 4 of Diago et al. 2009a) and HD 181231 (B5 IV, Figs. 1 and 8 of Neiner et al. 2009) are good examples how the multiperiodicity of Be stars can produce such an appearance through its frequency groupings.

Only early-type Be stars pulsate strongly enough to be detected from the ground. Nevertheless, pulsation extends to late-type Be stars, though with smaller amplitudes. It is interesting to note that *all* Be stars, regardless of spectral subtype, that were analyzed with high-cadence, long duration space-based photometry data have been reported to be multiperiodic and to pulsate. About half of these are nearby, prominent and well investigated Be stars (Table 1), the other half is basically drawn from a magnitude limited sample, namely the Be stars in the CoRoT target fields (Semaan 2012). Given that this is currently the most sensitive and best developed technique to study pulsation, this backs the claim that Be stars are non-radially pulsating stars in general, at least in the Milky Way (see Sect. 7.2.4 and Table 3 for other galaxies).

Be stars are not alone as pulsating stars in their region of the Hertzsprung–Russell diagram. Plain B stars have been found to pulsate in the entire range. However, non-pulsating normal B stars, even as early as B0.5 IV, exist as well (e.g., Pápics et al. 2011, with a detection threshold in the mmag regime). The rotation might be responsible for the pulsation in some way, so that it is not specific to Be stars, but again, in order to investigate this, a similar study on Bn stars is yet to be carried out.

Looking at the various types of variation seen in the stars listed in Table 1, one can sort the variability into a number of types:

1. In the earliest Be stars, down to about B3, β Cep-type pulsation can be present, i.e., high-ℓ p-modes (after the restoring force, pressure) driven by the κ mechanism, acting on the iron (Fe III) opacity bump.
2. All over the Be range, periods with about 0.5 to 2 d are found, for which different mechanisms have been proposed:
   (a) Low-ℓ g-modes (after the restoring force, gravity), likely of high radial order n. Asteroseismic modeling points to *prograde* $m = -1$ and higher modes (see references in Table 1), while from spectroscopic modeling *retrograde* $m = +2$ and higher modes are favored (Rivinius et al. 2003, it should be noted, however, that Rossby waves were not considered there). Like the β Cep-type pulsation, these are driven by the κ mechanism, but for g-modes the mechanism would not set in earlier than about B2 (see Fig. 1 of Saio 2013).
   (b) A variant type of Rossby waves (r-modes) has been suggested, taking into account the rapid rotation. The modes are driven by the interplay of buoyancy due to the κ mechanism exciting normal g-modes and the Coriolis force (called "mixed modes" by Townsend 2005, "quasi g-modes", q-modes, by Savonije 2005, and "gravito-inertial", gi-modes by Ballot et al. 2010). For stars of a type too early to excite these modes via the κ mechanism, Neiner et al. (2012a) have proposed an excitation through convection, which may explain such long periods in these early Be stars. The result of Mathis et al. (2013) shows that the resulting amplitudes indeed grow with rotation.
   (c) In some stars one of the observed frequencies seems to be rotational. However, this has not yet been confirmed by spectroscopy, which would be particularly important since rotation can only provide the clock, but the actual variability mechanism remains to be identified (but see below for a candidate process, namely small-scale magnetic fields). For instance, in ω Ori (B3 III , Neiner et al. 2003, 2012b) a persistent period of 1.37 days was found in UV and optical spectroscopy. Similarly, for the suggested rotational period of 1.21 d

in γ Cas, Henry and Smith (2012) report variable shape and amplitude of the light curve over 15 years, but a single, stable period.

3. Very low frequencies are eventually seen. Whether these are really photospheric, in which case they might be retrograde r-modes (i.e., Rossby waves), or rather reside in the circumstellar disk, is unclear. Such cycle time scales seem, e.g., to reside in the line emission region of the binary δ Sco (B0.2 IV), where for a few years a 60 d cycle was present (Jones et al. 2013). In ω CMa, additional variability with a mean cycle length of 20–25 d (Štefl et al. 2003a) becomes observable at times of outburst in emission lines, but not in photospheric ones.
4. During outburst, in particular, additional frequencies arise at similar values as the persistent g-modes mentioned above (Huat et al. 2009; Balona 2013). Again, such a behavior was first found in spectroscopy (Štefl et al. 1998, and references therein), but became much clearer with the advent of space-based photometry. This and the previous point will be discussed in detail in Sect. 4.

3.3 Be stars and magnetic fields

No magnetic field has been reliably detected in any Be star. In fact, the magnetic field detections which have been published for Be stars are all close to the 3σ-limit, and independent confirmation is important. Such detections, based on both techniques described in Sect. 2.4, were published for ω Ori (B3 III, Neiner et al. 2003, using LSD), for 27 CMa (B3 III) and χ Oph (B2 V, Hubrig et al. 2007, slope method), and for μ Cen (B2 V), o Aqr (B7 IV), ε Tuc (B9 IV), and HD 62367 (B9, Hubrig et al. 2009, slope method). Independent observations in order to test these claims were obtained for four stars. For ω Ori and μ Cen, these gave negative results (Neiner et al. 2012b; Wade and Grunhut 2012), while for χ Oph (Silvester et al. 2009) and HD 62367 (Wade priv. comm., 2013) as well no field was detected, but the precision required to confirm the claimed fields was not reached for these two objects. For a while, β Cep was as well listed as magnetic Be star (Henrichs et al. 2000), however, as said above it is a binary: The magnetic star is one and the Be star the other component (Schnerr et al. 2006).

All circular polarimetric data analyzed with the slope method so far have been taken with the FORS1/2 instruments at the VLT (for which the method was devised). Bagnulo et al. (2012) undertook a re-reduction of all archival data, and came to the conclusion that detections not well above the 3σ-limit are not entirely trustworthy. In particular for Be stars, they note that "most if not all of the detections ... are probably spurious, and that magnetic fields much above [a $\langle B_z \rangle$ of] 100 G rarely if ever occur in classical Be stars".

In that context, the "Magnetism in Massive Stars" (MiMeS) project dedicated a part of its Survey Component to classical Be stars. While in all other target subcategories positive magnetic field detections were made with an incidence of 5–10 %, not a single magnetic field was found in the about 100 observed Be stars (see, e.g., Wade and Grunhut 2012, final publications by the MiMeS group are in preparation). The MiMeS sample includes Be stars with projected rotational velocities as high as 350 km/s, as well as those with low projected rotational velocity, in which a Zeeman signature would be fairly easy to detect, even if the star itself is a rapid rotator. This

not only confirms the conclusion of the FORS re-reduction, but excludes the presence of *large-scale*, organized surface fields stronger than ∼250 G in about one-half of the sample (Wade and Grunhut priv. comm., 2013). Neither did MiMeS find any observational evidence for *small-scale* magnetic fields (which can have $\langle B_z \rangle = 0$ G across the stellar disk, e.g., for localized loops), but because of the multitude of possible geometries it is much harder to give a numerical upper limit. Adopting the random magnetic spot formalism of Kochukhov and Sudnik (2013) the typical MiMeS Be star observations conservatively rule out spots with angular radii of 20° or larger, and fields of 500 G or stronger, for a filling factor of 0.5 (Grunhut and Wade priv. comm., 2013).

Although there is no direct observational evidence for small-scale magnetic fields in classical Be stars, indirect evidence has been reported. It comes mainly from observations of small-scale and rapid line profile variability in the visual regime (e.g., Smith et al. 1996), flux and line profile variations in the ultraviolet regime (e.g., Smith 2006), and X-ray flux variations (e.g., Smith and Robinson 1999), which are all related to each other (e.g., Robinson et al. 2002). All these observations point to the transient presence of circumstellar plasma heated to well above photospheric temperatures, of which magnetic fields (which could be created, e.g., by subsurface convection, see Cantiello and Braithwaite 2011) are one possible origin.

In this context, γ Cas (B0.5 IV), as one of the best-studied Be stars, has proven to be a rather unique case (and thus far from being the archetype it was often considered). It has hard, thermal X-ray emission, which is variable on all observed time scales, including short-lived flaring. This distinct behavior has prompted the postulation of a distinct group of γ Cas-analogues, by now consisting of ten members, including one Oe star (see, Smith et al. 2012b; Rauw et al. 2013, for a list). The emitting plasma seems to be associated with the Be star, rather than with a potential secondary (Smith et al. 2012b; Torrejón et al. 2012). Together with the correlated UV variations this is interpreted as evidence for magnetic star–disk interaction (Smith et al. 2012a) as the cause for the heated plasma, although a disk intrinsic magnetic field, i.e., not connecting to the star, is a possibility as well.

4 The star-disk connection

Neither the properties of the central stars themselves, nor the physical mechanisms in the disks are unique to Be stars, except possibly in their combinations. This is different for the connection between star and disk, and the name "Be-phenomenon" has been used to designate the still largely unknown physics of the actual mechanism that expels the material from the star with properties suited to form a Keplerian disk. What may have been seen in the past as an artificial separation has now been observationally verified: The mechanisms that feed the disk are different from the mechanism that makes the disk grow. In other words, once material is ejected and orbits the star, its fate is governed by an entirely different physics, and all memory on the process that brought it there is lost. This also happens in accretion disks of young stellar objects, once the accreting material crosses the so-called "X point", which decouples

the inner magnetic field from the Keplerian disk (Papaloizou and Lin 1995). Differently than an accretion disk, however, a viscous decretion disk has no inner radius other than the stellar surface (see Sect. 5.3).

4.1 Mass and angular momentum transport

A circumstellar decretion disk will not persist unless its inner boundary is constantly supplied with angular momentum to prevent re-accretion (Sect. 5.4). Since most Be stars likely do not rotate critically, a mechanism in addition to rotation is needed for this. The intrinsic rotational velocity distribution provides a strong constraint for any such mechanism: it defines the order of magnitude of the problem. For instance, at $W = 0.75$, an excess velocity of the order of 100 $\mathrm{km\,s^{-1}}$ is needed to bring material into a Keplerian orbit for main sequence B star parameters, while close to $W = 1$ already the photospheric turbulence will be sufficient for some particles to enter orbit. The fact that Be star disks may dissipate and form anew over relatively short time scales, much shorter than any evolution time scale of the central star, points to a mechanism that is capable of switching on and off. An important point was made by Kroll (1995, see also Kroll and Hanuschik 1997), who explored smooth particle hydrodynamic simulations of localized mass ejections: It is not necessary that all the ejected material has the right kinematic properties to form a Keplerian disk. Even in an un-directional, spherical ejection a "kinematic filter" will naturally act to select the particles with the right parameters to remain in orbit, as the others will either fall back or escape.

Finally, a constraint is posed by the realization that the circumstellar disks are Keplerian (i.e., subject to a $1/r$ potential, as is shown later by the explanation of V/R-variations, in Sect. 5.3.2) and governed by viscosity. This means that whatever mechanism puts the material in orbit, it must not act strongly on the material that already is in orbit, as otherwise the settling into a Keplerian disk, i.e., a disk free of external forces besides gravity, would be prevented.

4.1.1 Pulsation

Pulsation has been suggested early on to be responsible for the Be-phenomenon (Baade 1988). However, pulsational velocities are restricted to the order of magnitude of the sound speed ($\approx$20 $\mathrm{km\,s^{-1}}$); much larger velocities—or to be precise, larger local velocity differentials—would create supersonic turbulence and be damped quickly, the damping details depending on the mode type. Rivinius et al. (1998b) observed that for the multiperiodic Be star μ Cen (B2 V), at times of constructive interference of the pulsational velocity fields, mass was ejected into the circumstellar environment. Then the overall amplitude can well exceed the sound speed for some time. In the particular case of μ Cen, the interfering modes are of identical mode numbers ℓ and m, differing in the number of radial nodes n only. This means that the surface velocity fields are of identical structure, so that in constructive interference the velocities co-add on the entire surface. Superposition of modes with different ℓ and m is likely much less efficient to temporarily enhance the mass loss. Indeed, although most Be stars seem multiperiodic (see above), it is clear from spectroscopy that multiple periods with identical mode numbers and comparably high

pulsational amplitudes are uncommon (Rivinius et al. 2003). However, some correlation between photometric pulsation amplitude and circumstellar activity has as well been observed in some stars not showing such superposition.

Goss et al. (2011), for instance, report observations of α Eri (B3 V) showing such behavior. There are only two frequencies, out of which one is well known to be pulsational from ground-based spectra (0.775 c/d, see, e.g., Rivinius et al. 2003). This frequency is stable in value and phase, i.e., it is long-term coherent. The second frequency, 0.725 c/d, is not, it varies in frequency from 0.69 to 0.73 in various seasons, and is incoherent in phase over a longer time. Both frequencies rose in strength 2005 to 2007, which according to spectroscopy coincides with an emission-line phase (e.g., Carciofi et al. 2008). In CoRoT 102719279, a shell star, fadings supposedly caused by newly ejected matter are preceded by a strong amplitude increase of the periodic variations (Gutiérrez-Soto et al. 2010), which is also similar to what has been observed in μ Cen. In HD49330 the observed strength of short period p-modes decreased, while additional longer, transient periods arose during outburst. Huat et al. (2009) interpret those as g-modes. However, other scenarios are conceivable as well (see below).

One more example of interdependency between the circumstellar activity and the stellar pulsation was seen in ω CMa (B2 IV). Štefl et al. (2003b, their Fig. 8) report a single, very stable and coherent pulsation period over several years of disk dissipation. After the next outburst, however, the phase of the pulsation period is suddenly advanced by $\Delta\phi = -0.2$. The behavior could then be traced back several outbursts. Whether pulsation here is cause or consequence is unclear, but in any case the phase lag is a constraint to be explained by a mass-ejection theory.

Theoretically, the ability of linear non-radial pulsation (i.e., not taking into account possible multi-mode beating effects driving the amplitude temporarily well beyond the usual limits) to eject material seems insufficient to form a Be star disk. The pulsational amplitudes are not high enough (Owocki 2006), and works where pulsation is shown to achieve the task (Cranmer 2009) seem to be based on rather optimistic assumptions.

Retrograde modes, as spectroscopic modeling indicates, would as well be a problem. In retrograde modes the part of the wave associated with the maximal prograde particle velocity turns out to be a density minimum, and retrograde modes tend to remove angular momentum from the uppermost atmosphere layers, if they are excited in the star and damped in the atmosphere (see, e.g., Townsend 2007). It should be noted, however, that "mixed modes"/gi-modes (see Sect. 3.2) can have a retrograde phase but a prograde group velocity (see, e.g., Townsend 2005), which would solve the problem. Rogers et al. (2013) have modeled such modes as internal gravity waves, transporting angular momentum upwards. Neiner et al. (2013) suggest that such a mechanism was observed in HD 49330, where, when enough angular momentum has accumulated in the surface layers, transient g-modes were triggered, driving the outburst and at the same time suppressing the p-modes. A variable surface angular momentum at the equator was possibly observed in Achernar (Rivinius et al. 2013). While the variation is correlated with the circumstellar activity, the causal relation between the two needs further scrutinization.

4.1.2 Magnetic fields

Magnetic fields can provide angular momentum to the circumstellar domain in a very straightforward way, just by leverage. The most mature theoretical approach to magnetic fields as an ingredient to Be stars is that of the magnetically torqued disk (MTD) (e.g., Cassinelli et al. 2002; Brown et al. 2004, 2008). Assuming a rotation at about 80 % of the critical velocity (see above), one can estimate from Fig. 9 of Cassinelli et al. (2002) a minimum required "average surface field" for a magnetically torqued disk to be above 1 kG for a B0 star, about 300 G for a B2 star, and a few tens of Gauss for a B9 star. Although the "average surface field" is not exactly the usually measured quantity of $\langle B_z \rangle$, for practical purposes they are of the same order of magnitude. Maheswaran (2003), using a somewhat different method of angular momentum transport, derives only about one tenth of the field strength necessary to form a Keplerian disk.

However, the MTD faces some difficulties. For one, the field properties and the rotation rate in this model cannot be fully independent of each other, since the release radius for the torque to produce a Keplerian disk must neither be too small, as the material would fall back, nor can it be too large, as the released material would escape from the system. Secondly, it would require a relatively sharp transition from a field-governed region to a completely field-free region, as a Keplerian disk needs to be largely free from external forces (apart from gravity) in order to form. Indeed, magneto-hydrodynamic (MHD) modeling fails to produce a Keplerian disk by magnetic torquing, even with parameters expected to be optimally suited for the task (see Figs. 1 and 2 of Owocki 2006 and ud Doula et al. 2008). Brown et al. (2008) thus suggested a transition region between the magnetically governed inner and a Keplerian outer disk region, where the transition is controlled by an increase of viscous effects, similar to the "X point" in accretion disks. However, while an X point necessarily forms in accretion disks, as the increasing inner disk density forces such a point to emerge against the magnetic field, it is not clear why such a point should be stable or even form in a decretion disk. Moreover, as is seen from Sect. 3.3, magnetic fields of sufficient strength to produce a MTD, at least in the form originally proposed by Cassinelli et al. (2002), are observationally ruled out.

For small-scale magnetic fields only indirect evidence has been reported. In particular in stars with anomalous flaring X-ray activity, however, such fields may provide an opportunity to lift material into the circumstellar domain, where upon release at least some part of the material will have kinematical properties appropriate to end in Keplerian orbits.

4.1.3 Other mechanisms

Binarity has as well been proposed to be responsible for the Be-phenomenon (e.g., Kříž and Harmanec 1975), but statistical arguments on Be binarity continue to speak against it as a widespread mechanism (Abt and Levy 1978; Oudmaijer and Parr 2010), and as pointed out in Sect. 1.1.1 classical Be stars with Roche lobe filling companions are not known to exist. Theoretical work dedicated to binary driven disk formation came to the conclusion that also there a rotation rate very close to critical is required (Harmanec et al. 2002a; Bisikalo et al. 2006). The mechanism suggested acts by

tidal forces, lowering the effective gravity on the Be star equator at the point towards the companion to zero or below. However, at the required very high W other weak mechanisms, such as single pulsation, are effective as well.

The highly eccentric binary δ Sco (B0.2 IV) was for some time considered an example for binary driven disk formation during periastron. However, upon closer investigation, it turned out the disk was already present before the periastron (Miroshnichenko et al. 2001), and its rotational direction is not aligned with the binary orbital plane, and possibly even counter-aligned (Štefl et al. 2012b; Che et al. 2012).

The wind-compressed disk model (WCD, Bjorkman and Cassinelli 1993) was the first dynamical physical model of Be star-disk formation, providing clear falsifiable predictions. Unfortunately, theoretical work including second order effects did not confirm the WCD mechanism (Owocki et al. 1996). In addition, the WCD naturally formed an angular momentum conserving disk, which was later ruled out by observations. Notwithstanding the falsification, much of the new theoretical work on disks and disk formation reported in this review was triggered by the WCD one way or the other, and it certainly deserves to be called a ground-breaking work for the field of Be stars.

4.2 Observations of actual mass transfer

In ω CMa, Štefl et al. (2003a) investigated the 1996 and 2001/2 outbursts vs. the photometric quiescent state. They found a *red-shifted persistent* absorption at a velocity of about $+2 \times v \sin i$ in He I and Mg II lines, which was present during the outbursts, but not in the quiescent state. It is noteworthy that ω CMa is considered a pole-on Be star. This means that the region against which the absorption forms would have to be either the stellar pole, meaning material falling back to the star, or the disk continuum, that forms within about the first stellar radius of the disk. In the latter case the material would be fed into the disk from above, similarly to the original WCD scenario.

Another important observation was made of μ Cen by Peters (1986), and later the same phenomenon was re-observed by Rivinius et al. (1998a). During outbursts, they observed distinct and very short-lived *blue-shifted transient* absorption components (up to $\approx -2 \times v \sin i$) in the same lines. μ Cen is seen only somewhat more equatorial than ω CMa. The question is, therefore, whether this is really the aspect dependency of one and the same process acting in two stars, or rather two different processes. Given that μ Cen shows multiperiodically triggered relatively weak outbursts every few weeks, while ω CMa has a single strong pulsation period and a strong outburst every few years only, the latter is well possible.

It is quite possible that the observations of the γ Cas-analogues introduced in Sect. 3.3 also are observations of mass-transfer events into the disk. However, this connection has not been firmly established and remains speculative.

4.3 The disk behavior during outburst

While some Be stars have never shown any strong variability of the emission, in most the disks are replenished, at least partly, by outburst events, in which the disk

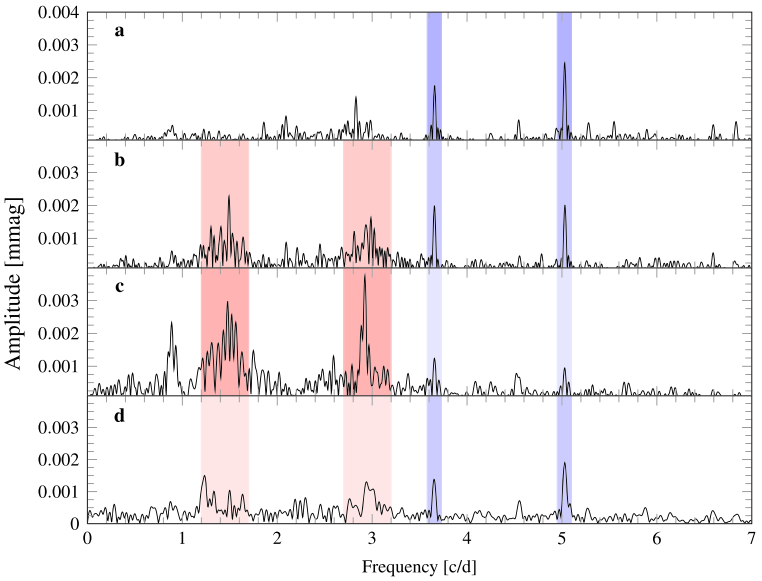

Fig. 10 The cyclic photometric variability of HD 49330. In quiescence (**a**) it shows narrow and persistent pulsation frequency peaks (examples underlaid in *blue*, the one at $f \approx 5$ c/d is actually an alias of a higher p-mode frequency), while in outburst (**b** and **c**) additional transient frequencies and their harmonics arise (groups underlaid in *red*) and the persistent frequencies weaken. As the outburst ceases, the frequency spectrum returns to the quiescence appearance (**d**). Adapted from Huat et al. (2009)

emission and polarization rises steeply, signifying a density increase in the innermost parts. While actual observations of the mass transfer are rare (see above), and their interpretation is debated, these events do have a repercussion on the disk that is much more frequently observed.

Carciofi et al. (2007) reported such a behavior in polarimetry: very short-term changes of the polarization degree of some 0.01 percent and polarization angle by a few degree of α Eri, were interpreted as due to mass ejections creating transient azimuthal asymmetries orbiting the star.

With respect to point 4 in the list in Sect. 3.2, HD 49330 (B0.5 IV, Huat et al. 2009) deserves closer inspection: HD 49330 was observed from relative quiescence through an outburst and back (See Fig. 1 of Floquet et al. 2009 and Figs. 4 and 5 of Huat et al. 2009). The frequencies form two morphological groups: Some are present over the entire time span, and with narrow frequency peaks. These are interpreted as β Cep p-modes and weaken during the outburst. Others are undetectable before and after outburst, but *strong in outburst* (around 1.47 c/d, 2.94 c/d). The Fourier peaks for these frequencies are wider and less well defined than those for the other frequencies (see Fig. 10). Instead of ascribing these frequencies to temporary g-modes, as Huat et al. (2009) do, Balona (2013) suggests a circumstellar origin, an ensemble of short-lived, transient cyclic events, like the ones known from spectroscopy to accompany outbursts (Štefl et al. 1998; Rivinius et al. 1998a). These would likely be caused by locally ejected matter not yet circularized. In Balona's picture, these would temporar-

ily veil the photosphere, and thus only the observable amplitude of the photospheric modes weaken, their actual strength unaffected.

An outburst can indeed alter the observational properties of the pulsation. Spectroscopic observations of ω CMa show, for the same photospheric period, a different line profile variability pattern in outburst than in quiescence. The differences are more pronounced for lines with stronger circumstellar contribution (see Fig. 9 of Štefl et al. 2003b). Maintz et al. (2003) model this as an effect of a significantly puffed up disk (up to stellar latitudes of 40°) veiling the photosphere. However, while the pattern is more or less reproduced, the amplitude is not at all, being stronger in outburst, rather than weaker as predicted by the model. Regardless whether there is a puffed up disk or not, this makes it plausible that part of this variability is intrinsic to the disk.

Finally, medium-term cyclic light variations on the scale of dozens of days and with an amplitude of few tenths of a magnitude are sometimes observed in outbursts. The best known case is again in ω CMa, where Štefl et al. (2003a) report 12–25 d cycles anticorrelated in photometry and emission-line strength. This is observed only in the photometric "high state", i.e., during active mass transfer between star and disk. The mechanism of this variability is unknown, but given the formation process of the photometric signature (see Sect. 2.1), it must be linked to the innermost parts of the disk. Similar observations of the binary δ Sco, however, with a cycle time of 60–100 d, were made outside the time of mass transfer, judging from the overall light curve (Jones et al. 2013). It is, therefore, possible that such variations are not or only loosely related to outbursts.

5 Be star disks

The term "classical Be star" is now inextricable from the idea of a circumstellar disk. This section reviews the observational clues that established that the circumstellar environment of Be stars is a flattened, disk-like, structure, and provided both a qualitative and quantitative confirmation of the schematic view shown in Fig. 1. With very few exceptions (see, e.g., Sect. 5 of Nemravová et al. 2010), the presence of a disk has become the generally accepted view, and all models currently used to reproduce/predict Be star observables have incorporated such a disk. Observational phenomena such as the transition between B and Be phases, quasi-periodic long-term V/R variations, phase-locked V/R variations, etc., are generally viewed as pieces of a single, well-defined puzzle. Throughout this section, observational disk diagnostics and theory are considered jointly for the interpretation of the data.

5.1 Geometry of the circumstellar material

The general idea of a flattened envelope around Be stars has been confirmed spectacularly by OLBI (see Quirrenbach et al. 1994, for the first of many such observations), which invalidated the class of spherical models practically overnight (the night in question being an observing night). However, OLBI data alone do not allow for an *independent* determination of both the inclination angle and the thickness of the disk, since both quantities affect how the disk appears on the sky.

5.1.1 Disk height and opening angle

Even a flattened geometry, as was shown to be present interferometrically, is not necessarily a disk, but might just be an oblate envelope. This issue was successfully addressed by combining interferometry with polarimetry. While Quirrenbach et al. (1997) derived an upper limit of 20° for the disk opening angle[20] of ζ Tau (B2 IV) and other Be stars, the spectropolarimetric observations of ζ Tau by Wood et al. (1997) could only be explained by either a very thin or a very thick disk of opening angles of 2.5° or 52°, respectively. Hence, the disk of ζ Tau must have a very small opening angle. A similar analysis for the continuum polarization of δ Sco (B0.2 IV, Carciofi et al. 2006) corroborates the thin disk hypothesis.

From a theoretical point of view, a rotationally supported (Sect. 5.2), geometrically thin disk in vertical hydrostatic equilibrium has a Gaussian vertical density distribution if one assumes an isothermal gas. In this case the scale height, $H(r)$, is controlled only by the gas pressure and the gravity of the star (Bjorkman 1997)

$$H(r) = \frac{c_s}{v_{\rm orb}} \frac{r^{3/2}}{{R_\star}^{1/2}}, \tag{15}$$

where c_s is the isothermal sound speed.[21] The scale height is proportional to the ratio between the sound speed and the orbital velocity. Such a disk is said to be flaring because the aspect of the opening angle grows with distance from the star. For a disk somewhat below the photospheric temperature, the scale height starts with a value of 0.04 $R_\star$, which corresponds to an opening angle of about 2°, and puffs up to 3.5 $R_\star$ (10°) at a distance of 20 $R_\star$ from the star.

There are other, less conclusive, arguments favoring a small geometric thickness. One comes from the statistics of shell stars, which was found to be about 23 % by Hanuschik (1996). Assuming a random distribution of inclinations this translates to an opening angle of 13°. In another study, Porter (1996) found a value of 5°. If the disk is flaring these values are not in contradiction with the polarimetric results, since Hα is formed farther out in the disk than the polarized continuum (Fig. 2 vs. Fig. 7). Another indication of small opening angles comes from the fact that, so far, almost all observations that could be cross-checked with OLBI measurements indicate that the polarization angle of the disk is perpendicular to the disk equator (see Sects. 2.2 and 5.1.4). If the disk were both geometrically and optically thick, the polarization angle would be aligned with the optically thin poles, i.e., parallel to the disk (Wood et al. 1996a).

Zorec et al. (2007) derived a much larger opening angle in the inner disk ($H \gtrsim 0.5\ R_\star$) from an analysis of Fe II emission lines. However, that statistics depends critically on the inclination to be known independently, which, as outlined in Sect. 3.1, is prone to biases with current photospheric models. An enhanced scale height, larger

[20] Values given here are the half-opening angle of the disk, i.e., as measured from the disk equatorial plane. Twice this value is sometimes given, but designations are used incoherently in the literature.

[21] $c_s = [(kT)/(\mu m_{\rm H})]^{1/2}$, where μ is the mean molecular weight of the gas, T the (isothermal) electron temperature and $m_{\rm H}$ the hydrogen mass.

than that of a pressure-supported disk in thermal equilibrium with the stellar radiation field, would likely be a result of further interactions between the star and the disk. Certainly, this is a topic that deserves further investigation (see Sect. 4.3).

5.1.2 Disk size

The physical extent of a Be disk[22] is quite challenging to be determined observationally. In view of the discussion in Sect. 2, a distinction must be made between the *disk physical extent* and the *size of the emitting region* of a given line or continuum band. Observations can only probe the latter, unless the disk is truncated by some physical mechanism (see Sect. 6.1) and the emitting region then really extends to the farthest reaches of the disk. In fact, to date the physical extent of a Be disk has not yet been unambiguously determined for any Be star.

As seen in Sect. 2, the size of the emitting region reflects the physical conditions in the disk. OLBI currently is the only technique that provides a direct measurement of this for optical wavelengths, but care must be taken when analyzing data from the literature. Size estimates come from fitting the interferometric data with either a geometrical (e.g., uniform disk, ring, flattened Gaussian, etc.) or a physical model, and the results will depend on the model used. Also, some works remove the emission of the central (usually unresolved) star, before doing the fit.

Table 2 lists OLBI measurements of the size of the emitting region for 22 Be stars. To make the different determinations more meaningfully comparable, only estimates made from Gaussian fitting are listed. This procedure provides an estimate of the total encircled energy within a given radius. The angular size given in the table corresponds to the FWHM of the Gaussian, which, in turn, corresponds to an encircled energy of 80 % of the total energy. Figure 2 indicates that there is a strong dependence of the size of the disk emitting region on density. Since the density varies from star to star, and with time for a given star, the large scatter in Table 2 is to be expected. A closer comparison of the data with Fig. 7, panels h and i, shows that the measurements are largely consistent with that Figure (noting that the $R_\star$ given in the Table is probably somewhat smaller than the $R_{\rm eq}$ used in the figure, due to oblateness effects often not taken into account or being of unknown size in a given star, see Sect. 2.3.1). Exceptions are φ Per and possibly κ Dra and α Ara (spectral types see Table 2). For φ Per the estimated K'-band continuum sizes are about 50 % larger than the high-density case of Fig. 7. It should be kept in mind, however, that φ Per is the prototype of Be binaries with a hot companion (see Sect. 6.3), and κ Dra is a binary as well; tidal effects and the additional radiation source may invalidate the model assumptions (Sect. 6). In the case of α Ara the reported large K-band size may be due to issues with the absolute calibration of the visibilities (see Sect. 5.1.5).

ψ Per remains the only star resolved in the radio domain to date. Dougherty and Taylor (1992) fully resolved the emission at 2 cm (15 GHz) along its major axis, giving the extent of 111 ± 16 mas, which converts to about 450 $R_\star$.

[22]This quantity actually lacks a definition in the literature, and probably cannot be unambiguously defined. See Sect. 5.4 for one possible definition.

Table 2 Size of the emitting region estimated from Gaussian fits, for different wavelengths

Star	Sp. type	$R_\star$ [$R_\odot$]	Measured FWHM [mas]	Diameter [AU]	Radius [$R_\star$]	Refs.
Hα						
γ Cas	B0.5 IVe	10	3.47 ± 0.02	0.652 ± 0.004	7.01 ± 0.04	a
γ Cas	B0.5 IVe	10	3.59 ± 0.04	0.675 ± 0.008	7.25 ± 0.08	b
φ Per	B2 Vsh	7.0	2.67 ± 0.20	0.588 ± 0.044	9.03 ± 0.68	a
φ Per	B2 Vsh	7.0	2.89 ± 0.09	0.637 ± 0.020	9.77 ± 0.30	b
χ Oph	B2 Ve	5.7	3.46 ± 0.07	0.557 ± 0.011	10.5 ± 0.2	c
υ Cyg	B2 Ve	4.7	1.0 ± 0.2	0.20 ± 0.04	4.5 ± 0.9	d
ζ Tau	B2 IVsh	7.7	4.53 ± 0.52	0.618 ± 0.071	8.63 ± 0.99	a
ζ Tau	B2 IVsh	7.7	3.14 ± 0.21	0.428 ± 0.029	5.98 ± 0.40	e
48 Per	B3 Ve	6.0	2.77 ± 0.56	0.41 ± 0.08	7.3 ± 1.5	a
48 Per	B3 Ve	6.0	2.10 ± 0.2	0.31 ± 0.03	5.5 ± 0.5	f
ψ Per	B5 Vsh	4.7	3.26 ± 0.23	0.583 ± 0.041	13.34 ± 0.94	a
ψ Per	B5 Vsh	4.7	4.00 ± 0.2	0.716 ± 0.036	16.36 ± 0.82	f
o Cas	B5 IIIe	7.7	1.90 ± 0.10	0.409 ± 0.022	5.71 ± 0.30	g
β Psc	B6 Ve	3.5	2.4 ± 0.2	0.30 ± 0.03	9.3 ± 0.8	d
κ Dra	B6 IIIe	6.4	2.0 ± 0.3	0.30 ± 0.05	5.1 ± 0.76	d
η Tau	B7 IIIe	8.5	2.65 ± 0.14	0.328 ± 0.017	4.15 ± 0.22	a
η Tau	B7 IIIe	8.5	2.08 ± 0.18	0.257 ± 0.022	3.26 ± 0.28	h
β CMi	B8 Ve	3.5	2.65 ± 0.10	0.131 ± 0.005	4.03 ± 0.15	a
β CMi	B8 Ve	3.5	2.13 ± 0.15	0.106 ± 0.007	3.24 ± 0.23	h
R						
γ Cas	B0.5 IVe	10	0.76 ± 0.05	0.143 ± 0.009	1.54 ± 0.10	i
H						
δ Sco	B0.2 IVe	7.3	0.72 ± 0.08	0.11 ± 0.01	1.6 ± 0.2	j
γ Cas	B0.5 IVe	10	0.82 ± 0.08	0.154 ± 0.015	1.66 ± 0.16	i
ζ Tau	B2 IVsh	7.7	1.61 ± 0.05	0.220 ± 0.007	3.07 ± 0.10	k
48 Lib	B3 Vsh	2.7	1.72 ± 0.20	0.247 ± 0.029	5.64 ± 0.66	l

5.1.3 Disk density

OLBI measurements of the size of the emitting region can be linked to the bulk properties of the disk gas by means of radiative transfer modeling. Historically, however, the main source of information about the disk density has been the continuum SED, as the continuum excess flux bears the imprint of the physical properties of the emitting region (Sect. 2). First approaches to the problem (e.g., Gehrz et al. 1974; Waters 1986, to cite a few) used ad hoc physical descriptions for the disk, so comparison of the results was hampered by the different model assumptions made. We note that the difficulty of explaining the infrared excess of Be stars with thin disks reported by Porter (1997) has found a solution by adopting viscous models (see below).

Most recent analyses have adopted a somewhat common view of the disk as consisting of material that is pressure-supported vertically (Eq. (15)) and falls-off radially

Table 2 (*Continued*)

Star	Sp. type	$R_\star$ [$R_\odot$]	Measured FWHM [mas]	Diameter [AU]	Radius [$R_\star$]	Refs.
K or K'						
γ Cas	B0.5 IVe	10	1.95 ± 0.07	0.367 ± 0.013	3.94 ± 0.14	m
γ Cas	B0.5 IVe	10	1.24 ± 0.06	0.232 ± 0.012	2.50 ± 0.13	d
κ CMa	B1.5 IVe	5.9	1.0 ± 0.3	0.20 ± 0.06	3.7 ± 1.10	n
α Ara	B2 Ve	4.8	7.3 ± 2.0	0.60 ± 0.16	13.4 ± 3.7	o
α Ara	B2 Ve	4.8	2.4 ± 1.1	0.2 ± 0.1	4.4 ± 2.0	n
α Ara	B2 Ve	4.8	1.9 ± 1.3	0.2 ± 0.1	3.5 ± 2.4	n
φ Per	B2 Vsh	7.0	2.30 ± 0.08	0.507 ± 0.018	7.78 ± 0.27	m
φ Per	B2 Vsh	7.0	2.44 ± 0.2	0.537 ± 0.044	8.25 ± 0.68	d
χ Oph	B2 Ve	5.7	0.86 ± 0.14	0.138 ± 0.023	2.61 ± 0.43	d
υ Cyg	B2 Ve	4.7	1.21 ± 0.79	0.24 ± 0.16	5.5 ± 3.6	d
ζ Tau	B2 IVsh	7.7	1.79 ± 0.07	0.244 ± 0.010	3.41 ± 0.13	m
ζ Tau	B2 IVsh	7.7	1.790 ± 0.073	0.244 ± 0.010	3.41 ± 0.14	d
48 Lib	B3 Vsh	2.7	1.65 ± 0.05	0.237 ± 0.007	5.41 ± 0.16	p
48 Lib	B3 Vsh	2.7	0.84 ± 0.16	0.120 ± 0.024	2.74 ± 0.54	d
48 Per	B3 Ve	6.0	0.6 ± 0.25	0.088 ± 0.037	1.58 ± 0.66	d
6 Cep	B3 IVe	12.9	0.528 ± 0.087	0.322 ± 0.053	2.68 ± 0.44	d
p Car	B4 Ve	6.0	1.1 ± 0.3	0.16 ± 0.04	2.9 ± 0.8	q
ψ Per	B5 Vsh	4.7	1.03 ± 0.26	0.184 ± 0.047	4.2 ± 1.1	d
o Cas	B5 IIIe	7.7	1.03 ± 0.17	0.222 ± 0.037	3.09 ± 0.51	d
κ Dra	B6 IIIe	6.4	1.83 ± 0.11	0.275 ± 0.017	4.62 ± 0.28	m
κ Dra	B6 IIIe	6.4	3.12 ± 0.75	0.47 ± 0.11	7.9 ± 1.9	d
α Col	B7 IVe	5.8	1.3 ± 0.7	0.10 ± 0.06	1.9 ± 1.0	n
α Col	B7 IVe	5.8	1.0 ± 0.2	0.08 ± 0.02	1.5 ± 0.3	n
o Aqr	B7 IVsh	3.8	1.53 ± 0.64	0.204 ± 0.086	5.7 ± 2.4	d
β CMi	B8 Ve	3.5	0.78 ± 0.18	0.039 ± 0.009	1.19 ± 0.27	d
ω Car	B8 IIIsh	6.2	1.7 ± 0.5	0.18 ± 0.05	3.1 ± 0.9	n
8 μm						
α Ara	B2 Ve	4.8	4.0 ± 1.5	0.33 ± 0.12	7.3 ± 2.8	q
α Ara	B2 Ve	4.8	5.5 ± 0.3	0.45 ± 0.03	10.1 ± 0.6	o
δ Cen	B2 IVe	6.5	4.9 ± 1.8	0.62 ± 0.23	10.3 ± 3.8	o
12 μm						
α Ara	B2 Ve	4.8	8.1 ± 0.6	0.66 ± 0.05	14.9 ± 1.1	o
δ Cen	B2 IVe	6.5	6.9 ± 2.7	0.88 ± 0.34	14.5 ± 5.7	o
ζ Tau	B2 IVsh	7.7	5.7 ± 2.2	0.78 ± 0.30	10.9 ± 4.2	o
2 cm						
ψ Per	B5 Vsh	4.7	111 ± 16	19.9 ± 2.9	454 ± 65	r

[a]Quirrenbach et al. (1997), [b]Tycner et al. (2006), [c]Tycner et al. (2008), [d]Touhami et al. (2013), [e]Tycner et al. (2004), [f]Delaa et al. (2011), [g]Koubský et al. (2010), [h]Tycner et al. (2005), [i]Stee et al. (2012), [j]Che et al. (2012), [k]Schaefer et al. (2010), [l]Štefl et al. (2012a), [m]Gies et al. (2007), [n]Meilland et al. (2012), [o]Meilland et al. (2009), [p]Pott et al. (2010), [q]Chesneau et al. (2005), [r]Dougherty and Taylor (1992)

as a power law:[23]

$$\rho = \rho_0 \left(\frac{r}{R_\star} \right)^{-n}, \tag{16}$$

therefore making comparisons more meaningful. Using a simple radiative transfer model, Touhami et al. (2011) showed that a power law + Gaussian model (for radial and vertical density profile, respectively) could reproduce the statistical properties of the color excesses of a sample of 130 stars. By fitting Hα profiles of 56 stars, Silaj et al. (2010) concluded that the observed line profiles were generally well reproduced. Their determination of the density slope n showed that it is in the range of 1.5–4, with a statistically significant peak at 3.5.

Studies for individual stars that include a simultaneous fit of more than one observable also successfully verified the power law + Gaussian scenario. A non-exhaustive list includes Tycner et al. (2008), who modeled interferometry and spectroscopy of χ Oph and found $n = 2.5$ and $\rho_0 = 2 \times 10^{-11}$ g cm^{-3}, although they point out that acceptable fits are also found for $n = 2.5$–4. These results are in good agreement with the ones by Porter (1999) for the same star. Similar analysis by Jones et al. (2008b) for κ Dra, β Psc, and υ Cyg found $n = 2.5$, 4.2, 2.1, and $\rho_0 = 2 \times 10^{-11}$, 1.5×10^{-10} and 3×10^{-12} g cm^{-3}, respectively, and comparable results were found by Gies et al. (2007).[24] The Be stars α Eri, ζ Tau and δ Sco were analyzed by Carciofi et al. (2007, 2009, 2006, respectively). In their analysis, n was fixed to 3.5, and the SED, polarization and line profiles were fitted to obtain $\rho_0 = 7 \times 10^{-13}$, 5.6×10^{-11}, and 4.5×10^{-10} g cm^{-3}, respectively.

Barring differences in the detailed methodology of the above studies and the fact that some of the fits are not unique, the following picture emerges from the results of this and the previous section.

- Observational properties of Be stars are well described by a simple model consisting of a vertical Gaussian fall-off and a radial power law;
- The base density of the disk lies in the range between about 10^{-12} to a few times 10^{-10} g cm^{-3}.
- Radial density slopes are usually in the range 2–4, with a peak in the range 3–4.

The theoretical implications of these results will be discussed in Sect. 5.4.

5.1.4 Position angle

The first confirmation that the polarization angle is perpendicular to the major elongation axis, as predicted by scattering models (Sect. 2.2), was given by Quirrenbach et al. (1997). Since polarization probes more the inner part of the disk and OLBI at Hα the outer part, the agreement reported by Quirrenbach et al. (op. cit.), and since then confirmed by many other similar studies, indicates that there is no misalignment between the large-scale disk and the inner part. The only counterexample where disk

[23] An exception are the studies that make use of the SIMECA code (Stee and de Araujo 1994), which employs a two-component outflowing model for the Be disk.

[24] κ Dra being an exception; possible reasons for the discrepancy are discussed in Jones et al. (2008b).

and polarization angle seem not to be perpendicular is 48 Per, reported by Delaa et al. (2011). However, since 48 Per is a near pole-on Be star, the intrinsic polarization signal is very small, much smaller than the interstellar contribution, and the determination of the interferometric position angle is as well tricky for a source that deviates little from a circular shape. A possible density wave (Sect. 5.3) could further complicate the picture. A careful independent confirmation of that result would be required.

The position angle of the disk, as measured by either polarization or interferometry, has not been reported to vary in most stars, but some exceptions are known. The most striking of these exceptions are associated with the Be $\Leftrightarrow$ shell phase transitions, that have so far been observed in three stars only, γ Cas (B0.5 IV), Pleione (28 Tau, B8 V), and 59 Cyg (B1.5 V). In γ Cas these transitions were observed only in the first half of the 20th century and in 59 Cyg they ceased before the advent of electronic detectors (Underhill and Doazan 1982, p. 325ff), but in Pleione they are ongoing. The most recent transition Be $\Rightarrow$ Shell took place in 2006 (Tanaka et al. 2007), after the Shell $\Rightarrow$ Be transition in 1988. During this entire time, the system has been monitored polarimetrically (Hirata 2007) and the polarization position angle was found to change dramatically, from about 60° in the last shell phase to about 130° in 2003. These variations were suggested by Hummel (1998) to be due to the precession of a disk, e.g., under the influence of a misaligned binary orbit. Indeed, all three stars are known binaries. Hirata's result is in good agreement with this. We note that in Hirata's picture (op. cit., Fig. 2) shell phases occur twice per cycle, i.e., the full precession takes 80 years. Martin et al. (2011) worked out a theoretical framework for the precession and obtained about 45 years as tidal time scale in Pleione.

Less strongly changing position angles have been found to be related to mass transfer into the disk and V/R cycles, and are discussed in the respective parts of this work (Sects. 4.1.3 and 5.3.2).

5.1.5 Above the disk

Regardless of remaining uncertainties, the result that Be stars indeed have disks was a breakthrough also in the sense that many older observations, which were understood differently for different circumstellar geometries, could now be interpreted on a firm basis. This was particularly true for IUE data. For instance Grady et al. (1987, 1989) report a correlation of the stellar wind features in Be stars with $v \sin i$. Already then this was suggested to be an inclination dependence, but only with the disk picture being established was this conclusion confirmed. The details found by Grady et al. are still relevant for current work:

- Low $v \sin i$ Be stars ($\leq$150 km s^{-1}) have winds similar to non-Be stars.
- Intermediate to high $v \sin i$ Be stars have stronger winds than similar B-type stars, but only when they actually are in Be phases (see the example of ϑ CrB reported in Sect. 5.3.1).
- The excess wind absorption over the winds of normal main sequence B stars is almost exclusively in the form of discrete components. The respective strongest discrete components, in terms of velocity normalized to C IV blue edge velocity of P Cygni absorption, are distributed in three distinct classes:
  - At zero velocity. These are mostly the UV-equivalents of shell lines.

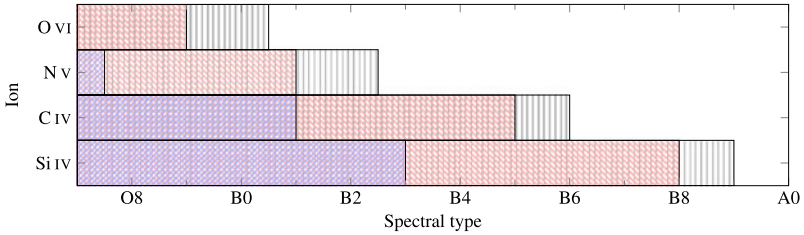

Fig. 11 Occurrence of wind superionization in supergiants (*hatched black*) and active Oe/Be stars (*hatched red*) vs. the photospheric occurrence in main sequence stars (*hatched blue*). Figure adapted from Kogure and Hirata (1982)

- At around 20 % of the edge velocity.
- At around 80 % of the edge velocity. This is similar to discrete absorption components observed in non-Be stars.

– When present, the excess wind in Be stars is seen over the entire spectral range, i.e, in much later subtypes than winds are normally observed in main sequence B stars, more similar to B-type supergiant winds (see Fig. 11).

Given that Be star winds when not in Be phases *are* normal B star winds, and in Be phases show enhanced density, but are still radiation driven, there is no reason to postulate an additional mechanism, i.e., beyond the one acting in B stars, around a Be star or above the disk in a Be phase to explain superionization of species like C IV and Si IV (Sect. 2.3). Rather, the observed distribution of superionization vs. normal B main sequence and B supergiant stars (see Fig. 11) may provide constraints for the interaction between disk and wind: superionization is meanwhile understood as being produced by shock-induced X-rays (see Sect. 6.1 of Puls et al. 2008). The enhanced winds at intermediate inclinations are probably due to disk ablation, i.e., the source of material for the enhanced wind outflow is likely the disk, and not directly the star (see, e.g., the correlation reported by Telting and Kaper 1994). Other than by an erosive process on the surface of the disk, observationally shown to be present but not yet further constrained, a viscous disk can be dissipated by either re-accretion or material crossing the critical radius outwards. Both is discussed in Sect. 5.4.

The first point in the above list is as well worth emphasizing in terms of circumstellar geometry: From the point of UV-observations, highly sensitive to additional absorbers between the star and the observer, there is no evidence for a noticeably enhanced stellar wind at polar latitudes.

This is at variance with interferometric reports of polar winds above two Be stars, α Eri and α Ara (Kervella and Domiciano de Souza 2006; Meilland et al. 2007b). These observations were taken in the H- and K-band continuum, contributing up to 5 % of the flux and opening angles of some ten degree (Kanaan et al. 2008; Stee 2011). In the case of α Eri the observations were taken in an almost diskless state, so that the suggested wind might be unrelated to the presence of a disk.

The report on α Ara may have been triggered by a problematic absolute calibration of the data, which is known to be a difficult task. For instance, the original estimate of the K-band continuum size of Meilland et al. (2009), that used the same data as Meilland et al. (2007b), was 7.3 ± 2.0 mas, while a more recent determination by

the same group, using different data, is 1.9 ± 1.3 mas (Table 2). According to Stee et al. (2012), "this star was observed 11 times in low resolution mode in 2007 but the data quality was too low to obtain more than an estimate of the disk extension." An improperly calibrated visibility can easily introduce biases in the model fitting.

The α Eri data, however, did not suffer from such calibration issues, and the star certainly deserves further observational and theoretical investigation to clarify polar winds above Be stars.

5.2 Kinematics

Since the earliest detections of Be stars it was clear that a flattened rotating structure offered the most natural explanation for the observed double peak of emission lines. Once the disk picture became established, the kinematics needed to be constrained, and this was an open issue until recently. The fashion the disk rotates bears the imprint of its formation mechanism; therefore, determining the disc kinematics observationally is of great importance.

5.2.1 Disk rotation

Over time, three distinct cases for the disk kinematics were under consideration, as well as mixed forms. Firstly, in a line-driven wind off a rotating star, the dominant force on the material is the radially directed radiation pressure that does not exert torques. In such a flow, the specific angular momentum of the material is conserved, which means the azimuthal velocity, v_ϕ, falls as the inverse of the distance to the star. Secondly, in a Keplerian velocity field, in which $v_\phi \propto r^{-1/2}$, the specific angular momentum grows with radius as $r^{1/2}$. So, for example, material that is ejected at the stellar photosphere must have its specific angular momentum doubled in order to reach an orbit of 4 $R_\star$. This change in the specific angular moment requires a torque, such as can be provided by viscous shear (Sect. 5.4). Note that in a Keplerian disk with circular orbits the radial velocity, in the frame of the star, is zero. Finally, another limiting case for the disk velocity field is the case of plasma trapped by strong magnetic fields and forced to corotate with the star, in which case $v_\phi \propto r$.

This case is actually the one most easily disproven, because an increase of the azimuthal velocity leads to entirely different shapes of emission and shell lines than actually observed (seen, e.g., in stars like σ Ori E Landstreet and Borra 1978). For the first two cases, however, the line shapes can be very similar to each other (see for instance Hummel and Vrancken 2000).

Theoretical evidence that the disk must be Keplerian came from V/R variations, attributed to a precessing one-armed density wave (Okazaki 1991; Papaloizou et al. 1992). The fact that the precession periods are two orders of magnitude larger than the orbital period of the disk particles (years vs. days) imposes that, in order for the modes to survive, the radial motions must be quite small, as non-Keplerian motion would render the oscillation modes unstable (Sect. 5.4.3). This requires a potential with only minor deviations from a $\propto 1/r$ shape.

Unambiguous observational determination of the kinematics from spectroscopy is generally difficult, as demonstrated by Hummel and Vrancken (2000), but shell stars

do provide strong evidence for near-Keplerian rotation: The central quasi-emissions observed in some Be-shell stars (Rivinius et al. 1999) can only occur if the radial velocity component is smaller than a few $\mathrm{km\,s^{-1}}$ (Hanuschik 1995). The same conclusion is drawn from the radial velocities of sharp metallic absorption lines in shell stars not undergoing V/R variations (Rivinius et al. 2006).

Spectrally resolved interferometry and spectroastrometry of emission lines finally confirmed Keplerian rotation (Meilland et al. 2007b; Delaa et al. 2011; Kraus et al. 2012; Wheelwright et al. 2012). The report of a possible exception, for the star κ CMa, relied on medium resolution data (Meilland et al. 2007a). Further analysis using high-resolution data, however, found the disk to be Keplerian, along with a number of other Be stars (Meilland et al. 2012).

5.2.2 Evidence for non-circular motion

If the disk is axisymmetric and Keplerian, it follows that the orbits are necessarily circular; a Keplerian disk with non-circular orbits would have azimuthal asymmetries because density maxima would be found at apastron, due to the slow orbital velocities, and minima at periastron, for the converse reason. Such a scenario is thought to occur in the global oscillation modes present in some Be stars (Sect. 5.4.3). A corollary is that for stars undergoing such V/R variations, there will always be some non-zero velocity component projected in the line of sight towards the observer in front of the star. This has been observed in many shell stars, ζ Tau and 48 Lib being well-studied examples. Figure 3 of Štefl et al. (2009) and Fig. 3 of Štefl et al. (2012a) illustrate the rich phenomenology of shell lines observed across V/R cycles and associated with strong (several tens of $\mathrm{km\,s^{-1}}$) projected radial motions. For 48 Lib there is another interesting observation by Hanuschik and Vrancken (1996), who report on distinct narrow components in shell line absorption cores, varying in radial velocity on time scales of less than a day.

5.3 Disks as dynamical structures

The Keplerian orbital period increases with radius as $r^{3/2}$. So, if at the stellar equator the disk material has an orbital period of typically 1 d, this increases to about 30 d at $r = 10\ R_\star$ and 1000 d at $r = 100\ R_\star$. From this simple time scale consideration one can associate short-term variations to the photosphere proper (Sect. 3) or the immediate vicinity of the star (Sect. 4), and variations with longer periods to the disk as a whole. Exceptions to this are short-term variations caused in the outer disk by the periastron passage of a secondary (e.g., Štefl et al. 2012b; Che et al. 2012) and in the wind UV lines, the latter being due to the large bulk velocity of the wind material vs. the small spatial region where the absorption is formed. Below we focus on two aspects of the variability associated with the bulk of the disk. Section 5.3.1 discusses how the disk changes in response to a varying disk-feeding rate, and Sect. 5.3.2 reviews the observational characteristics of the cyclic V/R variations.

5.3.1 Disk growth and decay

Many Be stars are known to possess very stable disks for very long times (e.g., ζ Tau B2 IV, 1 Del A1, α Col B7 IV, β CMi B8 V), which indicates these disks are fed

at nearly steady rates. Numerous examples exist, on the other hand, in which the dissipation of a pre-existing disk is observed as a gradual disappearance of emission lines, continuum polarization, and visible and infrared excesses. The dissipation is thought to occur as a result of the mass loss from the star being turned off. Examples of well-documented cases are the disk dissipation of π Aqr (B1 V) between 1986 and 1996 (Wisniewski et al. 2010; Draper et al. 2011) and the transition, seen for ϑ CrB, between a strong shell spectrum from the late 1970s to one of a B star towards the end of 1980 (Doazan et al. 1986). The disk dissipation of ϑ CrB (B6 V) offers evidence for the connection between the disk and the wind, since the UV shell lines were strong during the disk phase, fading in the course of 1981 and finally vanishing in early 1982.

Conversely, there are cases in which a B star, which has never been known to possess a disk in the past, suddenly builds a disk, δ Sco (B0.2 IV) being a spectacular recent example. Here, the Be-phenomenon must have been turned on by some mechanism. Disk build-up from scratch is well documented for a number of Be stars, for instance in the case of ω Ori (B3 III) in the early 1980s by Guinan and Hayes (1984) and Sonneborn et al. (1988), who observed it as well polarimetrically.

In between the limiting cases of clear-cut disk growth/dissipation, most stars display either a very irregular variability, alternating periods of disk growth with disk dissipation, or, what is more rare, a quasi-cyclic variability, ω CMa (B2 V) being the best-studied example of such behavior (Štefl et al. 2003a). On top of the large-scale, long-term variation there is often short-term "flickering activity", characterized by small-scale variability in photometry, polarization and also in emission lines with time scales from days to weeks. This flickering activity was observed, for instance, in μ Cen (B2 V), with a variety of different techniques (Hanuschik et al. 1993; Rivinius et al. 1998a). This variability is characterized by a sudden increase of light or line emission over just a few days, followed by a decay back to the ground state over up to a few weeks.

Stars monitored spectroscopically during the disk dissipation phase show evidence of inside-out clearing (Rivinius et al. 2001, and references therein). What is observed, mainly in the optically thin metal and helium lines, is a gradual disappearance of the high velocity components of the line, which indicates that the high velocity material close to the star has been partially depleted, though it can be replenished by a subsequent outburst. The suggestion that this was due to the formation of an inner ringlike void, however, is inadequate, as this would be dynamically unstable in a viscous disk.

It has often been observed that the late-type Be stars are less variable than early-type ones. Depending on the definition of early vs. late and observational technique and thresholds used to define variability, between 45 % and 98 % of the early-type Be stars are variable, but only 29 % to 46 % of the late-type Be stars (photometry: Hubert and Floquet 1998 98 %/45 %; Hα spectroscopy: Jones et al. 2011 45 %/29 % and Barnsley and Steele 2013 84 %/46 %).

Some examples of disk formation and dissipation are shown in Fig. 12. For the Be star MACHO 23.4148.53 (panel a), a disk formed after several years of quiescence, giving rise to an excess in the R-band of 0.6 mag. The brightening can be explained in terms of the growth of the R-band pseudo-photosphere as the density grows. The disk stayed stable for about 2 years then and slowly declined. A similar behavior was

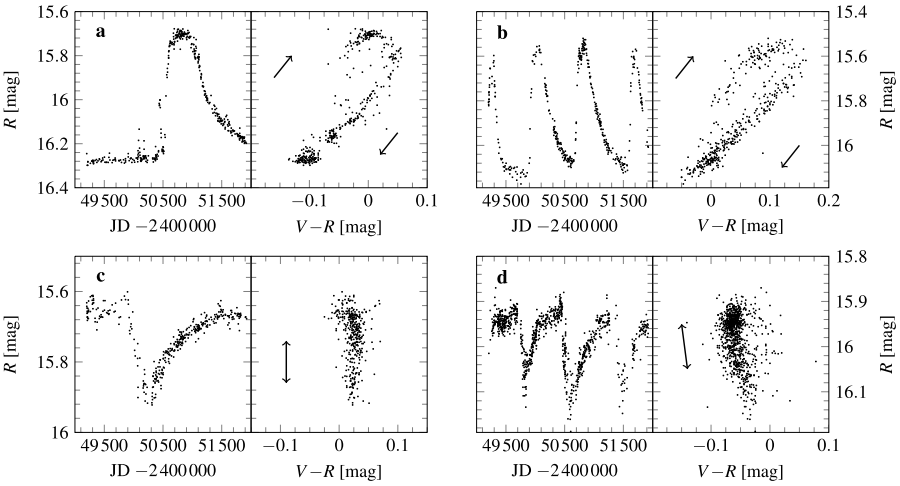

Fig. 12 Color and magnitude variation for four SMC Be stars. *Upper row*: MACHO 23.4148.53 (**a**) and 17.2109.68 (**b**), showing brightening. *Lower row*: MACHO 17.2594.208 (**c**) and 77.7427.129 (**d**), showing dimming. The temporal sense of the color changes is indicated by arrows. Plotted similarly as by de Wit et al. (2006), with data provided by S. Keller

seen for MACHO 17.2594.208 (panel c), but in this case the disk growth causes a *dimming* in the light curve as a result of obscuration of photospheric light by a disk seen close to edge-on (see below). MACHO 17.2109.68 and 77.7427.129 (panels b and d) offer examples of quasi-cyclic behavior, similar to what is seen for ω CMa.

Harmanec (1983) studied contemporaneous observations of Be stars and found two classes of correlations between photometric and spectroscopic features

– *Positive correlation*: the stronger the H I line emission, the brighter the star in the Paschen continuum (up to 0.5 mag in V), the larger (redder) $B–V$ and the smaller (bluer) $U–B$.
– *Negative correlation*: the stronger the H I line emission, the fainter the star (up to 0.3 in V), the larger $B–V$ and the larger $U–B$,

Positive correlations are associated with Be stars (not seen edge-on) and the negative correlations with shell stars. For the pole-on case, the positive correlation is quite apparent in Fig. 12: as the star gets brighter, its $V–R$ increases by more than ≈0.1 mag. The case is not so clear for the edge-on stars, which, according to Harmanec should also get redder as the star dims owing to a progressively denser disk. What is observed in Fig. 12 is a downward movement in the color-magnitude diagram, meaning that the star is not significantly changing color. Harmanec (1983)'s correlations were discussed in Haubois et al. (2012) who argue that the large change of color of some shell stars reported by Harmanec (1983) might actually be governed by other phenomena, such as V/R-cycle related changes, rather than by the mass injection. Haubois et al. (2012) suggest that the change of $B–V$ for shell stars is of rather small amplitude only.

Recent hydrodynamic models show that the observed disk variability of Be stars, associated with the secular process of disk growth and dissipation due to mass injection, are naturally explained by a viscous disk (Sect. 5.4).

5.3.2 Cyclic violet-to-red peak height variations

The observational properties of the cyclic V/R variations were reviewed and summarized by Okazaki (1991). The most relevant parts of his summary are quoted below, supplemented with some more recent findings

1. V/R periods range from years to decades, with a statistical mean of about 7 years, which is thousands of times longer than the rotation period of the star and hundreds of times longer than the typical disk orbital periods.
2. Periods are not sensitive to the spectral types of the central stars.
3. Cycle lengths are not constant, but vary from cycle to cycle (Štefl et al. 2009; Ruždjak et al. 2009).
4. The profile as a whole shifts blueward (redward) when the red (blue) component is the stronger.
5. V/R variations of binary shell stars suggest that for some of them the variability is phase locked to the orbital motions (Štefl et al. 2007), but for others this behavior is not seen (see Sect. 6.1).
6. A peculiarity of some shell stars with V/R variability is the appearance of Hα profiles with three peaks (or possibly an additional, non-central absorption), whose occurrence seems restricted to a narrow phase interval, more specifically when $V \approx R$ in the transition from $V < R$ to $V > R$ (Štefl et al. 2009, see as well Sect. 6.1).
7. V/R phase lags between different lines in the optical have been observed for some stars. Recently, these phase lags have also been detected in infrared lines (Wisniewski et al. 2007).
8. Studies of UV lines (Doazan et al. 1987; Telting and Kaper 1994) find a positive correlation between the V/R variability in emission lines and the presence of discrete absorption components (DACs) in the UV spectra.

In addition to the above spectroscopic characteristics, McDavid et al. (2000) presents evidence of a V/R phase-locked variation of the linear polarization, with a 2:1 period ratio, for the stars ζ Tau and 48 Lib. However, no correlation between the brightness and V/R was found in ζ Tau by Ruždjak et al. (2009). Using both own data and a compilation from the literature, Schaefer et al. (2010) found that the interferometric position angle of ζ Tau varies with a semi-amplitude of $8.1 \pm 1.7°$ (Fig. 14d). Since the polarimetric position angle seems to be stable (Štefl et al. 2009), this suggests that the changes of the disk geometry, as seen by interferometry, are confined to the outer parts of the disk. The above observational features will be confronted with the theory of one-armed global oscillations in Sect. 5.4.3.

5.4 Disk scenarios and physical models

After disks became generally accepted in the 1990s, models were put forward to explain the disk formation, conceptually viewed as line-driven outflows becoming

equatorially enhanced due to the rapid stellar rotation (Bjorkman 2000). However, because a Keplerian velocity law requires transport of angular momentum, Keplerian disks cannot be driven by radial forces since they exert no torque.[25] Out of the models proposed, the one that offers an explanation for angular momentum transport and naturally leads to a Keplerian velocity field was the viscous decretion disk (henceforth VDD) model of Lee et al. (1991). In the past decade this model was further developed theoretically and was compared to observations by different groups. This section reviews the structural information predicted by this model and the efforts in modeling the observational features reviewed in the previous sections.

5.4.1 Steady-state viscous disks

The basic hydrodynamics of a VDD are the same as viscous accretion disks around young stellar objects (YSO, Balbus 2003; Pringle 1981; Shakura and Sunyaev 1973), except that the sign of the rate at which mass flows through the disk, $\dot{M}$, is opposite: a negative sign denotes accretion while a positive one means decretion. Typically, accretion models assume a torque free inner boundary (i.e., accretion is allowed on to the central object) whereas in a decretion disk the inner boundary prevents inward flow by assuming a source of matter at Keplerian angular velocities at the disk inner rim. Here lies an important difference between YSO and Be disks: in the first, while being quite variable, matter is always flowing outside in; Be disks, on the other hand, can become accretion disks once the Be-phenomenon is turned off and the torque exerted at the inner rim vanishes (Sect. 5.4.2).

Several authors studied viscous decretion disks fed at a constant rate (Bjorkman 1997; Porter 1999; Okazaki 2001; Bjorkman and Carciofi 2005; Krtička et al. 2011) and the solutions agree in their essentials. Assuming that (1) the gas is isothermal, (2) the pressure gradient term in the fluid equations is small compared to gravity, so that the gas orbits the star with circular orbits and Keplerian velocities, it is possible to obtain an analytical solution for the surface density[26] vs. the distance from the star (e.g., Bjorkman and Carciofi 2005)

$$\Sigma(r) = \frac{\dot{M} v_{\rm orb} R_\star^{1/2}}{3\pi\alpha {c_s}^2 r^{3/2}} \left[\left(\frac{R_0}{r} \right)^{1/2} - 1 \right]. \tag{17}$$

Here R_0 is an arbitrary integration constant, associated with the size of the disk, and α relates the kinematic viscosity, ν, with its characteristic velocity and vertical size scale: $\nu = \alpha c_s H$ (Shakura and Sunyaev 1973). Note that Eq. (17) further assumes that α is constant throughout the disk. In the inner disk ($r \ll R_0$), the surface density has a simple power law dependence with radius, $\Sigma(r) \propto r^{-2}$.

If assumption 2 above is relaxed (i.e., the ϕ-component of momentum is explicitly solved), an analytical solution is no longer available (Okazaki 2001; Krtička et al. 2011). In this case, numerical results show two distinct regimes for the disk

[25] Close to the star there are non-radial components to the radiative force vector (see Bjorkman 2000, for a discussion).

[26] The surface density is defined as the vertically integrated disk density, ρ: $\Sigma(r) = \int_{-\infty}^{\infty} \rho(r, z)\, {\rm d}z$.

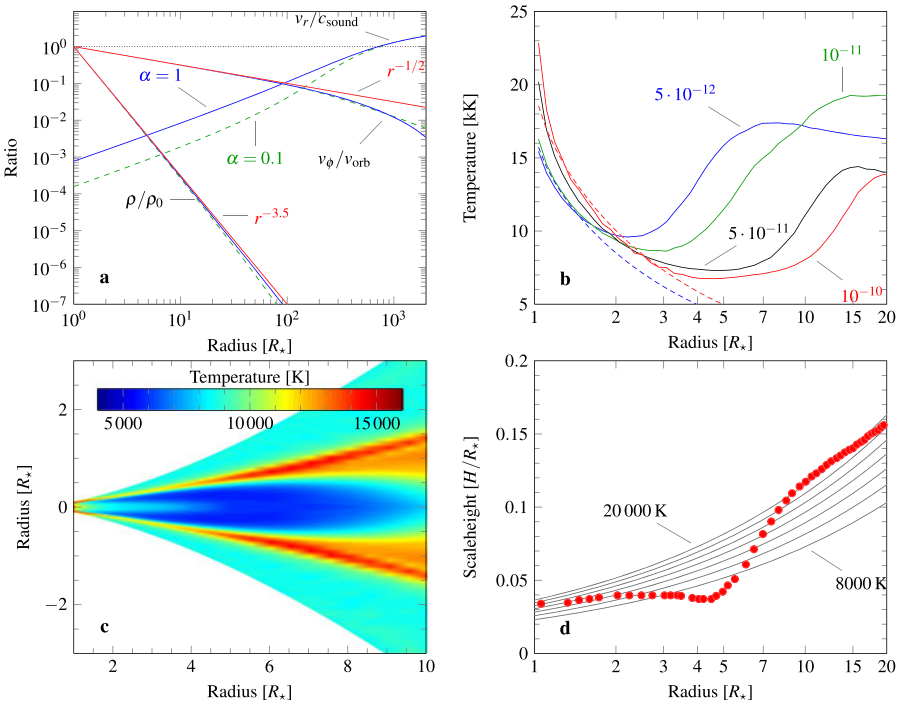

Fig. 13 Structure of a steady-state VDD. *Upper left*: Okazaki's (2001) calculation of the disk density ρ normalized to the value at the base of the disk, radial expansion velocity, v_r, in units of the local sound speed $c_{\rm s}$ and azimuthal velocity, v_ϕ, in units of the orbital speed at the base of the star, $v_{\rm orb}$. The *solid blue lines* are for $\alpha = 1$ and the *dashed lines* are for $\alpha = 0.1$. *Upper right*: Electron temperature along the disk midplane, computed with HDUST. *Curves* are labeled according to their base density ρ_0 in $\mathrm{g\,cm^{-3}}$. The *dashed lines* represent a fit of the temperature fall-off with a thin re-processing disk, Eq. (21), for the lowest and highest densities. *Lower Left*: Temperature map of the disk (*vertical cut*) with a base density of $\rho_0 = 1 \times 10^{-10}$ $\mathrm{g\,cm^{-3}}$, computed by Halonen and Jones (2013). *Lower Right*: Sigut et al. (2009) calculation of the scale height of a non-isothermal hydrostatic VDD, compared with the corresponding isothermal values in the temperature range of 8000 K to 20 000 K

– *subsonic inner part*, for which the radial velocity $v_r \ll c_s$. In this part, the surface density is nearly a power law, the azimuthal velocity is nearly Keplerian and the radial velocity grows linearly with radius (Fig. 13a). The near-Keplerian rotation follows from the fact that gravity is the dominant force and the radial velocity is small, so the gas orbits the star in nearly closed circular orbits.
– *transonic outer part*, for which $v_r \gtrsim c_s$. In this part, the surface density becomes much steeper, as a result of larger outflow velocities, and the azimuthal velocity is no longer Keplerian, but angular momentum conserving.

The critical point, $R_{\rm c}$, which marks the transition between these two regimes, occurs roughly when the orbital velocity is $\approx c_s$. The distinction between the two regimes has an important physical meaning: In the inner part the flow is driven by viscosity but for $r > R_{\rm c}$ gas pressure overcomes gravity and becomes the mechanism that supplies the radial acceleration. As a result, *after the critical point the specific*

angular momentum no longer grows with radius. For an isothermal disk, R_c is given approximately by (Krtička et al. 2011)

$$\frac{R_c}{R_\star} = \frac{3}{10}\left(\frac{v_{orb}}{c_s}\right)^2. \tag{18}$$

Typical values for R_c are about 430 $R_\star$ for a B9 V star and 350 $R_\star$ for a B0 V. These regions can only be probed at radio wavelengths (Eq. (1)). Indeed, a steeper spectral slope in the radio (Waters et al. 1991) has been interpreted as due to either a truncated disk or changing conditions in the outer disk. An analysis of radio data with current Be disk models must still be carried out to settle this issue.

Evolutionary models (Sect. 3) suggest that the outer layers of B stars spin up during the main sequence evolution. Since the rotation rate cannot grow beyond critical rotation, the excess angular momentum must be shed somehow. If $\dot{W}$ denotes the spin-up rate of the star, the mass-loss rate to maintain critical rotation is (Krtička et al. 2011)

$$\dot{M} = \frac{I}{R_\star^2}\frac{\dot{W}}{W}\left(\frac{R_\star}{R_{out}}\right)^{1/2}, \tag{19}$$

where I is the stellar moment of inertia and R_{out} represents the radius up to which angular momentum is transported. In an isolated star, $R_{out} \approx R_c$ (see above), but in a binary system (Sect. 6) the angular momentum is transferred from the disk to the binary system at the so-called truncation radius.[27] So, depending on the binary parameters, R_{out} can be much smaller than R_c, and a larger mass-loss rate is needed to shed the excess angular momentum in this case. The value of R_{out} has, thus, implications on both the mass-loss evolution and the mechanism behind the Be-phenomenon itself.

The mass loss of a steady-state system is quite difficult to determine observationally. Even though the density scale of the disk is something easily obtainable from observations, $\dot{M}$ cannot be known unless α is known or some information about the outflow velocities is available. Direct measurement of the outflow velocity is not a simple task, however, given that close to the star it is several thousand times smaller than the orbital velocities.

The disk mass density can be calculated from the surface density, recalling that the conservation of z-component of momentum implies hydrostatic vertical equilibrium. In the isothermal case

$$\rho(r,z) = \frac{\Sigma}{\sqrt{2\pi}H(r)}\exp\left[-\frac{1}{2}\left(\frac{z}{H(r)}\right)^2\right], \tag{20}$$

where the scale height is given by Eq. (15). The radial fall-off of the density is $\rho \propto \Sigma/H \propto r^{-3.5}$, which gives a physical basis for using Eq. (16) for Be disks. It should be noted that an index of $n = 3.5$ is the *minimum* value required for an outflowing, isothermal VDD (Porter 1999). In other words, an isothermal VDD should

[27] "Truncation radius" seems an unfortunate expression because the disk does not cease to exist past that radius.

always have a density slope of 3.5 or larger. This is at odds with the results shown in Sect. 5.1 that suggest that many disks possess less steep density slopes. Here, non-isothermal effects (see below), non-constant disk-feeding rates (Sect. 5.4.2), and binary iterations (Sect. 6) may play a role in creating a more complex radial behavior for the density.

Millar and Marlborough (1998, 1999) first studied the energy-balance problem in Be disks to determine the disk temperature. Since then, several other studies, with progressively more detailed calculations (Jones et al. 2004; Carciofi et al. 2006; Sigut and Jones 2007; Carciofi and Bjorkman 2008; McGill et al. 2011, 2013), showed that Be disks can be quite non-isothermal, at least in the dense part close to the star. An example of the temperature structure is shown in Fig. 13b for three disk densities. The temperature initially falls quickly, reaching a minimum whose position depends on the density, and then rises back to a value of about 60 % of $T_{\rm eff}$. Carciofi et al. (2006) showed that the initial decline is well represented by an infinitesimally thin, flat (i.e., not flared) re-processing disk (Adams et al. 1987)

$$T_{\rm flat}(r) = \frac{T_\star}{\pi^{1/4}}\left[\sin^{-1}\left(\frac{R_\star}{r}\right) - \frac{R_\star}{r}\sqrt{1-\frac{R_\star^2}{r^2}}\right]^{1/4}, \tag{21}$$

where $T_\star$ is the temperature of the radiation that illuminates the disk. This shows that the inner part of the disk is very optically thick to photoionizing radiation. The point where the temperature departs from the above curve correlates well with the vertical electron scattering optical depth, meaning that the temperature stops falling because the disk becomes vertically optically thin. Thus, as the density of the disk increases, the point where the temperature departs from the above curve moves further out into the disk (Fig. 13b). Figure 13c shows a 2-D map of the temperature, indicating that the upper layers of the disk are nearly isothermal.

Because the viscous torque depends on the sound speed (Bjorkman 1997), viscous diffusion depends on the disk temperature. This problem was studied by Carciofi and Bjorkman (2008) by solving the energy balance and viscous diffusion. This represents an intricate problem, since while the disk temperature controls the geometry (via hydrostatic equilibrium and viscous diffusion), the geometry itself determines the disk heating, and therefore the temperature. Typically, the effects of non-isothermal viscous diffusion is that the density slope is smaller than 3.5 where the temperature gradient is negative and larger than 3.5 where the temperature gradient is positive. The non-isothermal structure also affects how the disk flares. The initial fast decline of the temperature actually prevents the disk from flaring; on the other hand, the fast rise of the temperature once the disk becomes optically thin causes the disk to flare quite dramatically. This is illustrated in Fig. 13d, which shows calculations carried out by Sigut et al. (2009).

It should be noted that the above model is only applicable to disks that were fed steadily for a long time (a generalization of the VDD for time-dependent calculations is presented in the next section), and where α is constant in time and across the disk. The case of ζ Tau is particularly emblematic. This star underwent a long and well-documented period in which the average properties of its disk remained essentially

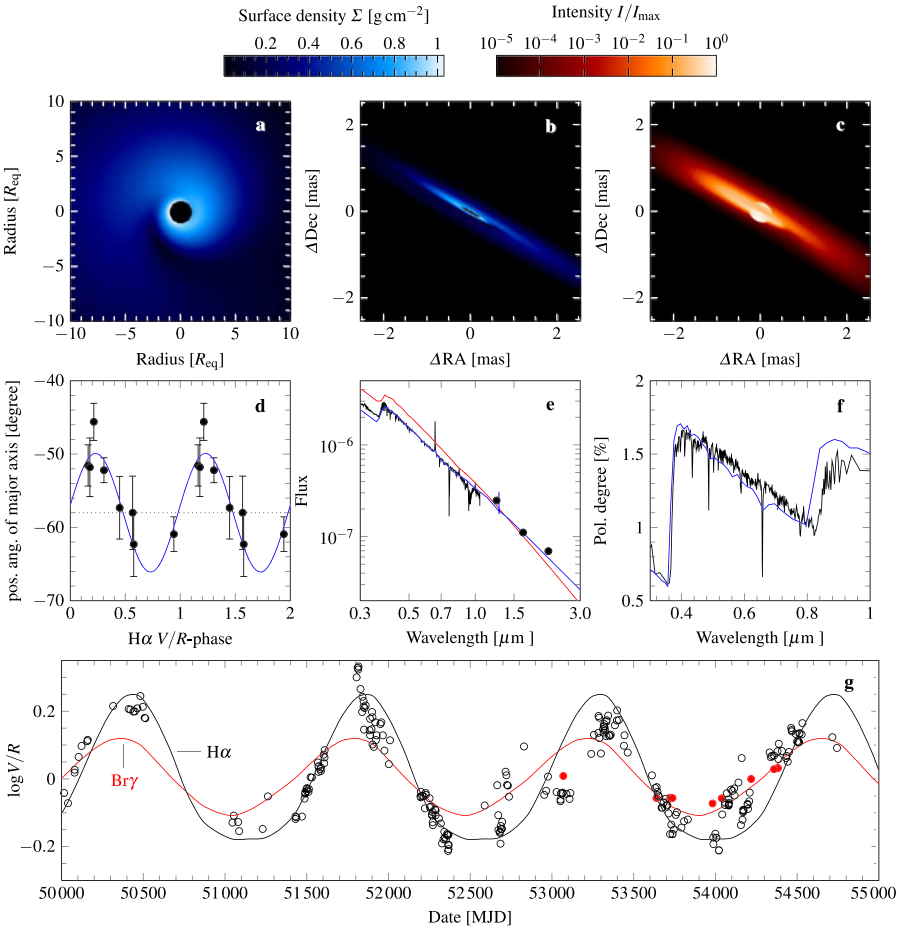

Fig. 14 Observations and models for ζ Tau. *Upper row*: Density perturbation pattern of the global oscillation model from above the disk; projected onto the plane of the sky; and the modeled continuum intensity image at 2.16 μm. *Middle row*: Changes of the interferometrically measured disk position angle vs. the Hα V/R phase; the observed SED (*black*) vs. model (*blue*) and pure photospheric stellar SED (*red*); and the observed linear polarization (*black*) vs. modeled (*blue*). *Lower row*: Observed V/R oscillations vs. model for Hα (*black*) and Brγ (*red*). Panel (**d**) adapted from Schaefer et al. (2010), all others from Carciofi et al. (2009)

constant (Štefl et al. 2009), thus being an ideal testbed for the steady-state VDD theory. In addition, it is a well-known single line binary, so it is reasonable to assume that the disk is truncated at the tidal radius of the system (Sect. 6). Therefore, neglecting second order truncation effects, theory predicts that the disk should have a power law density fall-off with $n = 3.5$ up to the truncation radius, and, therefore, the only free parameters are the disk density scale and inclination angle. Using this two-parameter model, Carciofi et al. (2009) were able to successfully fit the SED from the visible to the far infrared, the linear polarization and the spectral line profiles of H I lines (Fig. 14).

5.4.2 *Dynamical viscous disks*

Since variability is the rule rather than the exception for Be disks, steady-state models are only applicable to few systems. In this section we confront the observed time-variability features of Be disks (Sect. 5.3) with recent dynamical viscous decretion models.

The time-dependent viscous diffusion problem was examined by several authors. Okazaki (2007) points out that a decretion disk never actually experiences steady state: it either grows or decays. However, it can be shown that a disk subject to a constant mass injection rate, even though a steady state is never physically realized, tends to an asymptotic value when time goes to infinity. Jones et al. (2008a) presented self-consistent solutions for the 1-D viscous diffusion problem taking into account non-isothermal effects. The asymptotic solution for disk growth is qualitatively consistent with the non-isothermal steady-state calculations of Carciofi and Bjorkman (2008). They also obtain, from first principles, a velocity field that deviates little from Keplerian (<1 %) within 20 $R_\star$ or so.

The observed properties of Be disk variability (Sect. 5.3) are controlled by two different time scales (Haubois et al. 2012): $\tau_{\rm in}$, time scale for the variability of the mass *injection* into the disk, related to the rate of stellar mass-ejection events and the length of these events, and, $\tau_{\rm d}$, time scale for the disk to redistribute the injected material, which depends strongly on the disk volume considered: it is very short in the inner disk (days to weeks) and much longer for the outer disk. The temporal evolution of a given system will depend on an often complicated interplay between these two time scales. More specifically,

1. If $\tau_{\rm in} \ll \tau_{\rm d}$ of the inner disk, no significant observable effects should be produced.
2. If $\tau_{\rm in} \gg \tau_{\rm d}$ one can envisage two distinct limiting cases: the creation of a new disk fed at a constant mass injection rate and the dissipation of a pre-existing disk after the Be-phenomenon is turned off.
3. If $\tau_{\rm in} \sim \tau_{\rm d}$ there will be a complex interaction between the two competing time scales.

Haubois et al. (2012) studied idealized dynamical scenarios to describe the disk behavior under conditions 2 and 3 above. The main results are summarized below.

– *Disk growth:* In a forming disk fed at a constant rate, the density grows with time in the entire disk but at a rate that varies strongly with radius: the inner parts approach the steady-state values much faster than the outer parts. Initially, the slope of the density is very steep ($\gg$3.5), asymptotically reaching the steady-state value of 3.5 (Fig. 15a). For the most part the density cannot be approximated by a power law.
– *Disk dissipation:* Starting from a pre-existing disk, when the Be-phenomenon is turned off, the disk is no longer provided with mass and angular momentum by the star and quickly assumes a dual behavior in which the inner part reaccretes back onto the star while the outer part decretes outwards. These two regions are separated by a *stagnation point*, where the radial velocity is zero. The stagnation point moves away from the star with time (Fig. 15b). In the decreting part, the power law index of the density is about 3.5, whereas in the accreting part the slope goes from 3.0, which is the value for a steady-state accreting disk, to negative values closer to the star.

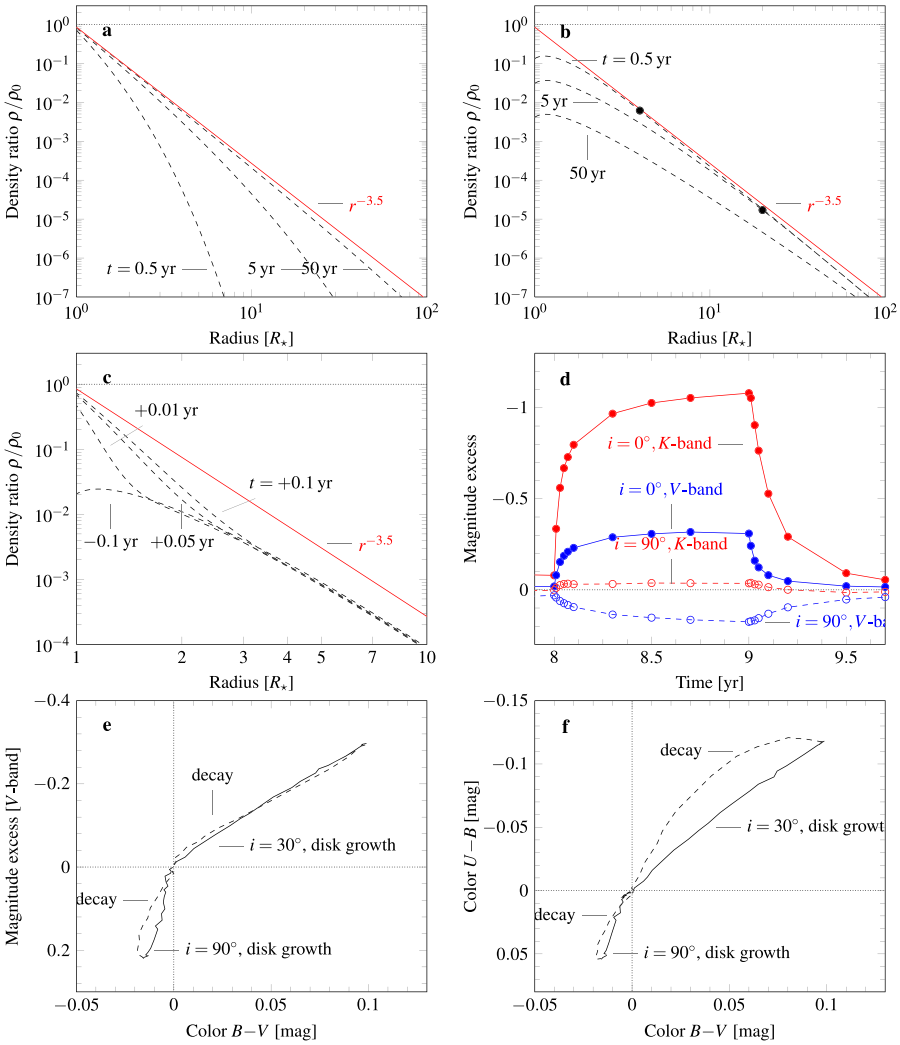

Fig. 15 Examples of the disk evolution for different dynamical scenarios computed by Haubois et al. (2012). *Upper left*: Density evolution of a disk fed at a constant rate, starting from a diskless state ($\alpha = 0.1$). *Upper right*: Density evolution of a disk decaying from a fully developed state after disk feeding has ceased ($\alpha = 0.1$). *Middle left*: Density evolution of a decaying disk into which mass feeding is restarted at epoch 0. *Middle right*: V- and K-band light curves for a disk scenario with periodic feeding, active every other year for one year, here from $t = 8$ to 9 yr. Pole-on ($i = 0°$) and edge-on ($i = 90°$, i.e., a shell star) cases are shown. *Bottom left*: Color-magnitude diagram for a disk growing steadily (panel **a**), then decaying (panel **b**) for near pole-on and edge-on cases. *Bottom right*: As panel (**e**), but color–color diagrams

– Role of α: In the above limiting cases α acts simply to scale time up and down, i.e., a forming disk with $\alpha = 1$ grows strictly 10 times faster than for $\alpha = 0.1$.
– *Periodic scenarios:* In case 3 above, for which $\tau_{\rm in} \sim \tau_{\rm d}$, the surface density can be a quite complicated function of radius and time. In the case of periodic scenarios, for instance, the details of how the surface density varies with time and radius depends

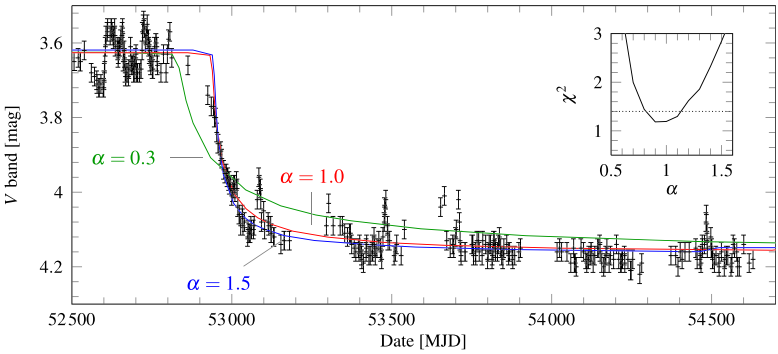

Fig. 16 Dynamical viscous models. Fit of the dissipation phase of ω CMa after the 2002 outburst. Visual observations are shown in comparison to model fits for different values of α (Carciofi et al. 2012). The inset shows the reduced chi-squared of fit for different values of the viscosity parameter α

very much on α, the cycle length and the duty cycle. An example of a periodic case is shown in Fig. 15c.

As outlined in Sect. 5.3, studies find disk density slopes in the range 2–4. The properties of dynamical viscous disks offer an additional explanation for this scatter, as decretion phases are associated with steeper slopes ($n > 3.5$) and accretion phases with flatter ones ($n < 3$). Furthermore, the slope varies wildly with distance from the star, and thus any determination of the index will be sensitive to the wavelength for which it is determined. Finally, the combination of dynamical and non-isothermal effects will likely result in even more complex density structures than predicted by isothermal models (Jones et al. 2008a).

Examples of theoretical V-band light curves and color-magnitude diagrams are shown in Fig. 15d to f for both edge-on and pole-on-on viewing. A comparison between these curves and the ones shown in Fig. 12 indicates that both model and theory agree in that the time scales for disk growth are much shorter (3–4 times) than the time scales for disk dissipation. This comes from the fact that during disk growth the time scales involved are set by the matter redistribution within a few stellar radii only. At disk dissipation, the time scales are controlled by re-accretion from a much larger area of the disk.

A comparison between the VDD theory and a time-varying system has been done for just one star to date. Carciofi et al. (2012) studied the disk dissipation of ω CMa that occurred between 2003 and 2008, after an outburst that began in 2001 and lasted for more than two years. The agreement between the dissipation curve and the model constitutes a quantitative test of the VDD theory. The fit of the observations (Fig. 16) provided the means to measure the viscosity parameter in the disk of ω CMa ($\alpha = 1.0 \pm 0.2$). The authors concluded that this large value of α "provides an important clue about the origin of the turbulent viscosity, suggesting that it likely is produced by an instability in the disk whose growth is limited by shock dissipation." This study allowed as well to determine a disk-feeding rate of $\dot{M} = (3.5 \pm 1.3) \times 10^{-8}\ \mathrm{M}_\odot\ \mathrm{yr}^{-1}$, which is at least one order of magnitude larger than the observed wind mass-loss rate

of B stars Puls et al. (2008). This may imply that the stellar wind is not the mechanism responsible for the Be-phenomenon.

5.4.3 Global oscillation models

Starting from the original ideas of Kato (1983), who studied the existence of global waves in Keplerian accretion disks, Okazaki (1991) proposed that the cyclic long-term V/R variations observed in Be stars were caused by global disk oscillations. In this initial formulation the predicted motion of the modes was retrograde. An important contribution was made by Papaloizou et al. (1992), who showed that the inclusion of a quadrupole potential due to a rotationally flattened star offers a more natural explanation of the observed periods. Such potential induces the *prograde* precession of the line of apsides of elliptical orbits. Since the precession period increases with the distance from the star, the result is a spiral pattern in the disk with $m = 1$ (e.g., Fig. 14a).

In this model, a density asymmetry between the approaching vs. receding sides of the disk causes the different heights of the line emission peaks ($V/R \neq 1$, Sect. 2.3). In addition, the spiral shape of the predicted density waves in viscous disks hinted that the model could offer a natural explanation for the observed phase lags between the higher and lower Balmer lines (item 7 of Sect. 5.3.2), due to the different formation loci of emission lines. Further observational support for this theory came, e.g., from spectroscopic, photometric, and interferometric evidence for prograde motion (Telting et al. 1994; Mennickent et al. 1997; Vakili et al. 1998).

It was generally expected that the modes should be confined to the inner part of the disk. Okazaki (1997) showed that the large disk temperature in early-type stars would prevent the confinement mechanism proposed by Papaloizou et al. (1992). In an attempt to achieve such confinement, Okazaki employed an ad hoc radiative force due to an ensemble of optically thin lines. Papaloizou and Savonije (2006) suggested that no radiative force is necessary to obtain prograde confined modes in hotter disks if there is an inner hole between the disk and the photosphere. More recently, Ogilvie (2008) solved the mode confinement problem taking into account previously ignored three-dimensional effects that caused an oscillatory vertical motion in the eccentric disk. Ogilvie's model allowed the confinement problem to be solved "without introducing uncertain radiative forces or modifying the inner boundary condition".

Spectrointerferometric data of ζ Tau provided evidence that the density wave is a spiral, as predicted by theory. Using the formalism of Okazaki (1997), Carciofi et al. (2009) developed a model for ζ Tau that is presented in Fig. 14. Panel a shows the spiral density pattern as seen from above, panel b the projected density on the sky and panel c a model image of the infrared continuum. Apparent from this plot is the brighter southern hemisphere of the star, which is little affected by the presence of the geometrically thin disk.[28] Radiative transfer calculations using this model successfully fitted the Hα and Brγ V/R cycle (panel g), in addition to the interferometric

[28] Carciofi et al. (2009) determined an inclination angle of 95° for ζ Tau, which means the southern side of the disk faces the Earth.

data. This model indicates that, at least in the case of ζ Tau, the oscillation mode cannot be confined to the inner disk, since the large amplitude of the V/R cycle requires that the oscillations extend all the way to the outer rim of the disk. Despite the general success, the model of Carciofi et al. (2009) has some issues. Both the prediction of a large polarization modulation across the V/R cycle, which is not observed, and the wrong V/R phase of the Br15 line indicates that the predicted spiral structure in the inner part of the disk may be incorrect.

The theory of global oscillations, briefly outlined above, has witnessed important theoretical developments and observational verifications in the past few years. However, much remains to be understood, such as what mechanism excites the oscillations.

6 Be stars in interacting binaries

Most massive stars ($M_\star > 8\ M_\odot$) either are binaries (about 75 %) or were so at some point of their evolution (Sana et al. 2012). Towards later spectral classes, the ratio decreases, but at least over the B star range not too steeply. Naturally, binarity is common in Be stars as well. We recall that we have excluded mass-transferring binaries from our definition of classical Be stars in Sect. 1.1.1, on grounds that the disk is not formed by a process as it is considered in Sect. 4, but rather by mass transfer from a secondary, so that their disks are constantly accreting. Indeed, in contrast to the situation for non (classical) Be stars, very few close systems, i.e., with periods shorter than about a month, are known, and all these have compact (neutron star) companions. Considering tidal forces, close companions may typically not allow the formation of a sufficiently dense disk out of self-ejected material. Even so, about one third of the Galactic Be stars are binaries (Oudmaijer and Parr 2010), and these companions often do interact with the Be star disks, either tidally (Sect. 6.1), as sources of high energy particles (Sect. 6.2), or radiatively (Sect. 6.3).

6.1 Tidal interaction

Tidal interaction, where one companion is a classical Be star, has for some time been considered as a mechanism to form a disk. However, due to the kinematic requirements concerning angular momentum transfer, this can only be the case in a minority of stars (see Sect. 4.1.3). Tidal interaction does, however, have important consequences for the disk structure.

Observationally, many cases of binarity induced behavior are known or suspected. The connection is obvious for phase-locked variability. For instance, the V/R ratio may vary with the orbital period, like in π Aqr (B1 V, Bjorkman et al. 2002; Pollmann 2012). Such behavior is often veiled when the disk is very massive, or by the typically much stronger density wave type V/R variations (since that usually involves a large fraction of the disk mass, see Sect. 5.3.2), but can be detected when the disk is not undergoing such oscillations or is dissipating.

Additionally, satellite absorptions, i.e., small dents sitting on top of the blue and/or red emission peaks, were observed to be phase locked for 4 Her (B9) and κ Dra

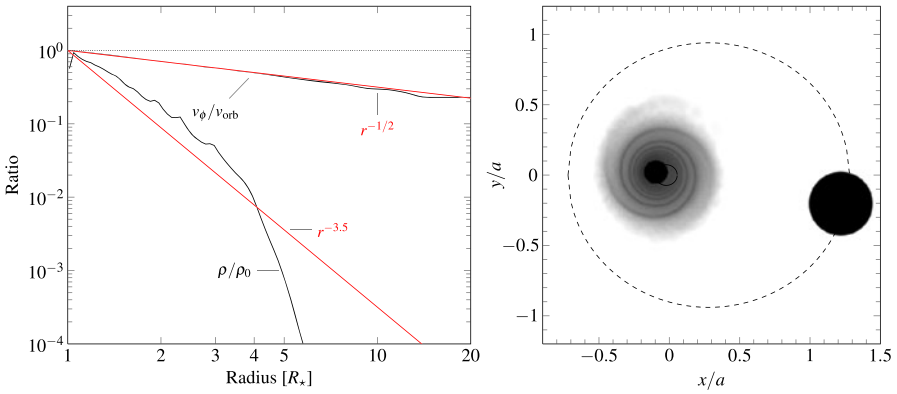

Fig. 17 Tidally disturbed structure of a Be star viscous disk, computed by Okazaki et al. (2002). *Left panel*: Disk density ρ, normalized to the value at the base of the disk and azimuthal velocity, v_ϕ, in units of the orbital speed at the stellar equator, $v_{\rm orb}$. The structure of the isothermal disk was computed for a viscosity of $\alpha = 0.1$. The spiral structure is seen as the "wiggling" on top of the density curve. The truncation radius is where the density slope changes from shallower than -3.5 to steeper than that value. *Right panel*: Spiral disk structure induced by the previous periastron passe of the binary (shown at an orbital phase close to apastron). The orbital paths ($a = 12\ R_\star$, $e = 0.34$, $q = 0.078$) relative to the center of gravity at $(0, 0)$ are indicated as *solid* and *dashed lines*. The *black areas* mark the Be star itself and, approximately, the Hill sphere of the secondary

(B6 III, Koubský et al. 1997; Saad et al. 2005, respectively). While such a clear phase-locked occurrence is rare, satellite absorptions, additional emission peaks and/or absorption, or flat topped emission profiles in general seem to be common for Balmer emission in binaries (e.g., ζ Tau B2 IV, Štefl et al. 2009; φ Per B2 V, Poeckert 1981; 59 Cyg B1.5 V, Harmanec et al. 2002b; κ Dra, Saad et al. 2004), although it is not clear whether they are unique to binary systems, and a thorough explanation for these structures is lacking.

Okazaki et al. (2002) studied tidal interaction in detail in the context of Be/X-ray binaries, but the results are valid for any type of Be binary system. They found the truncation radius to be where the tidal torque balances the viscous one. This radius depends on the system and disk properties, but it is reasonable to suspect it is near an orbital resonance.

Truncation does not just "cut" the outer parts from an otherwise unaltered disk. Rather, the truncation radius forms a watershed: Within that radius, the disk will not settle into a steady-state $\rho \propto r^{-3.5}$ density law, but become more dense and with a more shallow density gradient than would be the case for a single Be star. Outside the truncation radius, the radial density dependency becomes steeper than $r^{-3.5}$. Since the truncation process involves viscosity, the details will depend on the viscosity parameter. In any case, however, a disk with lower viscosity has a clearer truncation signature than a more viscous one; namely stronger deviations from $r^{-3.5}$ both in- and outside the truncation radius (see Fig. 17).

For eccentric orbits, the situation is more complicated, because the tidal torque becomes a function of phase. A viscous disk reacts to this by having a somewhat smaller truncation radius in periastron, and expanding while the companion is farther away until the next periastron. Additionally, in the models by Okazaki et al. (2002),

a tightly folded spiral structure in the inner disk arises, triggered at periastron. Viscosity and Keplerian shear then act to smooth the spiral, until next periastron, when the structure is re-invigorated. Thus, the spiral structure becomes phase locked. Eccentricity may as well trigger the "eccentric mode" of the disk, a special case of density waves discussed in Sect. 5.3.

We note that these theoretical results on truncation are strictly valid only for aligned orbit and disk. In slightly misaligned cases, the additional phenomenon of tidally induced disk warping is expected to occur in all but the widest binaries (Martin et al. 2011), and may actually explain the precessing disk of 28 Tau (B8 V, see Sect. 5.1.4).

In strongly misaligned, or even counter-aligned systems these results do not hold, because the tidal torque, due to reduced interaction time scales, is much smaller and truncation or other strong interaction does not occur (Martin et al. 2011). The small tidal interaction signature in the δ Sco (B0.2 IV) system during its recent periastron might, actually, be caused by a such a counter alignment (Štefl et al. 2012b; Che et al. 2012).

The relatively well developed theory on Be star binaries has been worked out as a framework for Be/X-ray binaries, and thus special emphasis was put on accretion onto the companion, not so much on the observables of the disk. Work remains to be done confronting the theory with the emission-line behavior in normal Be star binaries.

6.2 High energy interaction

Of the objects counted under high-mass X-ray binaries, the Be/X-ray type (BeXRB) is the most common. An extensive review was given only recently by Reig (2011), so this section is limited to a basic summary only.

The canonical picture is that of a classical Be star, orbited by a compact object onto which the material of the disk accretes. Because of the tidal effects, the BeXRB disks show structural differences vs. single Be star disks, such as a higher density with a shallower density profile (see Sect. 6.1) or more frequent V/R variability with shorter periods, but in principle the disks are well explained by the same mechanisms and principles as acting in single Be stars.

Black holes, as well as white dwarf companions, are among the potential companion objects; however, so far only neutron star (NS) companions have been confirmed. Evolutionary studies suggest black hole companions to be rare, consistent with none of them having been found so far (Podsiadlowski et al. 2003), though the lack of white dwarf systems remains surprising (Pols et al. 1991). The above discussed γ Cas-analogues (Sect. 3.3) might fill that gap, but this is a matter of debate and recent results seem not in favor (Smith et al. 2012a). The further discussion only mentions NS, therefore.

In a spin-orbit diagram of XRBs, BeXRBs occupy a distinct position with relatively long orbits $\gtrsim$20 d (see above for the lack of short period Be binaries in general). A positive correlation between rotational and orbital period of the companion is caused by the density law of the Be star disk. The density is a function of disk radius. The disk density in the vicinity of the NS vs. the magnetic field strength of the NS

governs the size of the magnetosphere. If it is larger than the Keplerian co-rotation radius, angular momentum is lost from the NS as material is not accreted but accelerated away, if it is smaller angular momentum is gained through accretion until the "equilibrium period" is reached. This way, if the orbit is large, the disk, locally in the vicinity of the NS, is of low density, hence the magnetosphere larger, and the rotation brakes to a longer period (e.g., Waters and van Kerkwijk 1989).

As the neutron star accretes material from the Be disk, the name-giving X-rays emerge. Due to the truncation radius being smaller than the orbit, see above, the NS does typically *not* pass through the disk. Eccentric orbits, misaligned disk and orbital planes, or density inhomogeneities in the disk (Sect. 5.4.3, very common in BeXRBs) modulate the X-ray production. Exceptions not showing modulation but only persistent X-ray production are usually very wide, low eccentricity systems with a low X-ray luminosity (Reig and Roche 1999). The transient X-ray behavior of BeXRBs is classified by this modulation. Two types of outbursts are generally recognized, following Reig (2011):

Type I outbursts are regular and (quasi-)periodic, short-lived ($\approx$0.2–0.3 $P_{\rm orb}$) flux increases by about a factor of 10 to 100 ($L_{\rm X} \leq 10^{37}$ erg s^{-1}), peaking at or close to periastron.

Type II outbursts are major flux increases by a factor of 10^3–10^4. They can occur at any orbital phase and last longer than Type I outbursts, up to several orbital cycles in extreme cases. An accretion disk may form around the NS during a type II event.

Both types can occur in a given system. Type II outbursts are violent events which can even completely disperse the Be star disk.

BeXRBs are particularly well investigated in the Magellanic Clouds (MCs) due to the low X-ray extinction and the fairly small area of the sky covered (Coe et al. 2010; Haberl et al. 2012). The total number of BeXRBs in the Large Magellanic Cloud (LMC) is small compared to the Small Magellanic Cloud (SMC) and Milky Way (MW) (Sturm et al. 2012). An additional population of Be/X-ray binaries was discovered in the Magellanic bridge between the SMC and LMC by McBride et al. (2010), where the gravitational/tidal interaction between those galaxies may have triggered local star formation episodes. The spectral-type distribution is as in the MW, in particular it does not depend on the metallicity, but angular momentum evolution in the binary system, i.e., the interaction of the neutron star with the Be star component (McBride et al. 2008). Otherwise, MC BeXRBs properties relate to classical Be stars in the MCs (see Sect. 7.2.2) as they do in the MW.

Finally, there are a few objects with Be stars as optical counterparts that emit γ-rays in the MeV to TeV range. Their nature is very uncertain, but radio observations of jets indicate relativistic particles. In at least one case the companion of the Be star is a non-accreting NS. For a summary of current hypotheses on γ-ray binaries see Sect. 1.2.3 of Reig (2011) and references therein.

6.3 Radiative interaction

Finally, Be binaries interact "radiatively", meaning that the radiation of the secondary affects the conditions in the primary's disk. This is most obvious when the secondary

is a hotter star than the primary, and such binaries are known as "Be + sdO" type. In these, the secondary is a subdwarf B or O star. The subdwarf is the remaining core of a more massive star after mass transfer has stripped the outer layers. Typical masses of the secondaries are around 1 $M_{\odot}$. Their evolutionary history is resembling Be + neutron star systems. For the current Be stars in such systems this means that they have been spun up by mass transfer, so the mass-transfer history is an important part of their "Be-story", even if the currently acting Be-phenomenon might be unrelated to it. While Be + NS binaries are fairly easy to detect via their X-ray properties, Be + sdO systems are far less conspicuous, and even though they are supposed to exist in abundance, only three systems are known with certainty, in the sense that the nature of the secondary has been proven by finding its spectral features. These are φ Per (B2 V), 59 Cyg (B1.5 V), and FY CMa (B0.5 IV, Thaller et al. 1995; Peters et al. 2008, 2013), while two more candidates have been proposed, HR 2142 (B2 V) and o Pup (B1 IV, Peters 2001; Peters and Gies 2002; Vanzi et al. 2012).

The subdwarf in the φ Per system, for instance, has $T_{\rm eff} \approx 53\,000$ K (Gies et al. 1998). The hard UV photons irradiate the outer part of the disk along the line of sight between the two components. This heats this region and stimulates fluorescence emission, such as the Balmer lines. Hence the irradiated region forms an additional emission component, which will trace the outer rim of the disk facing the secondary (Hummel and Štefl 2001).

7 Extragalactic Be stars

Modern instruments and large telescopes have enabled observations of individual stars, including main sequence stars, in other galaxies. In particular for the Large and Small Magellanic Clouds (LMC and SMC, respectively) this allowed to build extensive databases of the Be stars in these galaxies, and their photometric and spectroscopic behavior. Parallel to such instrumental development, understanding of stellar physics at low metallicity has advanced on the grounds of theory.

7.1 Be stars viewed as statistical samples

Since nearby and hence apparently bright Be stars exist in abundance, many in depth studies of individual objects exist, as shown above. However, the selection of truly homogeneous and unbiased samples from these nearby objects is not as simple as it may seem, since these Be stars were discovered by chance over a long time range, and not in a coordinated way. Samples drawn from the SMC and LMC Be stars, on the other hand, do typically not suffer these biases, and are homogeneous in distance, metallicity, and interstellar/intergalactic reddening. There is, though, a detection bias against weak and inactive Be stars (see below), which may not be constant vs. spectral type.

7.1.1 Identifying extragalactic Be stars

There are several ways to identify Be stars in bulk. The ones based on single epoch observations all rely on the detection of flux peculiarities in Hα w.r.t. the purely photospheric flux. Photometrically, this is done by taking narrow-band images centered

on Hα and on the adjacent continuum, and then analyzing the residuals after subtracting them from each other (as, e.g., by Reid and Parker 2012).

Spectroscopic identification of Be stars can, for instance, be done using objective-prism, i.e., slitless spectroscopy of an entire field. Such studies provided very large catalogs of emission-line stars including PNe, Be stars, pre-main sequence stars in the SMC, LMC, and Milky Way (MW) (Mathew et al. 2008; Martayan et al. 2008, 2010a). These lists are then typically refined using higher spectroscopic resolution observations (Martayan et al. 2007a), but also Spitzer photometric observations (Bonanos et al. 2009, 2010). However, since the Be-phenomenon is transient, single epoch observations can only identify a fraction of the actual Be stars in a field (McSwain et al. 2008, about half to two thirds). The remaining Be stars are either currently inactive, possess an only weakly developed disk, or are shell stars, of which only the strongest cases develop emission clearly detectable by the above techniques.

Another approach to identify Be stars is related to their photometric variability. Based on data from the microlensing surveys MACHO and OGLE, a large number of candidate Be stars were identified by their colors and sorted into four types according to their variability behavior (see, e.g., Fig. 12 and Keller et al. 2002; Mennickent et al. 2002). Some of these candidates were observed spectroscopically in the near-infrared, with the result that, while not all of these types correspond to classical Be stars, the majority probably does (Paul et al. 2012). Further candidate catalogs were obtained by McSwain and Gies (2005), Bonanos et al. (2009, 2010), Wisniewski and Bjorkman (2006), Wisniewski et al. (2007a), using optical or infrared photometry and/or polarimetry.

A problem in the crowded fields of SMC and LMC is the cross-identification of stars between these studies. E.g. Paul et al. (2012) could only match about 3/4 of their stars between two catalogs. It is to be hoped that with new catalogs from space missions, online archival data, and the Virtual Observatory tools, it will be possible to cross-match all those studies, and compile a complete and reliable catalog of Be stars for the purpose of statistical studies.

7.1.2 Evolutionary status of Be stars

The evolutionary status of Be stars, as a sample, can, among other things, be used to draw conclusions on the cause of rapid rotation, and thus on the internal evolution of the stars. Many studies found Be stars at all evolutionary states, independently of the metallicity environment. However, some of these results might not be taken at face value: Studies relying on photometry to determine the exact evolutionary status of Be stars are affected by the intrinsic reddening (Sect. 2.1) due to the circumstellar disk, and as well the rapid rotation may mimic evolution effects (Fig. 5), which will differ from star to star. Spectroscopy is needed to measure and correct for the disk contribution in order to determine the evolutionary status of Be stars.

– For the MW, Zorec et al. (2005) investigated the evolutionary status of Be stars, and obtained the age, measured in units of main sequence lifetime, versus the mass of the respective Be stars. Their result indicates that late-type Be stars mainly appear in the second half of their main sequence lifetime. Intermediate-type Be stars can appear throughout the main sequence phase and keep the Be star status for the

remaining main sequence life. At stark contrast, the early-type Be stars seem *only* to exist in the first part of the main sequence.
– At the intermediate metallicity of the LMC, the evolutionary states of Be stars seem to be quite similar to the MW (Martayan et al. 2006a).
– In the SMC, results for low- and intermediate mass Be stars are again similar to the MW. However, high-mass Be and Oe stars are also found in the second half of the main sequence in the SMC, unlike in the MW (Martayan et al. 2007b).

These differences concerning early-type Be stars are possibly related to either the evolution of W through the main sequence, which is affected by the relative strengths of stellar winds at different metallicities, more effectively losing angular momentum at higher metallicities (see below), or a less efficient disk dissipation process than in the MW (which might as well be metallicity related).

7.1.3 Surface abundance evolution of Be stars

The high rotation rate of B stars in low metallicity environments (see below) should lead to efficient rotational mixing of the chemical elements in Be stars (Maeder and Meynet 2001), in particular one would expect to find some nitrogen enrichment and carbon depletion. However, most of the chemical studies of Be stars (Dunstall et al. 2011) do not find such a pattern, and Hunter et al. (2009) pointed out in general that some stars may follow another chemical evolution path. Porter (1999) suggested that due to photospheric temperature gradients in such fast rotators, elements/ions may fractionate and become enriched/depleted depending on latitude, which would affect the abundance determination.

7.2 Metallicity and Be stars

Among the main questions about extragalactic Be stars is whether the metallicity (Z) affects the stellar parameters and the stellar evolutionary paths of Be stars, and whether incidence and properties differ between galaxies. To study these effects, one has to observe Be stars in environments of various metallicities. MW, LMC, and SMC are well suited, at respective metallicities of about $Z = 0.020$, 0.008, and 0.004 (see Westerlund 1997, and references therein).

7.2.1 Stellar rotation

Theoretical work predicts that at low metallicity the radiatively driven stellar winds are less efficient (Puls et al. 2008). Indeed, the radiatively driven stellar winds in OB stars are found to be weaker in the SMC (Bouret et al. 2003), and a comparative study of the MW, LMC, and SMC has found a gradient of mass loss with metallicity (Mokiem et al. 2007). Due to the weaker winds the mass loss is lower, and consequently less angular momentum is lost, meaning the stars should rotate faster (e.g., Ekström et al. 2008). This was confirmed observationally: O, B, and Be stars rotate faster in the SMC than in the LMC, and in the LMC faster than in the MW (Keller 2004; Hunter et al. 2008; Martayan et al. 2006a, 2007b). Although precise determination is subject to problems and biases discussed in Sect. 3.1, Martayan et al. (2006a, 2007b)

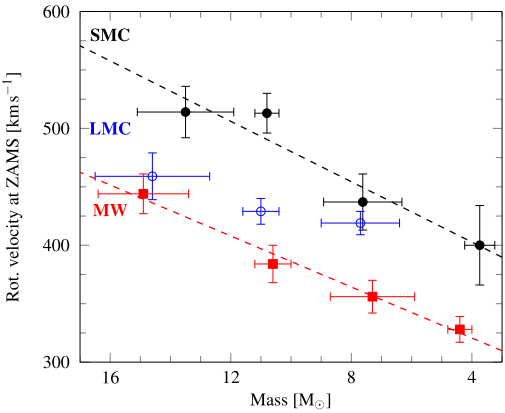

Fig. 18 Rotational velocities of Be stars computed back to their ZAMS values for MW (*red squares*), LMC (*blue open circles*), and SMC (*black filled circles*) and linear regressions to the MW and SMC values. Data from Martayan et al. (2007b), standard deviation of mass samples, shown as error bar, from Martayan (priv. comm., 2013)

use metallic lines, which are less affected by these issues, and find W of about 65 % and higher in the LMC and 75–100 % in the SMC, while in the MW a lower threshold is found at about 60 % (see Sect. 3.1).

Martayan et al. (2007b) then determined zero-age main sequence (ZAMS) rotational velocity distributions for Be stars in MW, LMC, and SMC (see Fig. 18). The explanation of the observed gradient with the metallicity was suggested to be an opacity effect: lower metallicity implies smaller stellar radii. Therefore, for the same angular momentum, stars with smaller radii rotate faster. Martayan et al. (op. cit.) indicated that over the stellar mass range of ∼4 to ∼15 $M_\odot$, the slope of the linear rotational velocity versus the stellar mass is about similar in the SMC and MW, but there was not enough data to obtain such a slope for the LMC.

7.2.2 Incidence

As a consequence of the higher rotation rate, one may expect more Be stars in the SMC/LMC than in the MW. Maeder et al. (1999) indeed found that the mean fraction of Be stars in open clusters is increasing with lower metallicity, although the scatter between individual clusters is very large. While the samples for this initial study were quite small, later studies with larger samples confirmed the result (Wisniewski and Bjorkman 2006; Martayan et al. 2006b, 2007a). In cluster studies, between 26 and 40 ± 4 % of all B stars were found to be Be stars in the SMC (Martayan et al. 2007a), and between 20 and 17.5 ± 2.5 % in the LMC (Martayan et al. 2006b). As can be seen from the results reported in Sect. 7.1.2, it is most important to compare clusters of similar age. For MW field stars the incidence is about 17 % across the entire B range, and 34 ± 1 % for B1 stars (Zorec and Briot 1997).

In particular the results for the SMC might be due to rotation closer to the critical one (Martayan et al. 2007b): $W = 0.75$, while for LMC and MW $W = 0.6$ and 0.55, respectively. Theoretically, already Maeder and Meynet (2000) linked the occurrence of Be stars in low Z environments with the higher stellar rotational velocities for B-type stars.

Regarding the spectral-type distribution of Be stars at low metallicity with respect to the MW, the distributions found by Martayan et al. (2006a, 2007b) are similar to

those in the MW, indicating that the spectral-type distribution of Be stars vs. B stars does not directly depend on metallicity. It is, however, related to the W evolution, the disk properties, and initial mass function evolution (Zorec and Frémat 2005). In a later study, Martayan et al. (2010a) found that among early-type stars (B0–B3) the frequency of Be stars is 3 to 5 times higher in the SMC than in the MW as reported by McSwain and Gies (2005) or Mathew et al. (2008). The high ZAMS W found at low Z (Martayan et al. 2007b, 2010a), especially in the SMC, indicates that some Be stars may be born as Be stars, and due to the low metallicity can keep this status all along their main sequence life.

7.2.3 Effect of metallicity on the disk

The metallicity may also have repercussions on the disk itself, by affecting the formation mechanism and/or its efficiency, as well as by altering the cooling function of the disk plasma.

For early Be stars with strong Hα emission, Martayan et al. (2007a) showed that the equivalent width (EW) tend to be more negative in the SMC than in the LMC and MW. For a limit of $EW < -20$ Å the fractions are 74 %, 62 %, and 50 %, respectively. As well the shape of the distribution is different in the SMC (see Fig. 2 of Martayan et al., op. cit.), peaking around -35 Å while in LMC and MW values of EW closest to zero are most frequent.

In the same work it is found that SMC Be stars have lower Hα full width at half maximum (FWHM), at more negative EW, than their LMC and MW counterparts. This might indicate that, in the framework of Keplerian rotating disk and using the relationship between the radius and the equivalent width (e.g., Grundstrom and Gies 2006), the typical disk radius is larger in the SMC than it is in the LMC and MW.

On the other hand, Wisniewski et al. (2007a) report that forming large disk systems is either *more* difficult at low Z or that the average disk temperature should be higher in these low Z environments. Hotter disks at SMC metallicity are also supported by model calculations (Ahmed and Sigut 2012), when assuming the same density structure as in MW disks. However, if the disks are hotter, this would result in lower Hα equivalent widths for SMC Be stars.

7.2.4 Effect of metallicity and rotation on the stellar pulsations

Pulsations in Be stars are commonly thought to be opacity driven, see Sect. 3.2. At low Z, it would obviously be more difficult to drive pulsations this way. Indeed the pulsational instability strips for B stars is shifted towards hotter regions (Martayan et al. 2007a; Diago et al. 2008, see Table 3). Note, however, that these results as well indicate that the SMC hosts a higher fraction of Be pulsators than the LMC.

The light-curve analysis summarized in Table 3 as well points out that Be stars in general are more likely to pulsate than B stars, regardless of the metallicity environment. It is possible that the fast rotation either favors the pulsating mechanisms, or increases the amplitude (Diago et al. 2009b), which might as well explain the higher fraction of pulsating Be stars in the SMC than in the LMC. More recent studies on Galactic Be stars confirm that the rotation may amplify the amplitude of pulsations

Table 3 Incidence and $\overline{W}$ of photometrically identified pulsating B and Be stars in MW, LMC, and SMC. Data from Table 1 of Diago et al. (2009b), the uncertainties of the incidence are about ±3 % for the B pulsators and ±5 % for Be pulsators, for $\overline{W}$ it is about ±5 % in all cases (Martayan, priv. comm., 2013)

	MW	LMC	SMC
	B star pulsators		
Incidence	16 %	7 %	5 %
$\overline{W}$	0.23	0.21	0.34
	Be star pulsators		
Incidence	74 %	15 %	25 %
$\overline{W}$	0.63	0.59	0.75

(Neiner et al. 2012a). However, it is worth to note that up to now no classical Be pulsators have been observed spectroscopically in the Magellanic Clouds, although they were searched for Baade et al. (2002).

7.3 Be stars, gamma-ray bursts, and the first stars

7.3.1 Post main sequence evolution and gamma-ray bursts

As a Be star evolves beyond the main sequence, the drop in surface rotation due to the expansion will stop the Be mechanism, and the circumstellar disk dissipates. However, the fact that the star has been a Be star previously may affect the post main sequence evolution, at least because the fast rotation has altered the stellar and chemical evolution. According to Yoon et al. (2006) and Georgy et al. (2009) the most massive Be- and Oe stars could become S Dor variables, especially at low metallicity.

They could also follow the quasi homogeneous chemical evolution and be progenitors of certain supernovae or gamma ray burst (GRB) explosions (Yoon et al. 2006; Martayan et al. 2010b). Woosley (1993) suggested that long GRBs could result from rapidly rotating stellar evolution at low Z. Another proposed channel to produce long GRBs is via binary evolution (Cantiello et al. 2007), and Tutukov and Fedorova (2007) predict GRB explosion in specific Be binary systems. Using the models of Yoon et al. (2006) for SMC stars, Martayan et al. (2010b) argue from B0/1e and Oe stars populations that the number of long GRBs at low redshift in dwarf galaxies and low Z would be between 2 and 14 LGRBs in 11 years, while 8 LGRBs were actually observed in this time frame.

7.3.2 Be stars and the first stars

At very low metallicity Be stars may evolve very differently, since the maximally possible rotational velocities increase and can reach more than 800 $\mathrm{km\,s^{-1}}$ at very low metallicity (Chiappini et al. 2006, see also above for the interplay of metallicity, opacity, and stellar radius). At such a rotation, the Be-phenomenon might reach much farther across the spectral types: earlier O-types, later A- and possibly F-types (Meynet and Maeder 2002; Ekström et al. 2008; Georgy et al. 2009). As a consequence, one might expect a higher fraction of Be stars in galaxies of very low metallicity. The only study of a very low metallicity galaxy (IC 1613) looking at such stars so far identified six main sequence B-type stars, and all of them were found to be Be stars (Bresolin et al. 2007).

8 Summary and conclusion

While the definition of Be stars by Collins (1987) is still the most useful one for taxonomical purposes, strict adherence will include not only classical Be stars, as discussed in this review, but as well other types of objects (see Sect. 1.1.1), which can only be distinguished with further in-depth analysis. The remaining classical Be stars, then, are found to have properties as listed below. Since such an additional analysis is hardly feasible for large samples, contamination biases will have to be worked out.

In the last few decades, Be stars have firmly been shown to be rapidly rotating objects, surrounded by gaseous decretion disks governed by viscous processes. Observationally, interferometry and space-based precision photometry are at the heart of the most important results. Theoretically, better understanding of the physics of rapidly rotating stars and the realization of the disk as being governed by viscous processes hold that position.

Rotation: Concerning the rotation, after some doubt has been cast on previous results, a new consensus seems to emerge: Be stars rotate at and above $W \gtrsim 0.75$. A mean value for the entire class is hard to derive due to gravity darkening being a problem for determining $v \sin i$. The often quoted value of $\overline{W} \approx 0.75$ is likely a lower limit only for the mean rotation of Be stars as a group. For an upper limit, at least if the rotation is to be explained by single star evolution, $\overline{W} > 0.95$ is probably excluded by the high incidence of Be stars. At least for late-type Be stars the fraction of Be stars increases towards the end of the main sequence as a consequence of rotational evolution, spinning the star up by core contraction. Future results are expected from better asteroseismic modeling, and from improving interferometric constraints on the disk inclination angles.

Pulsation: The periodic variability of early-type Be stars has been well known since more than 30 years. While initially both rotation and pulsation were proposed as underlying mechanism, first spectroscopy, then space-based photometry provided increasing evidence for pulsation, in most cases in grouped multiperiodicity. The great accuracy of dedicated space missions make it possible to identify pulsational variability for all observed Be stars, including late-type ones, though only at millimagnitude level and below. At present, it seems that detecting pulsation in Be stars is only limited by the detection threshold, not by the physical absence of pulsation. That said, a pulsating star may exhibit rotational modulation in addition, which has been suggested for several Be stars. The observational grounds have been laid by asteroseismic studies, and theoretical works are now building on these, investigating mode types and angular momentum transport.

Magnetic fields: There is no firm observational evidence for large-scale, i.e., dipolar magnetic fields at any strength, and such fields stronger than about a $\langle B_z \rangle$ of 100 G are excluded. Small-scale magnetic fields, such a localized loops, remain a possibility and have some indirect observational support, although a direct confirmation is lacking. With high resolution spectropolarimetry, this question is expected to find an answer, thanks to the Doppler effect elevating the detectability of such fields.

Disk formation: In order to be closer to the physical core of the problem of forming a disk and as well not to limit the statistics by the validity of the Roche approximation for critical rotation, we propose to abandon the notations of $\Upsilon = v_{\rm rot}/v_{\rm crit}$

and $\omega = \Omega_{\rm rot}/\Omega_{\rm crit}$ for the purpose of studying Be star rotation and instead use $W = v_{\rm rot}/v_{\rm orb}$. Even at $W = 0.9$, an ejection velocity of about 50 km s^{-1} is still required to form a circumstellar Keplerian disk (for a typical B star of luminosity class V). Although the mechanisms, at least in principle, seem well constrained as either pulsation-driven or involving small-scale magnetic fields, no detailed modeling has yet produced a disk, unless highly optimistic assumptions are made. In some objects pulsation certainly plays a role, in others no such connection could be made. It is quite unlikely that a single mechanism is responsible for all Be stars, since with increasing W more and more processes with sufficient strength to overcome the remaining threshold become available. As seen in Sect. 3.1, above a certain rotational threshold, independent of $T_{\rm eff}$, a B star can become a Be star, and above a somewhat higher threshold, decreasing as $T_{\rm eff}$ increases, it must. Reproducing this "efficiency gradient" would certainly be an important constraint for the disk forming processes. The main processes leading to the disk formation might be uncovered soon, quite possibly by a better understanding of the two points above. The details of the injection remains to be understood on theoretical grounds. The tools, such as smooth particle hydrodynamics and Monte Carlo modeling, have become very powerful and will probably soon deliver results not only for slowly evolving/steady-state cases, but as well for high temporal resolution.

Disk: Once the disk has formed and it well settled, after, e.g., an outburst replenishing the disk material, it is now generally accepted that the disks are in Keplerian rotation, geometrically thin and in vertical hydrostatic equilibrium. The further evolution of a disk is then governed by mainly viscous processes. As long as material with Keplerian properties is added at the inner part of the disk, material and angular momentum will be transported outwards. In a steadily fed disk, material transported outwards will eventually cross a critical radius and leave the system. Observations show that, in addition, some ablative mechanism is active, enhancing the wind in latitudes above the disk. As soon as the mass injection fades, the disk will gradually turn into an accretion mode, with matter falling back to the star.

The viscous decretion disk model has successfully been used to explain V/R variability in Be stars, interferometric observations, the observed photometric variations in disk build-up and decay, and the tidal interaction and truncation in Be binaries. Apart form future interferometry, long-term photometric databases, such as OGLE or MACHO, hold a great potential to be harvested, and spectroscopic databases, such as BeSS, are catching up.

Be stars in low metallicity environments: Of all Galactic field B stars, about 17 % are Be stars, with earlier types more likely to be Be stars than later types. The fraction is higher for low metallicity environments, and may even reach 100 % for very low metallicities. The most immediate reason for this is probably that the rotation, in terms of W, increases with decreasing metallicity. Be stars and their massive extension, the Oe stars, may prove to be progenitors of late stages of massive star evolution connected to rapid rotation, such as S Dor variables, or even the long GRBs. A full extension of Be star research to extragalactic environments will only be reached with future facilities, such as extremely large telescopes.

The question now is what the future research on Be stars will reveal. Having finally identified, and as well increasingly quantified, most of the basic ingredients that make Be stars tick is not the end of story; rather, it is a beginning.

Future and recently built facilities, in the optical as well as in other wavelength regimes, and both ground- (such as VLT/VLTI, GEMINIs, ALMA, the E-ELT) and space-based (JWST, HERSCHEL, GAIA, PLATO), will provide the perfect tools to perform combined multi-technique and multi-wavelength studies on Be stars to assess the remaining questions. These not only include the questions on physics and nature, but as well the parallaxes and stellar dynamics of Be stars in the Milky Way. These facilities will also enable observing stars in galaxies farther than the local group, to compare the physical processes acting in such extreme stars in various environments.

Be stars, precisely because of their relative ease of observation and meanwhile fairly well-understood nature, should be counted among the best suited laboratories to investigate some of the most important problems in contemporary astrophysics. Among these are, for instance, the effects of rapid rotation on stellar evolution, in the upper Hertzsprung–Russell diagram as well as at different metallicities, the interior structure of rapidly rotating stars, and the properties and consequences of turbulence in Keplerian disks, which are ubiquitous from planet formation around nearby young stellar objects to quasars at high redshift.

Acknowledgements We dedicate this review to the memory of the late John Porter. John was an outstanding colleague, scientifically as well as personally. He passed away Tuesday, June 7, 2005.

We are grateful to the Organizing Committee of the IAU Working Group on Active B stars for endorsing this review.

Valuable comments on the draft manuscript were provided by Dietrich Baade, Armando Domiciano de Souza, Jason Grunhut, Carol Jones, Ronald Mennickent, Florentin Millour, Coralie Neiner, Atsuo Okazaki, Stan Owocki, Geraldine Peters, Myron Smith, Philippe Stee, Richard Townsend, and Gregg Wade.

We thank Carol Jones, Armando Domiciano de Souza, Cyril Escolano, Daniel M. Faes, Robbie Halonen, Xavier Haubois, Anne-Marie Hubert, Stefan Keller, Bruno C. Mota, Coralie Neiner, Atsuo Okazaki, Stan Owocki, Gail Schaefer, and Richard Townsend for providing data for figures.

For this work we made use of NASA's ADS, the ESO Science Archive Facility, the AMBER data reduction package of the Jean-Marie Mariotti Center, the pgfplots package by Ch. Feuersänger, and the computing facilities of the Laboratory of Astroinformatics (IAG/USP, NAT/Unicsul), whose purchase was made possible by the Brazilian agency Fapesp (grant 2009/54006-4) and the INCT-A.

TRi acknowledges ESO's support in the form of a temporary re-assignment to the Office for Science to complete this review. ACa acknowledges support from CNPq (grant 307076/2012-1) and Fapesp (grant 2010/19029-0).

References

Abt HA, Levy SG (1978) Binaries among B2-B5 IV, V absorption and emission stars. Astrophys J Suppl Ser 36:241–258. doi:10.1086/190498

Adams FC, Lada CJ, Shu FH (1987) Spectral evolution of young stellar objects. Astrophys J 312:788–806. doi:10.1086/164924

Aerts C, Christensen-Dalsgaard J, Kurtz DW (2010) Asteroseismology. Springer, Berlin. doi:10.1007/978-1-4020-5803-5

Ahmed A, Sigut TAA (2012) The temperature structure of Be star disks in the Small Magellanic Cloud. Astrophys J 744:191. doi:10.1088/0004-637X/744/2/191

Alecian E (2011) Activity of Herbig Be stars and their environment. In: Neiner C, Wade G, Meynet G, Peters G (eds) Active OB stars. IAU symposium, vol 272, pp 354–365. doi:10.1017/S1743921311010775

Baade D (1988) Nonradial pulsations and the be phenomenon. In: Cayrel de Strobel G, Spite M (eds) The impact of very high S/N spectroscopy on stellar physics. IAU symposium, vol 132, p 217

Baade D (1992) Binary Be-stars and Be-binaries. In: Kondo Y, Sistero R, Polidan RS (eds) Evolutionary processes in interacting binary stars. IAU symposium, vol 151, p 147

Baade D, Rivinius T, Štefl S, Kaufer A (2002) A spectroscopic search for variability of Be stars in the SMC. Astron Astrophys 383:L31–L34. doi:10.1051/0004-6361:20020090

Bagnulo S, Szeifert T, Wade GA, Landstreet JD, Mathys G (2002) Measuring magnetic fields of early-type stars with FORS1 at the VLT. Astron Astrophys 389:191–201. doi:10.1051/0004-6361:20020606

Bagnulo S, Landstreet JD, Fossati L, Kochukhov O (2012) Magnetic field measurements and their uncertainties: the FORS1 legacy. Astron Astrophys 538:A129. doi:10.1051/0004-6361/201118098

Balbus SA (2003) Enhanced angular momentum transport in accretion disks. Annu Rev Astron Astrophys 41:555–597. doi:10.1146/annurev.astro.41.081401.155207

Balbus SA, Hawley JF (1998) Instability, turbulence, and enhanced transport in accretion disks. Rev Mod Phys 70:1–53. doi:10.1103/RevModPhys.70.1

Ballot J, Lignières F, Reese DR, Rieutord M (2010) Gravity modes in rapidly rotating stars. Limits of perturbative methods. Astron Astrophys 518:A30. doi:10.1051/0004-6361/201014426

Balona LA (2013) Rotational modulation in Be stars. In: Suárez JC, Garrido R, Balona LA, Christensen-Dalsgaard J (eds) Stellar pulsations: impact of new instrumentation and new insights. Astrophysics and space science proceedings, vol 31, p 247. doi:10.1007/978-3-642-29630-7_45

Balona LA, Cuypers J, Marang F (1992) Intensive photometry of southern Be variables. II—Summer objects. Astron Astrophys Suppl Ser 92:533–563

Balona LA, Henrichs HF, Medupe R (eds) (2003) Magnetic fields in O, B and A stars: origin and connection to pulsation, rotation and mass loss. Astronomical society of the pacific conference series, vol 305

Balona LA, Pigulski A, Cat PD, Handler G, Gutiérrez-Soto J, Engelbrecht CA, Frescura F, Briquet M, Cuypers J, Daszyńska-Daszkiewicz J, Degroote P, Dukes RJ, Garcia RA, Green EM, Heber U, Kawaler SD, Lehmann H, Leroy B, Molenda-Zaaowicz J, Neiner C, Noels A, Nuspl J, Østensen R, Pricopi D, Roxburgh I, Salmon S, Smith MA, Suárez JC, Suran M, Szabó R, Uytterhoeven K, Christensen-Dalsgaard J, Kjeldsen H, Caldwell DA, Girouard FR, Sanderfer DT (2011) Kepler observations of the variability in B-type stars. Mon Not R Astron Soc 413:2403–2420. doi:10.1111/j.1365-2966.2011.18311.x

Barnsley RM, Steele IA (2013) A representative sample of Be stars. V: Hα variability. Astron Astrophys 556:A81. doi:10.1051/0004-6361/201220419

Bisikalo DV, Boyarchuk AA, Harmanec P, Kaigorodov PV, Kuznetsov OA (2006) Disc formation in binary Be stars. In: Fridman AM, Marov MY, Kovalenko IG (eds) Astrophysics and space science library, vol 337, p 75

Bjorkman JE (1997) Circumstellar disks. In: de Greve JP, Blomme R, Hensberge H (eds) Stellar atmospheres: theory and observations. Lecture notes in physics, vol 497. Springer, Berlin, p 239. doi:10.1007/BFb0113487

Bjorkman JE (2000) The formation and structure of circumstellar disks. In: Smith MA, Henrichs HF, Fabregat J (eds) IAU colloq 175: the Be phenomenon in early-type stars. Astronomical society of the pacific conference series, vol 214, p 435

Bjorkman JE, Bjorkman KS (1994) The effects of gravity darkening on the ultraviolet continuum polarization produced by circumstellar disks. Astrophys J 436:818–830. doi:10.1086/174958

Bjorkman JE, Carciofi AC (2005) Modeling the structure of hot star disks. In: Ignace R, Gayley KG (eds) The nature and evolution of disks around hot stars. Astronomical society of the pacific conference series, vol 337, p 75

Bjorkman JE, Cassinelli JP (1993) Equatorial disk formation around rotating stars due to ram pressure confinement by the stellar wind. Astrophys J 409:429–449. doi:10.1086/172676

Bjorkman KS, Nordsieck KH, Code AD, Anderson CM, Babler BL, Clayton GC, Magalhaes AM, Meade MR, Nook MA, Schulte-Ladbeck RE, Taylor M, Whitney BA (1991) First ultraviolet spectropolarimetry of Be stars from the Wisconsin ultraviolet photo-polarimeter experiment. Astrophys J Lett 383:L67–L70. doi:10.1086/186243

Bjorkman KS, Miroshnichenko AS, McDavid D, Pogrosheva TM (2002) A study of π Aquarii during a quasi-normal star phase: refined fundamental parameters and evidence for binarity. Astrophys J 573:812–824. doi:10.1086/340751

Bonanos AZ, Massa DL, Sewilo M, Lennon DJ, Panagia N, Smith LJ, Meixner M, Babler BL, Bracker S, Meade MR, Gordon KD, Hora JL, Indebetouw R, Whitney BA (2009) Spitzer SAGE infrared photometry of massive stars in the Large Magellanic Cloud. Astron J 138:1003–1021. doi:10.1088/0004-6256/138/4/1003

Bonanos AZ, Lennon DJ, Köhlinger F, van Loon JT, Massa DL, Sewilo M, Evans CJ, Panagia N, Babler BL, Block M, Bracker S, Engelbracht CW, Gordon KD, Hora JL, Indebetouw R, Meade

MR, Meixner M, Misselt KA, Robitaille TP, Shiao B, Whitney BA (2010) Spitzer SAGE-SMC infrared photometry of massive stars in the Small Magellanic Cloud. Astron J 140:416–429. doi:10.1088/0004-6256/140/2/416

Bouret JC, Lanz T, Hillier DJ, Heap SR, Hubeny I, Lennon DJ, Smith LJ, Evans CJ (2003) Quantitative spectroscopy of o stars at low metallicity: o dwarfs in NGC 346. Astrophys J 595:1182–1205. doi:10.1086/377368

Bresolin F, Urbaneja MA, Gieren W, Pietrzyński G, Kudritzki RP (2007) VLT spectroscopy of blue supergiants in IC 1613. Astrophys J 671:2028–2039. doi:10.1086/522571

Brown JC, McLean IS (1977) Polarisation by Thomson scattering in optically thin stellar envelopes. I. Source star at centre of axisymmetric envelope. Astron Astrophys 57:141

Brown JC, Telfer D, Li Q, Hanuschik R, Cassinelli JP, Kholtygin A (2004) The effect of rotational gravity darkening on magnetically torqued Be star discs. Mon Not R Astron Soc 352:1061–1072. doi:10.1111/j.1365-2966.2004.07997.x

Brown JC, Cassinelli JP, Maheswaran M (2008) Magnetically fed hot star Keplerian disks with slow outflow. Astrophys J 688:1320–1325. doi:10.1086/592558

Cameron C, Saio H, Kuschnig R, Walker GAH, Matthews JM, Guenther DB, Moffat AFJ, Rucinski SM, Sasselov D, Weiss WW (2008) MOST detects SPBe pulsations in HD 127756 and HD 217543: asteroseismic rotation rates independent of $v \sin i$. Astrophys J 685:489–507. doi:10.1086/590369

Cantiello M, Braithwaite J (2011) Magnetic spots on hot massive stars. Astron Astrophys 534:A140. doi:10.1051/0004-6361/201117512

Cantiello M, Yoon SC, Langer N, Livio M (2007) Binary star progenitors of long gamma-ray bursts. Astron Astrophys 465:L29–L33. doi:10.1051/0004-6361:20077115

Carciofi AC, Bjorkman JE (2006) Non-LTE Monte Carlo radiative transfer. I. The thermal properties of Keplerian disks around classical Be stars. Astrophys J 639:1081–1094. doi:10.1086/499483

Carciofi AC, Bjorkman JE (2008) Non-LTE Monte Carlo radiative transfer. II. Nonisothermal solutions for viscous Keplerian disks. Astrophys J 684:1374–1383. doi:10.1086/589875

Carciofi AC, Rivinius T (eds) (2012) Circumstellar dynamics at high resolution. Astronomical society of the pacific conference series, vol 464

Carciofi AC, Miroshnichenko AS, Kusakin AV, Bjorkman JE, Bjorkman KS, Marang F, Kuratov KS, García-Lario P, Calderón JVP, Fabregat J, Magalhães AM (2006) Properties of the δ Scorpii circumstellar disk from continuum modeling. Astrophys J 652:1617–1625. doi:10.1086/507935

Carciofi AC, Magalhães AM, Leister NV, Bjorkman JE, Levenhagen RS (2007) Achernar: rapid polarization variability as evidence of photospheric and circumstellar activity. Astrophys J Lett 671:L49–L52. doi:10.1086/524772

Carciofi AC, Domiciano de Souza A, Magalhães AM, Bjorkman JE, Vakili F (2008) On the determination of the rotational oblateness of Achernar. Astrophys J Lett 676:L41–L44. doi:10.1086/586895

Carciofi AC, Okazaki AT, Le Bouquin JB, Štefl S, Rivinius T, Baade D, Bjorkman JE, Hummel CA (2009) Cyclic variability of the circumstellar disk of the Be star ζ Tauri. II. Testing the 2D global disk oscillation model. Astron Astrophys 504:915–927. doi:10.1051/0004-6361/200810962

Carciofi AC, Bjorkman JE, Otero SA, Okazaki AT, Štefl S, Rivinius T, Baade D, Haubois X (2012) The first determination of the viscosity parameter in the circumstellar disk of a Be star. Astrophys J Lett 744:L15. doi:10.1088/2041-8205/744/1/L15

Casini R, Landi Degl'Innocenti E (1994) Properties of the first-order moments of the polarization profiles of hydrogen lines. Astron Astrophys 291:668–678

Cassinelli JP, Brown JC, Maheswaran M, Miller NA, Telfer DC (2002) A magnetically torqued disk model for Be stars. Astrophys J 578:951–966. doi:10.1086/342654

Chauville J, Zorec J, Ballereau D, Morrell N, Cidale L, Garcia A (2001) High and intermediate-resolution spectroscopy of Be stars. Astron Astrophys 378:861–882. doi:10.1051/0004-6361:20011202

Che X, Monnier JD, Tycner C, Kraus S, Zavala RT, Baron F, Pedretti E, ten Brummelaar T, McAlister H, Ridgway ST, Sturmann J, Sturmann L, Turner N (2012) Imaging disk distortion of Be binary system δ Scorpii near periastron. Astrophys J 757:29. doi:10.1088/0004-637X/757/1/29

Chesneau O, Meilland A, Rivinius T, Stee P, Jankov S, Domiciano de Souza A, Graser U, Herbst T, Janot-Pacheco E, Koehler R, Leinert C, Morel S, Paresce F, Richichi A, Robbe-Dubois S (2005) First VLTI/MIDI observations of a Be star: alpha Arae. Astron Astrophys 435:275–287. doi:10.1051/0004-6361:20041954

Chiappini C, Hirschi R, Meynet G, Ekström S, Maeder A, Matteucci F (2006) A strong case for fast stellar rotation at very low metallicities. Astron Astrophys 449:L27–L30. doi:10.1051/0004-6361:20064866

Coe MJ, Bird AJ, Buckley DAH, Corbet RHD, Dean AJ, Finger M, Galache JL, Haberl F, McBride VA, Negueruela I, Schurch M, Townsend LJ, Udalski A, Wilms J, Zezas A (2010) INTEGRAL deep observations of the Small Magellanic Cloud. Mon Not R Astron Soc 406:2533–2539. doi:10.1111/j.1365-2966.2010.16844.x

Collins GW II (1963) Continuum emission from a rapidly rotating stellar atmosphere. Astrophys J 138:1134. doi:10.1086/147712

Collins GW II (1987) The use of terms and definitions in the study of Be stars. In: IAU Colloq 92: physics of Be stars, p 3

Collins GW II, Harrington JP (1966) Theoretical H-beta line profiles and related parameters for rotating B stars. Astrophys J 146:152. doi:10.1086/148866

Conti PS, Leep EM (1974) Spectroscopic observations of O-type stars. V. The hydrogen lines and λ4686 He II. Astrophys J 193:113–124. doi:10.1086/153135

Cranmer SR (1996) Dynamical models of winds from rotating hot stars. Dissertation, Bartol Research Institute, University of Delaware. Available at https://www.cfa.harvard.edu/~scranmer/cranmer_thesis.html

Cranmer SR (2005) A statistical study of threshold rotation rates for the formation of disks around Be stars. Astrophys J 634:585–601. doi:10.1086/491696

Cranmer SR (2009) A pulsational mechanism for producing Keplerian disks around Be stars. Astrophys J 701:396–413. doi:10.1088/0004-637X/701/1/396

Curtiss RH (1926) Statistical studies of stars with spectra in class Be. J R Astron Soc Can 20:19

Cuypers J, Balona LA, Marang F (1989) Intensive photometry of southern Be variables. I—Winter objects. Astron Astrophys Suppl Ser 81:151–186

Delaa O, Stee P, Meilland A, Zorec J, Mourard D, Bério P, Bonneau D, Chesneau O, Clausse JM, Cruzalebes P, Perraut K, Marcotto A, Roussel A, Spang A, McAlister H, ten Brummelaar T, Sturmann J, Sturmann L, Turner N, Farrington C, Goldfinger PJ (2011) Kinematics and geometrical study of the Be stars 48 Persei and ψ Persei with the VEGA/CHARA interferometer. Astron Astrophys 529:A87. doi:10.1051/0004-6361/201015639

de Mink SE, Langer N, Izzard RG, Sana H, de Koter A (2013) The rotation rates of massive stars: the role of binary interaction through tides, mass transfer, and mergers. Astrophys J 764:166. doi:10.1088/0004-637X/764/2/166

de Wit WJ, Lamers HJGLM, Marquette JB, Beaulieu JP (2006) The remarkable light and colour variability of Small Magellanic Cloud Be stars. Astron Astrophys 456:1027–1035. doi:10.1051/0004-6361:20065137

Diago PD, Gutiérrez-Soto J, Fabregat J, Martayan C (2008) Pulsating B and Be stars in the Small Magellanic Cloud. Astron Astrophys 480:179–186. doi:10.1051/0004-6361:20078754

Diago PD, Gutiérrez-Soto J, Auvergne M, Fabregat J, Hubert AM, Floquet M, Frémat Y, Garrido R, Andrade L, de Batz B, Emilio M, Espinosa Lara F, Huat AL, Janot-Pacheco E, Leroy B, Martayan C, Neiner C, Semaan T, Suso J, Catala C, Poretti E, Rainer M, Uytterhoeven K, Michel E, Samadi R (2009a) Pulsations in the late-type Be star HD 50209 detected by CoRoT. Astron Astrophys 506:125–131. doi:10.1051/0004-6361/200911901

Diago PD, Gutiérrez-Soto J, Fabregat J, Martayan C (2009b) More on pulsating B-type stars in the Magellanic Clouds. Commun Asteroseismol 158:184

Doazan V, Marlborough JM, Morossi C, Peters GJ, Rusconi L, Sedmak G, Stalio R, Thomas RN, Willis A (1986) Ultraviolet and visual variability of ϑ CrB during a normal B-phase following a shell phase (1980–1985). Astron Astrophys 158:1–13

Doazan V, Bourdonneau B, Rusconi L, Sedmak G, Thomas RN (1987) Long-term variability of the far-UV high-velocity components in γ Cas (1978–1986). Astron Astrophys 182:L25–L28

Domiciano de Souza A, Kervella P, Jankov S, Abe L, Vakili F, di Folco E, Paresce F (2003) The spinning-top Be star Achernar from VLTI-VINCI. Astron Astrophys 407:L47–L50. doi:10.1051/0004-6361:20030786

Domiciano de Souza A, Hadjara M, Vakili F, Bendjoya P, Millour F, Abe L, Carciofi AC, Faes DM, Kervella P, Lagarde S, Marconi A, Monin JL, Niccolini G, Petrov RG, Weigelt G (2012a) Beyond the diffraction limit of optical/IR interferometers. I. Angular diameter and rotation parameters of Achernar from differential phases. Astron Astrophys 545:A130. doi:10.1051/0004-6361/201218782

Domiciano de Souza A, Zorec J, Vakili F (2012b) CHARRON: code for high angular resolution of rotating objects in nature. In: Boissier S, de Laverny P, Nardetto N, Samadi R, Valls-Gabaud D, Wozniak H (eds) SF2A-2012: proceedings of the annual meeting of the French society of astronomy and astrophysics, pp 321–324

Donati JF, Semel M, Carter BD, Rees DE, Collier Cameron A (1997) Spectropolarimetric observations of active stars. Mon Not R Astron Soc 291:658

Dougherty SM, Taylor AR (1992) Resolution of the circumstellar gas around the Be star ψ Persei. Nature 359:808–810. doi:10.1038/359808a0

Draper ZH, Wisniewski JP, Bjorkman KS, Haubois X, Carciofi AC, Bjorkman JE, Meade MR, Okazaki A (2011) A new diagnostic of the radial density structure of Be disks. Astrophys J Lett 728:L40. doi:10.1088/2041-8205/728/2/L40

Dunstall PR, Brott I, Dufton PL, Lennon DJ, Evans CJ, Smartt SJ, Hunter I (2011) The VLT-FLAMES survey of massive stars: nitrogen abundances for Be-type stars in the Magellanic Clouds. Astron Astrophys 536:A65. doi:10.1051/0004-6361/201117588

Ekström S, Meynet G, Maeder A, Barblan F (2008) Evolution towards the critical limit and the origin of Be stars. Astron Astrophys 478:467–485. doi:10.1051/0004-6361:20078095

Emilio M, Andrade L, Janot-Pacheco E, Baglin A, Gutiérrez-Soto J, de Suárez JC, Batz B, Diago P, Fabregat J, Floquet M, Frémat Y, Huat AL, Hubert AM, Espinosa Lara F, Leroy B, Martayan C, Neiner C, Semaan T, Suso J (2010) Photometric variability of the Be star CoRoT-ID 102761769. Astron Astrophys 522:A43. doi:10.1051/0004-6361/201014081

Espinosa Lara F, Rieutord M (2011) Gravity darkening in rotating stars. Astron Astrophys 533:A43. doi:10.1051/0004-6361/201117252

Faes DM, Carciofi AC, Rivinius T, Štefl S, Baade D, Domiciano de Souza A (2013) Differential interferometric phases at high spectral resolution as a sensitive physical diagnostic of circumstellar disks. Astron Astrophys 555:A76. doi:10.1051/0004-6361/201321313

Floquet M, Hubert AM, Huat AL, Frémat Y, Janot-Pacheco E, Gutiérrez-Soto J, Neiner C, de Batz B, Leroy B, Poretti E, Amado P, Catala C, Rainer M, Diaz D, Uytterhoeven K, Andrade L, Diago PD, Emilio M, Espinosa Lara F, Fabregat J, Martayan C, Semaan T, Suso J (2009) The B0.5 IVe CoRoT target HD 49330. II. Spectroscopic ground-based observations. Astron Astrophys 506:103–110. doi:10.1051/0004-6361/200911927

Fox GK (1991) Stellar occultation of polarized light from circumstellar electrons. III—General axisymmetric envelopes. Astrophys J 379:663–675. doi:10.1086/170540

Frémat Y, Zorec J, Hubert AM, Floquet M (2005) Effects of gravitational darkening on the determination of fundamental parameters in fast-rotating B-type stars. Astron Astrophys 440:305–320. doi:10.1051/0004-6361:20042229

Gehrz RD, Hackwell JA, Jones TW (1974) Infrared observations of Be stars from 2.3 to 19.5 microns. Astrophys J 191:675–684. doi:10.1086/153008

Georgy C, Meynet G, Walder R, Folini D, Maeder A (2009) The different progenitors of type Ib, Ic SNe, and of GRB. Astron Astrophys 502:611–622. doi:10.1051/0004-6361/200811339

Gies DR, Bagnuolo WG Jr, Ferrara EC, Kaye AB, Thaller ML, Penny LR, Peters GJ (1998) Hubble space telescope Goddard high resolution spectrograph observations of the Be + sdO binary φ Persei. Astrophys J 493:440. doi:10.1086/305113

Gies DR, Bagnuolo WG Jr, Baines EK, ten Brummelaar TA, Farrington CD, Goldfinger PJ, Grundstrom ED, Huang W, McAlister HA, Mérand A, Sturmann J, Sturmann L, Touhami Y, Turner NH, Wingert DW, Berger DH, McSwain MV, Aufdenberg JP, Ridgway ST, Cochran AL, Lester DF, Sterling NC, Bjorkman JE, Bjorkman KS, Koubský P (2007) CHARA array K'-band measurements of the angular dimensions of Be star disks. Astrophys J 654:527–543. doi:10.1086/509144

Goss KJF, Karoff C, Chaplin WJ, Elsworth Y, Stevens IR (2011) Variations of the amplitudes of oscillation of the Be star Achernar. Mon Not R Astron Soc 411:162–166. doi:10.1111/j.1365-2966.2010.17665.x

Grady CA, Bjorkman KS, Snow TP (1987) Highly ionized stellar winds in Be stars—the evidence for aspect dependence. Astrophys J 320:376–397. doi:10.1086/165551

Grady CA, Bjorkman KS, Snow TP, Sonneborn G, Shore SN, Barker PK (1989) Highly ionized stellar winds in Be stars. II—Winds in B6-B9.5e stars. Astrophys J 339:403–419. doi:10.1086/167306

Granada A, Ekström S, Georgy C, Krticka J, Owocki S, Meynet G, Maeder A (2013) Populations of rotating stars II. Rapid rotators and their link to Be-type stars. Astron Astrophys 553:A25. doi:10.1051/0004-6361/201220559

Groh JH, Damineli A, Hillier DJ, Barbá R, Fernández-Lajús E, Gamen RC, Moisés AP, Solivella G, Teodoro M (2009) Bona fide, strong-variable galactic luminous blue variable stars are fast rotators: detection of a high rotational velocity in HR Carinae. Astrophys J Lett 705:L25–L30. doi:10.1088/0004-637X/705/1/L25

Grundstrom ED, Gies DR (2006) Estimating Be star disk radii using Hα emission equivalent widths. Astrophys J Lett 651:L53–L56. doi:10.1086/509635

Grunhut JH, Rivinius T, Wade GA, Townsend RHD, Marcolino WLF, Bohlender DA, Szeifert T, Petit V, Matthews JM, Rowe JF, Moffat AFJ, Kallinger T, Kuschnig R, Guenther DB, Rucinski SM, Sasselov D, Weiss WW (2012) HR 5907: discovery of the most rapidly rotating magnetic early B-type star by the MiMeS collaboration. Mon Not R Astron Soc 419:1610–1627. doi:10.1111/j.1365-2966.2011.19824.x

Guinan EF, Hayes DP (1984) The abrupt onset of a major ω Orionis mass loss episode. Astrophys J Lett 287:L39–L42. doi:10.1086/184393

Gutiérrez-Soto J, Fabregat J, Suso J, Suárez JC, Moya A, Garrido R, Hubert AM, Floquet M, Neiner C, Frémat Y (2007) Multiperiodic pulsations in the Be stars NW Serpentis and V1446 Aquilae. Astron Astrophys 472:565–570. doi:10.1051/0004-6361:20077414

Gutiérrez-Soto J, Floquet M, Samadi R, Neiner C, Garrido R, Fabregat J, Frémat Y, Diago PD, Huat AL, Leroy B, Emilio M, Hubert AM, de Andrade OTL, Batz B, Janot-Pacheco E, Espinosa Lara F, Martayan C, Semaan T, Suso J, Auvergne M, Chaintreuil S, Michel E, Catala C (2009) Low-amplitude variations detected by CoRoT in the B8 IIIe star HD 175869. Astron Astrophys 506:133–141. doi:10.1051/0004-6361/200911915

Gutiérrez-Soto J, Semaan T, Garrido R, Baudin F, Hubert AM, Neiner C (2010) Amplitude variations of the CoRoT Be star 102719279. Astron Nachr 331:P51

Gutiérrez-Soto J, Neiner C, Fabregat J, Lanza AF, Semaan T, Rainer M, Poretti E (2011) Short-term variations in Be stars observed by the CoRoT and Kepler space missions. In: Neiner C, Wade G, Meynet G, Peters G (eds) Active OB stars. IAU symposium, vol 272, pp 451–456. doi:10.1017/S1743921311011094

Haberl F, Sturm R, Ballet J, Bomans DJ, Buckley DAH, Coe MJ, Corbet R, Ehle M, Filipovic MD, Gilfanov M, Hatzidimitriou D, La Palombara N, Mereghetti S, Pietsch W, Snowden S, Tiengo A (2012) The XMM-Newton survey of the Small Magellanic Cloud. Astron Astrophys 545:A128. doi:10.1051/0004-6361/201219758

Halonen RJ, Jones CE (2013) On the intrinsic continuum linear polarization of classical Be stars during disk growth and dissipation. Astrophys J 765:17. doi:10.1088/0004-637X/765/1/17

Hanuschik RW (1995) Shell lines in disks around Be stars. 1: Simple approximations for Keplerian disks. Astron Astrophys 295:423–434

Hanuschik RW (1996) On the structure of Be star disks. Astron Astrophys 308:170–179

Hanuschik RW, Vrancken M (1996) Shell lines in 48 Lib: the discovery of narrow optical absorption components (NOACs). Astron Astrophys 312:L17–L20

Hanuschik RW, Dachs J, Baudzus M, Thimm G (1993) Hα outbursts of μ Centauri—a clue to the Be phenomenon. Astron Astrophys 274:356

Harmanec P (1983) Review of observational facts about Be stars. Hvar Obs Bull 7:55–88

Harmanec P, Bisikalo DV, Boyarchuk AA, Kuznetsov OA (2002a) On the role of duplicity in the Be phenomenon. I. General considerations and the first attempt at a 3-D gas-dynamical modelling of gas outflow from hot and rapidly rotating OB stars in binaries. Astron Astrophys 396:937–948. doi:10.1051/0004-6361:20021534

Harmanec P, Bozić H, Percy JR, Yang S, Ruzdjak D, Sudar D, Wolf M, Iliev L, Huang L, Buil C, Eenens P (2002b) Properties and nature of Be stars. XXI. The long-term and the orbital variations of V832 Cyg = 59 Cyg. Astron Astrophys 387:580–594. doi:10.1051/0004-6361:20020453

Harrington DM, Kuhn JR (2009a) Spectropolarimetric observations of herbig Ae/Be stars. II. Comparison of spectropolarimetric surveys: HAeBe, Be and other emission-line stars. Astrophys J Suppl Ser 180:138–181. doi:10.1088/0067-0049/180/1/138

Harrington DM, Kuhn JR (2009b) Ubiquitous Hα-polarized line profiles: absorptive spectropolarimetric effects and temporal variability in post-AGB, herbig Ae/Be, and other stellar types. Astrophys J 695:238–247. doi:10.1088/0004-637X/695/1/238

Hartmann L, Calvet N, Gullbring E, D'Alessio P (1998) Accretion and the evolution of T Tauri disks. Astrophys J 495:385. doi:10.1086/305277

Haubois X, Carciofi AC, Rivinius T, Okazaki AT, Bjorkman JE (2012) Dynamical evolution of viscous disks around Be stars. I. Photometry. Astrophys J 756:156. doi:10.1088/0004-637X/756/2/156

Henrichs HF, de Jong JA, Donati JF, Catala C, Wade GA, Shorlin SLS, Veen PM, Nichols JS, Kaper L (2000) The magnetic field of β Cep and the Be phenomenon. In: Smith MA, Henrichs HF, Fabregat J (eds) IAU colloq 175: the Be phenomenon in early-type stars. Astronomical society of the pacific conference series, vol 214, p 324

Henry GW, Smith MA (2012) Rotational and cyclical variability in γ Cassiopeiae. II. Fifteen seasons. Astrophys J 760:10. doi:10.1088/0004-637X/760/1/10

Hirata R (2007) Disk precession in Pleione. In: Štefl S, Owocki SP, Okazaki AT (eds) Active OB-stars: laboratories for stellar and circumstellar physics. Astronomical society of the pacific conference series, vol 361, p 267

Hoffleit D, Jaschek C (1991) The bright star catalogue. Yale University Observatory, New Haven

Hoffman JL, Bjorkman J, Whitney B (eds) (2012) Stellar polarimetry: from birth to death. American institute of physics conference series, vol 1429

Howarth ID (2007) Rotation and the circumstellar environment. In: Štefl S, Owocki SP, Okazaki AT (eds) Active OB-stars: laboratories for stellar and circumstellar physics. Astronomical society of the pacific conference series, vol 361, p 15

Huang W, Gies DR, McSwain MV (2010) A stellar rotation census of B stars: from ZAMS to TAMS. Astrophys J 722:605–619. doi:10.1088/0004-637X/722/1/605

Huat AL, Hubert AM, Baudin F, Floquet M, Neiner C, Frémat Y, Gutiérrez-Soto J, Andrade L, de Batz B, Diago PD, Emilio M, Espinosa Lara F, Fabregat J, Janot-Pacheco E, Leroy B, Martayan C, Semaan T, Suso J, Auvergne M, Catala C, Michel E, Samadi R (2009) The B0.5 IVe CoRoT target HD 49330. I. Photometric analysis from CoRoT data. Astron Astrophys 506:95–101. doi:10.1051/0004-6361/200911928

Hubert AM, Floquet M (1998) Investigation of the variability of bright Be stars using HIPPARCOS photometry. Astron Astrophys 335:565–572

Hubrig S, Yudin RV, Pogodin M, Schöller M, Peters GJ (2007) Evidence for weak magnetic fields in early-type emission stars. Astron Nachr 328:1133. doi:10.1002/asna.200710877

Hubrig S, Schöller M, Savanov I, Yudin RV, Pogodin MA, Štefl S, Rivinius T, Curé M (2009) Magnetic survey of emission line B-type stars with FORS 1 at the VLT. Astron Nachr 330:708. doi:10.1002/asna.200911236

Hummel W (1994) Line formation in Be star envelopes. 1: inhomogeneous density distributions. Astron Astrophys 289:458–468

Hummel W (1998) On the spectacular variations of Be stars. Evidence for a temporarily tilted circumstellar disk. Astron Astrophys 330:243–252

Hummel W, Štefl S (2001) The circumstellar structure of the Be shell star φ Persei. II. Modeling. Astron Astrophys 368:471–483. doi:10.1051/0004-6361:20000559

Hummel W, Vrancken M (2000) Line formation in Be star circumstellar disks Shear broadening, shell absorption, stellar obscuration and rotational parameter. Astron Astrophys 359:1075–1084

Hunter I, Brott I, Lennon DJ, Langer N, Dufton PL, Trundle C, de Smartt SJ, Koter A, Evans CJ, Ryans RSI (2008) The VLT FLAMES survey of massive stars: rotation and nitrogen enrichment as the key to understanding massive star evolution. Astrophys J Lett 676:L29–L32. doi:10.1086/587436

Hunter I, Brott I, Langer N, Lennon DJ, Dufton PL, Howarth ID, Ryans RSI, Trundle C, de Evans CJ, Koter A, Smartt SJ (2009) The VLT-FLAMES survey of massive stars: constraints on stellar evolution from the chemical compositions of rapidly rotating galactic and Magellanic cloud B-type stars. Astron Astrophys 496:841–853. doi:10.1051/0004-6361/200809925

Ignace R, Gayley KG (eds) (2005) The nature and evolution of disks around hot stars. Astronomical society of the pacific conference series, vol 337

Jackson S, MacGregor KB, Skumanich A (2004) Models for the rapidly rotating Be star Achernar. Astrophys J 606:1196–1199. doi:10.1086/383197

Jaschek M, Slettebak A, Jaschek C (1981) Be star terminology. Be Star Newsl 4:9

Jones CE, Sigut TAA, Marlborough JM (2004) Iron line cooling of Be star circumstellar discs. Mon Not R Astron Soc 352:841–846. doi:10.1111/j.1365-2966.2004.07970.x

Jones CE, Sigut TAA, Porter JM (2008a) The circumstellar envelopes of Be stars: viscous disc dynamics. Mon Not R Astron Soc 386:1922–1930. doi:10.1111/j.1365-2966.2008.13206.x

Jones CE, Tycner C, Sigut TAA, Benson JA, Hutter DJ (2008b) A parameter study of classical Be star disk models constrained by optical interferometry. Astrophys J 687:598–607. doi:10.1086/591726

Jones CE, Tycner C, Smith AD (2011) The variability of Hα equivalent widths in Be stars. Astron J 141:150. doi:10.1088/0004-6256/141/5/150

Jones CE, Wiegert P, Tycner C, Henry GW, Halonen R, Muterspaugh MW (2013) Using photometry to probe the environment of δ Scorpii. Astron J 145:142. doi:10.1088/0004-6256/145/5/142

Kaiser D (1989) Spectral energy distributions of Be stars. II—Determination of Be star parameters by comparison between measured and model spectra. Astron Astrophys 222:187–199

Kanaan S, Meilland A, Stee P, Zorec J, Domiciano de Souza A, Frémat Y, Briot D (2008) Disk and wind evolution of Achernar: the breaking of the fellowship. Astron Astrophys 486:785–798. doi:10.1051/0004-6361:20078868

Kato S (1983) Low-frequency, one-armed oscillations of Keplerian gaseous disks. Publ Astron Soc Jpn 35:249–261

Kaufer A, Stahl O, Prinja RK, Witherick D (2006) Multi-periodic photospheric pulsations and connected wind structures in HD 64760. Astron Astrophys 447:325–341. doi:10.1051/0004-6361:20053847

Keller SC (2004) Rotation of early B-type stars in the Large Magellanic Cloud: the role of evolution and metallicity. Publ Astron Soc Aust 21:310–317. doi:10.1071/AS04024

Keller SC, Bessell MS, Cook KH, Geha M, Syphers D (2002) Blue variable stars from the MACHO database. I. Photometry and spectroscopy of the Large Magellanic Cloud sample. Astron J 124:2039–2044. doi:10.1086/342548

Kervella P, Domiciano de Souza A (2006) The polar wind of the fast rotating Be star Achernar. VINCI/VLTI interferometric observations of an elongated polar envelope. Astron Astrophys 453:1059–1066. doi:10.1051/0004-6361:20054771

King AR, Pringle JE, Livio M (2007) Accretion disc viscosity: how big is alpha? Mon Not R Astron Soc 376:1740–1746. doi:10.1111/j.1365-2966.2007.11556.x

Kochukhov O, Sudnik N (2013) Detectability of small-scale magnetic fields in early-type stars. Astron Astrophys 554:A93. doi:10.1051/0004-6361/201321583

Kogure T, Hirata R (1982) The Be star phenomena I. General properties. Bull Astron Soc India 10:281

Koubský P, Harmanec P, Kubát J, Hubert AM, Božić H, Floquet M, Hadrava P, Hill G, Percy JR (1997) Properties and nature of Be stars. XVIII. Spectral, light and colour variations of 4 Herculis. Astron Astrophys 328:551–564

Koubský P, Hummel CA, Harmanec P, Tycner C, van Leeuwen F, Yang S, Šlechta M, Božić H, Zavala RT, Ruždjak D, Sudar D (2010) Properties and nature of Be stars. 28. Implications of systematic observations for the nature of the multiple system with the Be star o Cassiopeæ and its circumstellar environment. Astron Astrophys 517:A24. doi:10.1051/0004-6361/201014477

Kraus S, Monnier JD, Che X, Schaefer G, Touhami Y, Gies DR, Aufdenberg JP, Baron F, Thureau N, ten Brummelaar TA, McAlister HA, Turner NH, Sturmann J, Sturmann L (2012) Gas distribution, kinematics, and excitation structure in the disks around the classical Be stars β Canis Minoris and ζ Tauri. Astrophys J 744:19. doi:10.1088/0004-637X/744/1/19

Kříž S, Harmanec P (1975) A hypothesis of the binary origin of Be stars. Bull Astron Inst Czechoslov 26:65–81

Kroll P (1995) Dreidimensionale Simulationen zirkumstellarer Strukturen in Symbiotischen Doppelsternen und Be-Sternen mit der Methode der Smoothed-Particle-Hydrodynamics auf Parallelrechnern. Dissertation, Univ. Tübingen

Kroll P, Hanuschik RW (1997) Dynamics of self-accreting disks in Be stars. In: Wickramasinghe DT, Bicknell GV, Ferrario L (eds) IAU Colloq 163: accretion phenomena and related outflows. Astronomical society of the pacific conference series, vol 121, p 494

Krtička J, Owocki SP, Meynet G (2011) Mass and angular momentum loss via decretion disks. Astron Astrophys 527:A84. doi:10.1051/0004-6361/201015951

Lachaume R (2003) On marginally resolved objects in optical interferometry. Astron Astrophys 400:795–803. doi:10.1051/0004-6361:20030072

Lamers HJGLM, de Zickgraf FJ, Winter D, Houziaux L, Zorec J (1998) An improved classification of B[e]-type stars. Astron Astrophys 340:117–128

Landstreet JD, Borra EF (1978) The magnetic field of Sigma Orionis E. Astrophys J Lett 224:L5–L8. doi:10.1086/182746

Lee U (2012) Amplitudes of low-frequency modes in rotating B-type stars. Mon Not R Astron Soc 420:2387–2398. doi:10.1111/j.1365-2966.2011.20204.x

Lee U, Osaki Y, Saio H (1991) Viscous excretion discs around Be stars. Mon Not R Astron Soc 250:432–437

Levenhagen RS, Leister NV, Künzel R (2011) Spectroscopic variabilities in λ Pavonis. Astron Astrophys 533:A75. doi:10.1051/0004-6361/201116590

Lubow SH, Seibert M, Artymowicz P (1999) Disk accretion onto high-mass planets. Astrophys J 526:1001–1012. doi:10.1086/308045

Lucy LB (1967) Gravity-darkening for stars with convective envelopes. Z Astrophys 65:89

Maeder A (2009) Physics, formation and evolution of rotating stars. Astronomy and astrophysics library. Springer, Berlin. doi:10.1007/978-3-540-76949-1

Maeder A, Meynet G (2000) Stellar evolution with rotation. VI. The Eddington and Omega limits, the rotational mass loss for OB and LBV stars. Astron Astrophys 361:159–166

Maeder A, Meynet G (2001) Stellar evolution with rotation. VII. Low metallicity models and the blue to red supergiant ratio in the SMC. Astron Astrophys 373:555–571. doi:10.1051/0004-6361:20010596

Maeder A, Meynet G (2010) Evolution of massive stars with mass loss and rotation. New Astron Rev 54:32–38. doi:10.1016/j.newar.2010.09.017

Maeder A, Meynet G (2012) Rotating massive stars: from first stars to gamma ray bursts. Rev Mod Phys 84:25–63. doi:10.1103/RevModPhys.84.25

Maeder A, Grebel EK, Mermilliod JC (1999) Differences in the fractions of Be stars in galaxies. Astron Astrophys 346:459–464

Maheswaran M (2003) Magnetic rotator winds and Keplerian disks of hot stars. Astrophys J 592:1156–1172. doi:10.1086/375797

Maintz M, Rivinius T, Štefl S, Baade D, Wolf B, Townsend RHD (2003) Stellar and circumstellar activity of the Be star ω CMa. III. Multiline non-radial pulsation modeling. Astron Astrophys 411:181–191. doi:10.1051/0004-6361:20031375

Martayan C, Frémat Y, Hubert AM, Floquet M, Zorec J, Neiner C (2006a) Effects of metallicity, star-formation conditions, and evolution in B and Be stars. I. Large Magellanic Cloud, field of NGC 2004. Astron Astrophys 452:273–284. doi:10.1051/0004-6361:20053859

Martayan C, Hubert AM, Floquet M, Fabregat J, Frémat Y, Neiner C, Stee P, Zorec J (2006b) A study of the B and Be star population in the field of the LMC open cluster NGC 2004 with VLT-FLAMES. Astron Astrophys 445:931–937. doi:10.1051/0004-6361:20052760

Martayan C, Floquet M, Hubert AM, Gutiérrez-Soto J, Fabregat J, Neiner C, Mekkas M (2007a) Be stars and binaries in the field of the SMC open cluster NGC 330 with VLT-FLAMES. Astron Astrophys 472:577–586. doi:10.1051/0004-6361:20077390

Martayan C, Frémat Y, Hubert AM, Floquet M, Zorec J, Neiner C (2007b) Effects of metallicity, star-formation conditions, and evolution in B and Be stars. II. Small Magellanic Cloud, field of NGC 330. Astron Astrophys 462:683–694. doi:10.1051/0004-6361:20065076

Martayan C, Floquet M, Hubert AM, Neiner C, Frémat Y, Baade D, Fabregat J (2008) Early-type objects in NGC 6611 and the eagle nebula. Astron Astrophys 489:459–480. doi:10.1051/0004-6361:200809358

Martayan C, Baade D, Fabregat J (2010a) A slitless spectroscopic survey for Hα emission-line objects in SMC clusters. Astron Astrophys 509:A11. doi:10.1051/0004-6361/200911672

Martayan C, Zorec J, Frémat Y, Ekström S (2010b) Can massive Be/Oe stars be progenitors of long gamma ray bursts? Astron Astrophys 516:A103. doi:10.1051/0004-6361/200913079

Martayan C, Rivinius T, Baade D, Hubert AM, Zorec J (2011) Populations of Be stars: stellar evolution of extreme stars. In: Neiner C, Wade G, Meynet G, Peters G (eds) Active OB stars. IAU symposium, vol 272, pp 242–253. doi:10.1017/S1743921311010489

Martin RG, Pringle JE, Tout CA, Lubow SH (2011) Tidal warping and precession of Be star decretion discs. Mon Not R Astron Soc 416:2827–2839. doi:10.1111/j.1365-2966.2011.19231.x

Mathew B, Subramaniam A, Bhatt BC (2008) Be phenomenon in open clusters: results from a survey of emission-line stars in young open clusters. Mon Not R Astron Soc 388:1879–1888. doi:10.1111/j.1365-2966.2008.13533.x

Mathis S, Neiner C, Tran Minh N (2013) Impact of rotation on stochastic excitation of gravity and gravito-inertial waves in stars. Astron Astrophys (in press)

McAlister HA, ten Brummelaar TA, Gies DR, Huang W, Bagnuolo WG Jr, Shure MA, Sturmann J, Sturmann L, Turner NH, Taylor SF, Berger DH, Baines EK, Grundstrom E, Ogden C, Ridgway ST, van Belle G (2005) First results from the CHARA array. I. An interferometric and spectroscopic study of the fast rotator α Leonis (Regulus). Astrophys J 628:439–452. doi:10.1086/430730

McBride VA, Coe MJ, Negueruela I, Schurch MPE, McGowan KE (2008) Spectral distribution of Be/X-ray binaries in the Small Magellanic Cloud. Mon Not R Astron Soc 388:1198–1204. doi:10.1111/j.1365-2966.2008.13410.x

McBride VA, Bird AJ, Coe MJ, Townsend LJ, Corbet RHD, Haberl F (2010) The Magellanic bridge: evidence for a population of X-ray binaries. Mon Not R Astron Soc 403:709–713. doi:10.1111/j.1365-2966.2009.16178.x

McDavid D, Bjorkman KS, Bjorkman JE, Okazaki AT (2000) A connection between V/R and polarization in Be stars. In: Smith MA, Henrichs HF, Fabregat J (eds) IAU colloq 175: the Be phenomenon in early-type stars. Astronomical society of the pacific conference series, vol 214, p 460

McGill MA, Sigut TAA, Jones CE (2011) The thermal structure of gravitationally darkened classical Be star disks. Astrophys J 743:111. doi:10.1088/0004-637X/743/2/111

McGill MA, Sigut TAA, Jones CE (2013) The effect of density on the thermal structure of gravitationally darkened Be star disks. Astrophys J Suppl Ser 204:2. doi:10.1088/0067-0049/204/1/2

McSwain MV, Gies DR (2005) The evolutionary status of Be stars: results from a photometric study of southern open clusters. Astrophys J Suppl Ser 161:118–146. doi:10.1086/432757

McSwain MV, Huang W, Gies DR, Grundstrom ED, Townsend RHD (2008) The B and Be star population of NGC 3766. Astrophys J 672:590–603. doi:10.1086/523934

Meilland A, Millour F, Stee P, Domiciano de Souza A, Petrov RG, Mourard D, Jankov S, Robbe-Dubois S, Spang A, Aristidi E, Antonelli P, Beckmann U, Bresson Y, Chelli A, Dugué M, Duvert G, Gennari S, Glück L, Kern P, Lagarde S, Le Coarer E, Lisi F, Malbet F, Perraut K, Puget P, Rantakyrö F, Roussel A, Tatulli E, Weigelt G, Zins G, Accardo M, Acke B, Agabi K, Altariba E, Arezki B, Baffa C, Behrend J, Blöcker T, Bonhomme S, Busoni S, Cassaing F, Clausse JM, Colin J, Connot C, Delboulbé A, Driebe T, Feautrier P, Ferruzzi D, Forveille T, Fossat E, Foy R, Fraix-Burnet D, Gallardo A, Giani E, Gil C, Glentzlin A, Heiden M, Heininger M, Hernandez Utrera O, Hofmann KH, Kamm D, Kiekebusch M, Kraus S, Le Contel D, Le Contel JM, Lesourd T, Lopez B, Lopez M, Magnard Y, Marconi A, Mars G, Martinot-Lagarde G, Mathias P, Mège P, Monin JL, Mouillet D, Nussbaum E, Ohnaka K, Pacheco J, Perrier C, Rabbia Y, Rebattu S, Reynaud F, Richichi A, Robini A, Sacchettini M, Schertl D, Schöller M, Solscheid W, Stefanini P, Tallon M, Tallon-Bosc I, Tasso D, Testi L, Vakili F, von der Lühe O, Valtier JC, Vannier M, Ventura N (2007a) An asymmetry detected in the disk of κ Canis Majoris with AMBER/VLTI. Astron Astrophys 464:73–79. doi:10.1051/0004-6361:20065410

Meilland A, Stee P, Vannier M, Millour F, Domiciano de Souza A, Malbet F, Martayan C, Paresce F, Petrov RG, Richichi A, Spang A (2007b) First direct detection of a Keplerian rotating disk around the Be star α Arae using AMBER/VLTI. Astron Astrophys 464:59–71. doi:10.1051/0004-6361:20064848

Meilland A, Stee P, Chesneau O, Jones C (2009) VLTI/MIDI observations of 7 classical Be stars. Astron Astrophys 505:687–693. doi:10.1051/0004-6361/200911960

Meilland A, Millour F, Kanaan S, Stee P, Petrov R, Hofmann KH, Natta A, Perraut K (2012) First spectro-interferometric survey of Be stars. I. Observations and constraints on the disk geometry and kinematics. Astron Astrophys 538:A110. doi:10.1051/0004-6361/201117955

Mennickent RE, Sterken C, Vogt N (1997) Coupled long-term photometric and V/R variations in Be stars: evidence for prograde global one-armed disk oscillations. Astron Astrophys 326:1167–1175

Mennickent RE, Pietrzyński G, Gieren W, Szewczyk O (2002) On Be star candidates and possible blue pre-main sequence objects in the Small Magellanic Cloud. Astron Astrophys 393:887–896. doi:10.1051/0004-6361:20020916

Meynet G, Maeder A (2002) Stellar evolution with rotation. VIII. Models at $Z = 10^{-5}$ and CNO yields for early galactic evolution. Astron Astrophys 390:561–583. doi:10.1051/0004-6361:20020755

Meynet G, Georgy C, Revaz Y, Walder R, Ekström S, Maeder A (2010) Models of stars rotating near the critical limit. In: Revista Mexicana de astronomia y astrofisica conference series, vol 38, pp 113–116

Millar CE, Marlborough JM (1998) Rates of energy gain and loss in the circumstellar envelopes of Be stars: the Poeckert-Marlborough model. Astrophys J 494:715. doi:10.1086/305229

Millar CE, Marlborough JM (1999) Rates of energy gain and loss in the circumstellar envelopes of Be stars: diffuse radiation. Astrophys J 516:276–279. doi:10.1086/307098

Miroshnichenko AS, Fabregat J, Bjorkman KS, Knauth DC, Morrison ND, Tarasov AE, Reig P, Negueruela I, Blay P (2001) Spectroscopic observations of the δ Scorpii binary during its recent periastron passage. Astron Astrophys 377:485–495. doi:10.1051/0004-6361:20010911

Mokiem MR, de Koter A, Vink JS, Puls J, Evans CJ, Smartt SJ, Crowther PA, Herrero A, Langer N, Lennon DJ, Najarro F, Villamariz MR (2007) The empirical metallicity dependence of the mass-loss rate of O- and early B-type stars. Astron Astrophys 473:603–614. doi:10.1051/0004-6361:20077545

Moujtahid A, Zorec J, Hubert AM, Garcia A, Burki G (1998) Long-term visual spectrophotometric behaviour of Be stars. Astron Astrophys Suppl Ser 129:289–311. doi:10.1051/aas:1998186

Negueruela I, Steele IA, Bernabeu G (2004) On the class of Oe stars. Astron Nachr 325:749–760. doi:10.1002/ansa.200310258

Neiner C, Hubert AM, Frémat Y, Floquet M, Jankov S, Preuss O, Henrichs HF, Zorec J (2003) Rotation and magnetic field in the Be star ω Orionis. Astron Astrophys 409:275–286. doi:10.1051/0004-6361:20031086

Neiner C, Gutiérrez-Soto J, de Baudin F, Batz B, Frémat Y, Huat AL, Floquet M, Hubert AM, Leroy B, Diago PD, Poretti E, Carrier F, Rainer M, Catala C, Thizy O, Buil C, Ribeiro J, Andrade L, Emilio M, Espinosa Lara F, Fabregat J, Janot-Pacheco E, Martayan C, Semaan T, Suso J, Baglin A, Michel

E, Samadi R (2009) The pulsations of the B5 IVe star HD 181231 observed with CoRoT and ground-based spectroscopy. Astron Astrophys 506:143–151. doi:10.1051/0004-6361/200911971

Neiner C, de Batz B, Cochard F, Floquet M, Mekkas A, Desnoux V (2011a) The Be star spectra (BeSS) database. Astron J 142:149. doi:10.1088/0004-6256/142/5/149

Neiner C, Wade G, Meynet G, Peters G (eds) (2011b) Active OB stars: structure, evolution, mass loss, and critical limits. IAU symposium, vol 272

Neiner C, Floquet M, Samadi R, Espinosa Lara F, Frémat Y, Mathis S, de Leroy B, Batz B, Rainer M, Poretti E, Mathias P, Guarro Fló J, Buil C, Ribeiro J, Alecian E, Andrade L, Briquet M, Diago PD, Emilio M, Fabregat J, Gutiérrez-Soto J, Hubert AM, Janot-Pacheco E, Martayan C, Semaan T, Suso J, Zorec J (2012a) Stochastic gravito-inertial modes discovered by CoRoT in the hot Be star HD 51452. Astron Astrophys 546:A47. doi:10.1051/0004-6361/201219820

Neiner C, Grunhut JH, Petit V, ud-Doula A, Wade GA, Landstreet J, de Batz B, Cochard F, Gutiérrez-Soto J, Huat AL (2012b) An investigation of the magnetic properties of the classical Be star ω Ori by the MiMeS collaboration. Mon Not R Astron Soc 426:2738–2750. doi:10.1111/j.1365-2966.2012.21833.x

Neiner C, Mathis S, Saio H, Lee U (2013) Be star outbursts: transport of angular momentum by waves. In: Shibahashi H, Lynas-Gray AE (eds) Progress in physics of the sun and stars: a new era in helio- and asteroseismology. Astronomical society of the pacific conference series (in press)

Nelson RP, Papaloizou JCB, Masset F, Kley W (2000) The migration and growth of protoplanets in protostellar discs. Mon Not R Astron Soc 318:18–36. doi:10.1046/j.1365-8711.2000.03605.x

Nemravová J, Harmanec P, Kubát J, Koubský P, Iliev L, Yang S, Ribeiro J, Šlechta M, Kotková L, Wolf M, Škoda P (2010) Properties and nature of Be stars. 27. Orbital and recent long-term variations of the pleiades Be star Pleione = BU Tauri. Astron Astrophys 516:A80. doi:10.1051/0004-6361/200913885

Ogilvie GI (2008) 3D eccentric discs around Be stars. Mon Not R Astron Soc 388:1372–1380. doi:10.1111/j.1365-2966.2008.13484.x

Okazaki AT (1991) Long-term V/R variations of Be stars due to global one-armed oscillations of equatorial disks. Publ Astron Soc Jpn 43:75–94

Okazaki AT (1997) On the confinement of one-armed oscillations in discs of Be stars. Astron Astrophys 318:548–560

Okazaki AT (2001) Viscous transsonic decretion in disks of Be stars. Publ Astron Soc Jpn 53:119–125

Okazaki AT (2007) Theory vs observation of circumstellar disks and their formation. In: Štefl S, Owocki SP, Okazaki AT (eds) Active OB-stars: laboratories for stellar and circumstellar physics. Astronomical society of the pacific conference series, vol 361, p 230

Okazaki AT, Bate MR, Ogilvie GI, Pringle JE (2002) Viscous effects on the interaction between the coplanar decretion disc and the neutron star in Be/X-ray binaries. Mon Not R Astron Soc 337:967–980. doi:10.1046/j.1365-8711.2002.05960.x

Oudmaijer RD, Parr AM (2010) The binary fraction and mass ratio of Be and B stars: a comparative very large Telescope/NACO study. Mon Not R Astron Soc 405:2439–2446. doi:10.1111/j.1365-2966.2010.16609.x

Owocki SP (2006) Formation and evolution of disks around classical Be stars. In: Kraus M, Miroshnichenko AS (eds) Stars with the B[e] phenomenon. Astronomical society of the pacific conference series, vol 355, p 219

Owocki SP, Cranmer SR, Gayley KG (1996) Inhibition of wind compressed disk formation by nonradial line-forces in rotating hot-star winds. Astrophys J Lett 472:L115. doi:10.1086/310372

Papaloizou JCB, Lin DNC (1995) Theory of accretion disks I: angular momentum transport processes. Annu Rev Astron Astrophys 33:505–540. doi:10.1146/annurev.aa.33.090195.002445

Papaloizou JCB, Savonije GJ (2006) One-armed oscillations in Be star discs. Astron Astrophys 456:1097–1104. doi:10.1051/0004-6361:20065407

Papaloizou JCB, Savonije GJ, Henrichs HF (1992) On the long-term periodicities in Be stars. Astron Astrophys 265:L45–L48

Pápics PI, Briquet M, Auvergne M, Aerts C, Degroote P, Niemczura E, Vučković M, Smolders K, Poretti E, Rainer M, Hareter M, Baglin A, Baudin F, Catala C, Michel E, Samadi R (2011) CoRoT high-precision photometry of the B0.5 IV star HD 51756. Astron Astrophys 528:A123. doi:10.1051/0004-6361/201016131

Paul KT, Subramaniam A, Mathew B, Mennickent RE, Sabogal B (2012) Study of candidate Be stars in the Magellanic Clouds using near-infrared photometry and optical spectroscopy. Mon Not R Astron Soc 421:3622–3640. doi:10.1111/j.1365-2966.2012.20591.x

Peters GJ (1986) Observation of the onset of an emission episode in the Be star μ Centauri. Astrophys J Lett 301:L61–L65. doi:10.1086/184624
Peters GJ (2001) HR 2142, thirty years after it was hypothesized to be an interacting binary. Publ Astron Inst Czech Acad Sci 89:30–35
Peters GJ, Gies DR (2002) The interacting binary Be star HR 2142. In: Tout CA, van Hamme W (eds) Exotic stars as challenges to evolution. Astronomical society of the pacific conference series, vol 279, p 149
Peters GJ, Gies DR, Grundstrom ED, McSwain MV (2008) Detection of a hot subdwarf companion to the Be star FY Canis Majoris. Astrophys J 686:1280–1291. doi:10.1086/591145
Peters GJ, Pewett TD, Gies DR, Touhami YN, Grundstrom ED (2013) Far-ultraviolet detection of the suspected subdwarf companion to the Be star 59 Cygni. Astrophys J 765:2. doi:10.1088/0004-637X/765/1/2
Petit V, Owocki SP, Wade GA, Cohen DH, Sundqvist JO, Gagné M, Maíz Apellániz J, Oksala ME, Bohlender DA, Rivinius T, Henrichs HF, Alecian E, Townsend RHD, ud-Doula A (MiMeS Collaboration) (2013) A magnetic confinement versus rotation classification of massive-star magnetospheres. Mon Not R Astron Soc 429:398–422. doi:10.1093/mnras/sts344
Petrov HG, Lagarde S, N'guyen van Ky M (1996) Differential interferometry imaging. In: Strassmeier KG, Linsky JL (eds) Stellar surface structure. IAU symposium, vol 176, p 181
Podsiadlowski P, Rappaport S, Han Z (2003) On the formation and evolution of black hole binaries. Mon Not R Astron Soc 341:385–404. doi:10.1046/j.1365-8711.2003.06464.x
Poeckert R (1981) A spectroscopic study of the binary Be star φ Persei. Publ Astron Soc Pac 93:297–317. doi:10.1086/130828
Pollmann E (2012) Period analysis of the Hα line profile variation of the Be binary star π Aqr. Inf Bull Var Stars 6023:1
Pols OR, Cote J, Waters LBFM, Heise J (1991) The formation of Be stars through close binary evolution. Astron Astrophys 241:419–438
Porter JM (1996) On the rotational velocities of Be and Be-shell stars. Mon Not R Astron Soc 280:L31–L35
Porter JM (1997) Continuum IR emission of Be star wind-compressed discs. Astron Astrophys 324:597–605
Porter JM (1999) On outflowing viscous disc models for Be stars. Astron Astrophys 348:512–518
Porter JM, Rivinius T (2003) Classical Be stars. Publ Astron Soc Pac 115:1153–1170. doi:10.1086/378307
Pott JU, Woillez J, Ragland S, Wizinowich PL, Eisner JA, Monnier JD, Akeson RL, Ghez AM, Graham JR, Hillenbrand LA, Millan-Gabet R, Appleby E, Berkey B, Colavita MM, Cooper A, Felizardo C, Herstein J, Hrynevych M, Medeiros D, Morrison D, Panteleeva T, Smith B, Summers K, Tsubota K, Tyau C, Wetherell E (2010) Probing local density inhomogeneities in the circumstellar disk of a Be star using the new spectro-astrometry mode at the Keck interferometer. Astrophys J 721:802–808. doi:10.1088/0004-637X/721/1/802
Pringle JE (1981) Accretion discs in astrophysics. Annu Rev Astron Astrophys 19:137–162. doi:10.1146/annurev.aa.19.090181.001033
Pringle JE (1991) The properties of external accretion discs. Mon Not R Astron Soc 248:754–759
Pringle JE (1992) Circumstellar discs. In: Drissen L, Leitherer C, Nota A (eds) Nonisotropic and variable outflows from stars. Astronomical society of the pacific conference series, vol 22, p 14
Puls J, Vink JS, Najarro F (2008) Mass loss from hot massive stars. Astron Astrophys Rev 16:209–325. doi:10.1007/s00159-008-0015-8
Quirrenbach A, Buscher DF, Mozurkewich D, Hummel CA, Armstrong JT (1994) Maximum-entropy maps of the Be shell star ζ Tauri from optical long-baseline interferometry. Astron Astrophys 283:L13–L16
Quirrenbach A, Bjorkman KS, Bjorkman JE, Hummel CA, Buscher DF, Armstrong JT, Mozurkewich D, Elias NM II, Babler BL (1997) Constraints on the geometry of circumstellar envelopes: optical interferometric and spectropolarimetric observations of seven Be stars. Astrophys J 479:477. doi:10.1086/303854
Rauw G, Nazé Y, Spano M, Morel T, ud-Doula A (2013) HD45314: a new γ Cas analog among Oe stars. Astron Astrophys 555:L9. doi:10.1051/0004-6361/201321774
Reese DR, MacGregor KB, Jackson S, Skumanich A, Metcalfe TS (2009) Pulsation modes in rapidly rotating stellar models based on the self-consistent field method. Astron Astrophys 506:189–201. doi:10.1051/0004-6361/200811510

Reese DR, Prat V, Barban C, van 't Veer-Menneret C, MacGregor KB (2013) Mode visibilities in rapidly rotating stars. Astron Astrophys 550:A77. doi:10.1051/0004-6361/201220506

Reid WA, Parker QA (2012) Emission-line stars discovered in the UKST Hα survey of the Large Magellanic Cloud—I. Hot stars. Mon Not R Astron Soc 425:355–404. doi:10.1111/j.1365-2966.2012.21471.x

Reig P (2011) Be/X-ray binaries. Astrophys Space Sci 332:1–29. doi:10.1007/s10509-010-0575-8

Reig P, Roche P (1999) Discovery of two new persistent Be/X-ray pulsar systems. Mon Not R Astron Soc 306:100–106. doi:10.1046/j.1365-8711.1999.02473.x

Rivinius T, Curé M (eds) (2010) The interferometric view on hot stars. Revista Mexicana de astronomía y astrofísica conference series, vol 38

Rivinius T, Baade D, Štefl S et al (1998b) Predicting the outbursts of the Be star μ Cen. In: Kaper L, Fullerton AW (eds) Cyclical variability in stellar winds, p 207

Rivinius T, Baade D, Stefl S, Stahl O, Wolf B, Kaufer A (1998a) Stellar and circumstellar activity of the Be star μ Centauri. I. Line emission outbursts. Astron Astrophys 333:125–140

Rivinius T, Štefl S, Baade D (1999) Central quasi-emission peaks in shell spectra and the rotation of disks of Be stars. Astron Astrophys 348:831–842

Rivinius T, Baade D, Štefl S, Maintz M (2001) Evolution in circumstellar envelopes of Be stars: from disks to rings? Astron Astrophys 379:257–269. doi:10.1051/0004-6361:20011335

Rivinius T, Baade D, Štefl S (2003) Non-radially pulsating Be stars. Astron Astrophys 411:229–247. doi:10.1051/0004-6361:20031285

Rivinius T, Štefl S, Baade D (2006) Bright Be-shell stars. Astron Astrophys 459:137–145. doi:10.1051/0004-6361:20053008

Rivinius T, Szeifert T, Barrera L, Townsend RHD, Štefl S, Baade D (2010) Magnetic field detection in the B2Vn star HR 7355. Mon Not R Astron Soc 405:L46–L50. doi:10.1111/j.1745-3933.2010.00856.x

Rivinius T, Baade D, Townsend RHD, Carciofi AC, Štefl S (2013) Variable rotational line broadening in the Be star Achernar. Astron Astrophys (letter in press). doi:10.1051/0004-6361/201322515

Robinson RD, Smith MA, Henry GW (2002) X-ray and optical variations in the classical Be star γ Cassiopeia: the discovery of a possible magnetic dynamo. Astrophys J 575:435–448. doi:10.1086/341141

Rogers TM, Lin DNC, McElwaine JN, Lau HHB (2013) Internal gravity waves in massive stars: angular momentum transport. Astrophys J 772:21. doi:10.1088/0004-637X/772/1/21

Ruždjak D, Božić H, Harmanec P, Fiřt R, Chadima P, Bjorkman K, Gies DR, Kaye AB, Koubský P, McDavid D, Richardson N, Sudar D, Šlechta M, Wolf M, Yang S (2009) Properties and nature of Be stars. 26. Long-term and orbital changes of ζ Tauri. Astron Astrophys 506:1319–1333. doi:10.1051/0004-6361/200810526

Saad SM, Kubát J, Koubský P, Harmanec P, Škoda P, Korčáková D, Krtička J, Šlechta M, Božić H, Ak H, Hadrava P, Votruba V (2004) Properties and nature of Be stars Dra. XXIII. Long-term variations and physical properties of κ Dra. Astron Astrophys 419:607–621. doi:10.1051/0004-6361:20034241

Saad SM, Kubát J, Hadrava P, Harmanec P, Koubský P, Škoda P, Šlechta M, Korčáková D, Yang S (2005) Spectrum disentangling and orbital solution for κ Dra. Astrophys Space Sci 296:173–177. doi:10.1007/s10509-005-4438-7

Saio H (2013) Prospects for asteroseismology of rapidly rotating B-type stars. In: Goupil M, Belkacem K, Neiner C, Lignières F, Green JJ (eds) Lecture notes in physics, vol 865. Springer, Berlin, p 159. doi:10.1007/978-3-642-33380-4_8

Saio H, Cameron C, Kuschnig R, Walker GAH, Matthews JM, Rowe JF, Lee U, Huber D, Weiss WW, Guenther DB, Moffat AFJ, Rucinski SM, Sasselov D (2007) MOST detects *g*-modes in the late-type Be star β Canis Minoris (B8 ve). Astrophys J 654:544–550. doi:10.1086/509315

Sana H, de Mink SE, de Koter A, Langer N, Evans CJ, Gieles M, Gosset E, Izzard RG, Le Bouquin JB, Schneider FRN (2012) Binary interaction dominates the evolution of massive stars. Science 337:444. doi:10.1126/science.1223344

Savonije GJ (2005) Unstable quasi *g*-modes in rotating main-sequence stars. Astron Astrophys 443:557–570. doi:10.1051/0004-6361:20053328

Savonije GJ (2007) Non-radial oscillations of the rapidly rotating Be star HD 163868. Astron Astrophys 469:1057–1062. doi:10.1051/0004-6361:20077377

Schaefer GH, Gies DR, Monnier JD, Richardson ND, Touhami Y, Zhao M, Che X, Pedretti E, Thureau N, ten Brummelaar T, McAlister HA, Ridgway ST, Sturmann J, Sturmann L, Turner NH, Farrington CD, Goldfinger PJ (2010) Multi-epoch near-infrared interferometry of the spatially resolved disk around the Be star ζ Tau. Astron J 140:1838–1849. doi:10.1088/0004-6256/140/6/1838

Schnerr RS, Henrichs HF, Oudmaijer RD, Telting JH (2006) On the Hα emission from the β Cephei system. Astron Astrophys 459:L21–L24. doi:10.1051/0004-6361:20066392
Secchi A (1866) Schreiben des Herrn Prof. Secchi, Directors der Sternwarte des Collegio Romano, an den Herausgeber. Astron Nachr 68:63. doi:10.1002/asna.18670680405
Semaan T (2012) Caractéristiques spectrales et pulsationelles d'etoiles Be á l'aide de données sol (VLT/GIRAFFE et X-SHOOTER) et espace (CoRoT). Dissertation, École Doctorale d'Astronomie & Astrophysisque d'Île-de-France
Semaan T, Martayan C, Frémat Y, Hubert AM, Soto JG, Neiner C, Zorec J (2011) Spectral and photometric study of Be stars in the first exoplanet fields of CoRoT. In: Neiner C, Wade G, Meynet G, Peters G (eds) Active OB stars. IAU symposium, vol 272, pp 547–548. doi:10.1017/S1743921311011409
Shakura NI, Sunyaev RA (1973) Black holes in binary systems. Observational appearance. Astron Astrophys 24:337–355
Sigut TAA, Jones CE (2007) The thermal structure of the circumstellar disk surrounding the classical Be star γ Cassiopeiae. Astrophys J 668:481–491. doi:10.1086/521209
Sigut TAA, Patel P (2013) The correlation between Hα emission and visual magnitude during long-term variations in classical Be stars. Astrophys J 765:41. doi:10.1088/0004-637X/765/1/41
Sigut TAA, McGill MA, Jones CE (2009) Be star disk models in consistent vertical hydrostatic equilibrium. Astrophys J 699:1973–1981. doi:10.1088/0004-637X/699/2/1973
Silaj J, Jones CE, Tycner C, Sigut TAA, Smith AD (2010) A systematic study of Hα profiles of Be stars. Astrophys J Suppl Ser 187:228–250. doi:10.1088/0067-0049/187/1/228
Silvester J, Neiner C, Henrichs HF, Wade GA, Petit V, Alecian E, Huat AL, Martayan C, Power J, Thizy O (2009) On the incidence of magnetic fields in slowly pulsating B, β Cephei and B-type emission-line stars. Mon Not R Astron Soc 398:1505–1511. doi:10.1111/j.1365-2966.2009.15208.x
Slettebak A (1986) Hα and near-infrared spectra of late-type Be and A F-type shell stars. Publ Astron Soc Pac 98:867–871. doi:10.1086/131836
Slettebak A (1988) The Be stars. Publ Astron Soc Pac 100:770–784. doi:10.1086/132234
Smith MA (2006) Variations of the He II λ1640 line in B0e-B2.5e stars. Astron Astrophys 459:215–227. doi:10.1051/0004-6361:20065055
Smith MA, Robinson RD (1999) A multiwavelength campaign on γ Cassiopeiae. III. The case for magnetically controlled circumstellar kinematics. Astrophys J 517:866–882. doi:10.1086/307216
Smith MA, Plett K, Johns-Krull CM, Basri GS, Thomson JR, Aufdenberg JP (1996) Dynamic processes in Be star atmospheres. IV. Common attributes of line profile "Dimples". Astrophys J 469:336. doi:10.1086/177783
Smith MA, Lopes de Oliveira R, Motch C (2012a) Characterization of the X-ray light curve of the γ Cas-like B1e star HD 110432. Astrophys J 755:64. doi:10.1088/0004-637X/755/1/64
Smith MA, Lopes de Oliveira R, Motch C, Henry GW, Richardson ND, Bjorkman KS, Stee P, Mourard D, Monnier JD, Che X, Bücke R, Pollmann E, Gies DR, Schaefer GH, ten Brummelaar T, McAlister HA, Turner NH, Sturmann J, Sturmann L, Ridgway ST (2012b) The relationship between γ Cassiopeiae's X-ray emission and its circumstellar environment. Astron Astrophys 540:A53. doi:10.1051/0004-6361/201118342
Sonneborn G, Grady CA, Wu CC, Hayes DP, Guinan EF, Barker PK, Henrichs HF (1988) Mass loss in a B2 IIIe star—ω Orionis 1978-1984. Astrophys J 325:784–794. doi:10.1086/166049
Stee P (2011) Observations of circumstellar disks. In: Neiner C, Wade G, Meynet G, Peters G (eds) Active OB stars. IAU symposium, vol 272, pp 313–324. doi:10.1017/S1743921311010726
Stee P, de Araujo FX (1994) Line profiles and intensity maps from an axi-symmetric radiative wind model for Be stars. Astron Astrophys 292:221–238
Stee P, de Araujo FX, Vakili F, Mourard D, Arnold L, Bonneau D, Morand F, Tallon-Bosc I (1995) γ Cassiopeiae revisited by spectrally resolved interferometry. Astron Astrophys 300:219
Stee P, Delaa O, Monnier JD, Meilland A, Perraut K, Mourard D, Che X, Schaefer GH, Pedretti E, Smith MA, Lopes de Oliveira R, Motch C, Henry GW, Richardson ND, Bjorkman KS, Bücke R, Pollmann E, Zorec J, Gies DR, ten Brummelaar T, McAlister HA, Turner NH, Sturmann J, Sturmann L, Ridgway ST (2012) The relationship between γ Cassiopeiae's X-ray emission and its circumstellar environment. II. Geometry and kinematics of the disk from MIRC and VEGA instruments on the CHARA array. Astron Astrophys 545:A59. doi:10.1051/0004-6361/201219234
Stee P, Meilland A, Bendjoya P, Millour F, Smith M, Spang A, Duvert G, Hofmann KH, Massi F (2013) Evidence of an asymmetrical Keplerian disk in the Brγ and He I emission lines around the Be star HD 110432. Astron Astrophys 550:A65. doi:10.1051/0004-6361/201220302

Štefl S, Baade D, Rivinius T, Stahl O, Wolf B, Kaufer A (1998) Circumstellar quasi-periods accompanying stellar periods of Be stars. In: Bradley PA, Guzik JA (eds) A half century of stellar pulsation interpretation. Astronomical society of the pacific conference series, vol 135, p 348

Štefl S, Baade D, Rivinius T, Otero S, Stahl O, Budovičová A, Kaufer A, Maintz M (2003a) Stellar and circumstellar activity of the Be star ω CMa. I. Line and continuum emission in 1996–2002. Astron Astrophys 402:253–265. doi:10.1051/0004-6361:20030224

Štefl S, Baade D, Rivinius T, Stahl O, Budovičová A, Kaufer A, Maintz M (2003b) Stellar and circumstellar activity of the Be star ω CMa. II. Periodic line-profile variability. Astron Astrophys 411:167–180. doi:10.1051/0004-6361:20031179

Štefl S, Okazaki AT, Rivinius T, Baade D (2007) V/R variations of binary Be stars. In: Štefl S, Owocki SP, Okazaki AT (eds) Active OB-stars: laboratories for stellar and circumstellar physics. Astronomical society of the pacific conference series, vol 361, p 274

Štefl S, Owocki SP, Okazaki AT (eds) (2007) Active OB-stars: laboratories for stellar and circumstellar physics. Astronomical society of the pacific conference series, vol 361

Štefl S, Rivinius T, Carciofi AC, Le Bouquin JB, Baade D, Bjorkman KS, Hesselbach E, Hummel CA, Okazaki AT, Pollmann E, Rantakyrö F, Wisniewski JP (2009) Cyclic variability of the circumstellar disk of the Be star ζ Tauri. I. Long-term monitoring observations. Astron Astrophys 504:929–944. doi:10.1051/0004-6361/200811573

Štefl S, Le Bouquin JB, Carciofi AC, Rivinius T, Baade D, Rantakyrö F (2012a) New activity in the large circumstellar disk of the Be-shell star 48 Librae. Astron Astrophys 540:A76. doi:10.1051/0004-6361/201118054

Štefl S, Le Bouquin JB, Rivinius T, Baade D, Carciofi AC, Haubois X, Corder S, Curé M, Kanaan S (2012b) δ Sco 2011 periastron passage: near-IR interferometry and radio mm observations. In: Carciofi AC, Rivinius T (eds) Astronomical society of the pacific conference series, vol 464, p 197

Stoeckley TR (1968) Distribution of rotational velocities in Be stars. Mon Not R Astron Soc 140:141

Struve O (1931) On the origin of bright lines in spectra of stars of class B. Astrophys J 73:94

Sturm R, Haberl F, Rau A, Bartlett ES, Zhang XL, Schady P, Pietsch W, Greiner J, Coe MJ, Udalski A (2012) Discovery of the neutron star spin and a possible orbital period from the Be/X-ray binary IGR J05414-6858 in the LMC. Astron Astrophys 542:A109. doi:10.1051/0004-6361/201219093

Suárez JC, Garrido R, Balona LA, Christensen-Dalsgaard J (eds) (2013) Stellar pulsations. Astrophysics and space science proceedings, vol 31. doi:10.1007/978-3-642-29630-7

Tallon-Bosc I, Tallon M, Thiébaut E, Béchet C, Mella G, Lafrasse S, Chesneau O, Domiciano de Souza A, Duvert G, Mourard D, Petrov R, Vannier M (2008) LITpro: a model fitting software for optical interferometry. In: Society of photo-optical instrumentation engineers (SPIE) conference series, vol 7013. doi:10.1117/12.788871

Tanaka K, Sadakane K, Narusawa SY, Naito H, Kambe E, Katahira JI, Hirata R (2007) Dramatic spectral and photometric changes of Pleione (28 Tau) between 2005 November and 2007 April. Publ Astron Soc Jpn 59:L35

Telting JH, Kaper L (1994) Long-term periodic variability in UV absorption lines of the Be star γ Cassiopeiae: on the relation with V/R variations in the Hβ line. Astron Astrophys 284:515–529

Telting JH, Heemskerk MHM, Henrichs HF, Savonije GJ (1994) Observational evidence for a prograde one-armed density structure in the equatorial disc of a Be star. Astron Astrophys 288:558–560

Thaller ML, Bagnuolo WG Jr, Gies DR, Penny LR (1995) Tomographic separation of composite spectra. III. Ultraviolet detection of the hot companion of φ Persei. Astrophys J 448:878. doi:10.1086/176016

Torrejón JM, Schulz NS, Nowak MA (2012) Chandra and Suzaku observations of the Be/X-ray star HD110432. Astrophys J 750:75. doi:10.1088/0004-637X/750/1/75

Touhami Y, Gies DR, Schaefer GH (2011) The infrared continuum sizes of Be star disks. Astrophys J 729:17. doi:10.1088/0004-637X/729/1/17

Touhami Y, Gies DR, Schaefer GH, McAlister HA, Ridgway ST, Richardson ND, Matson R, Grundstrom ED, ten Brummelaar TA, Goldfinger PJ, Sturmann L, Sturmann J, Turner NH, Farrington C (2013) A CHARA array survey of circumstellar disks around nearby Be-type stars. Astrophys J 768:128. doi:10.1088/0004-637X/768/2/128

Townsend RHD (2005) κ-mechanism excitation of retrograde mixed modes in rotating B-type stars. Mon Not R Astron Soc 364:573–582. doi:10.1111/j.1365-2966.2005.09585.x

Townsend RHD (2007) The coupling between pulsation and mass loss in massive stars. In: Stancliffe RJ, Houdek G, Martin RG, Tout CA (eds) Unsolved problems in stellar physics: a conference in honor of Douglas Gough. American institute of physics conference series, vol 948, pp 345–356. doi:10.1063/1.2818992

Townsend RHD, Owocki SP, Howarth ID (2004) Be-star rotation: how close to critical? Mon Not R Astron Soc 350:189–195. doi:10.1111/j.1365-2966.2004.07627.x

Tutukov AV, Fedorova AV (2007) Formation and evolution of Ae and Be stars. Astron Rep 51:847–862. doi:10.1134/S1063772907100095

Tycner C, Hajian AR, Armstrong JT, Benson JA, Gilbreath GC, Hutter DJ, Lester JB, Mozurkewich D, Pauls TA (2004) The circumstellar envelope of ζ Tauri through optical interferometry. Astron J 127:1194–1203. doi:10.1086/381068

Tycner C, Lester JB, Hajian AR, Armstrong JT, Benson JA, Gilbreath GC, Hutter DJ, Pauls TA, White NM (2005) Properties of the Hα-emitting circumstellar regions of Be stars. Astrophys J 624:359–371. doi:10.1086/429126

Tycner C, Gilbreath GC, Zavala RT, Armstrong JT, Benson JA, Hajian AR, Hutter DJ, Jones CE, Pauls TA, White NM (2006) Constraining disk parameters of Be stars using narrowband Hα interferometry with the navy prototype optical interferometer. Astron J 131:2710–2721. doi:10.1086/502679

Tycner C, Jones CE, Sigut TAA, Schmitt HR, Benson JA, Hutter DJ, Zavala RT (2008) Constraining the physical parameters of the circumstellar disk of χ Ophiuchi. Astrophys J 689:461–470. doi:10.1086/592097

ud-Doula A, Owocki SP, Townsend RHD (2008) Dynamical simulations of magnetically channelled line-driven stellar winds—II. The effects of field-aligned rotation. Mon Not R Astron Soc 385:97–108. doi:10.1111/j.1365-2966.2008.12840.x

Underhill A, Doazan V (1982) B Stars with and without emission lines. NASA

Uytterhoeven K, Poretti E, Rodríguez E, De Cat P, Mathias P, Telting JH, Costa V, Miglio A (2007) Multiperiodicity in the newly discovered mid-late Be star V2104 Cygni. Astron Astrophys 470:1051–1057. doi:10.1051/0004-6361:20077657

Vakili F, Mourard D, Stee P, Bonneau D, Berio P, Chesneau O, Thureau N, Morand F, Labeyrie A, Tallon-Bosc I (1998) Evidence for one-armed oscillations in the equatorial disk of ζ Tauri from GI2T spectrally resolved interferometry. Astron Astrophys 335:261–265

van Belle GT (2012) Interferometric observations of rapidly rotating stars. Astron Astrophys Rev 20:51. doi:10.1007/s00159-012-0051-2

Vanzi L, Chacon J, Helminiak KG, Baffico M, Rivinius T, Štefl S, Baade D, Avila G, Guirao C (2012) PUCHEROS: a cost-effective solution for high-resolution spectroscopy with small telescopes. Mon Not R Astron Soc 424:2770–2777. doi:10.1111/j.1365-2966.2012.21382.x

Vink JS, Harries TJ, Drew JE (2005) Polarimetric line profiles for scattering off rotating disks. Astron Astrophys 430:213–222. doi:10.1051/0004-6361:20041463

Vink JS, Davies B, Harries TJ, Oudmaijer RD, Walborn NR (2009) On the presence and absence of disks around O-type stars. Astron Astrophys 505:743–753. doi:10.1051/0004-6361/200912610

von Zeipel H (1924) The radiative equilibrium of a slightly oblate rotating star. Mon Not R Astron Soc 84:684–701

Wade GA, Grunhut JF (MiMeS Collaboration) (2012) The MiMeS survey of magnetism in massive stars. In: Carciofi AC, Rivinius T (eds) Circumstellar dynamics at high resolution. Astronomical society of the pacific conference series, vol 464, p p 405

Walker GAH, Kuschnig R, Matthews JM, Cameron C, Saio H, Lee U, Kambe E, Masuda S, Guenther DB, Moffat AFJ, Rucinski SM, Sasselov D, Weiss WW (2005) MOST detects *g*-modes in the Be star HD 163868. Astrophys J Lett 635:L77–L80. doi:10.1086/499362

Walker GAH, Kuschnig R, Matthews JM, Reegen P, Kallinger T, Kambe E, Saio H, Harmanec P, Guenther DB, Moffat AFJ, Rucinski SM, Sasselov D, Weiss WW, Bohlender DA, Božić H, Hashimoto O, Koubský P, Mann R, Ruždjak D, Škoda P, Šlechta M, Sudar D, Wolf M, Yang S (2005) Pulsations of the Oe star ζ Ophiuchi from MOST satellite photometry and ground-based spectroscopy. Astrophys J Lett 623:L145–L148. doi:10.1086/430254

Waters LBFM (1986) The density structure of discs around Be stars derived from IRAS observations. Astron Astrophys 162:121–139

Waters LBFM, van Kerkwijk MH (1989) The relation between orbital and spin periods in massive X-ray binaries. Astron Astrophys 223:196–206

Waters LBFM, Waelkens C (1998) Herbig Ae/Be stars. Annu Rev Astron Astrophys 36:233–266. doi:10.1146/annurev.astro.36.1.233

Waters LBFM, Cote J, Geballe TR (1988) 51 Ophiuchi (B9.5 Ve)—a Be star in the class of Beta Pictoris stars? Astron Astrophys 203:348–354

Waters LBFM, Marlborough JM, van der Veen WEC, Taylor AR, Dougherty SM (1991) The structure of circumstellar discs of Be stars—millimeter observations. Astron Astrophys 244:120–130

Westerlund BE (1997) The Magellanic Clouds. Springer, Berlin
Wheelwright HE, Bjorkman JE, Oudmaijer RD, Carciofi AC, Bjorkman KS, Porter JM (2012) Probing the properties of Be star discs with spectroastrometry and NLTE radiative transfer modelling: β CMi. Mon Not R Astron Soc 423:L11–L15. doi:10.1111/j.1745-3933.2012.01241.x
Wisniewski JP, Bjorkman KS (2006) The role of evolutionary age and metallicity in the formation of classical Be circumstellar disks. I. new candidate Be stars in the LMC, SMC, and Milky Way. Astrophys J 652:458–471. doi:10.1086/507260
Wisniewski JP, Bjorkman KS, Magalhães AM, Bjorkman JE, Meade MR, Pereyra A (2007a) The role of evolutionary age and metallicity in the formation of classical Be circumstellar disks. II. Assessing the evolutionary nature of candidate disk systems. Astrophys J 671:2040–2058. doi:10.1086/522293
Wisniewski JP, Kowalski AF, Bjorkman KS, Bjorkman JE, Carciofi AC (2007) Toward mapping the detailed density structure of classical Be circumstellar disks. Astrophys J Lett 656:L21–L24. doi:10.1086/512123
Wisniewski JP, Draper ZH, Bjorkman KS, Meade MR, Bjorkman JE, Kowalski AF (2010) Disk-loss and disk-renewal phases in classical Be stars. I. Analysis of long-term spectropolarimetric data. Astrophys J 709:1306–1320. doi:10.1088/0004-637X/709/2/1306
Wood K, Brown JC, Fox GK (1993) Polarimetric line profiles from optically thin Thomson scattering circumstellar envelopes. Astron Astrophys 271:492
Wood K, Bjorkman JE, Whitney B, Code A (1996a) The effect of multiple scattering on the polarization from axisymmetric circumstellar envelopes. II. Thomson scattering in the presence of absorptive opacity sources. Astrophys J 461:847. doi:10.1086/177106
Wood K, Bjorkman JE, Whitney BA, Code AD (1996b) The effect of multiple scattering on the polarization from axisymmetric circumstellar envelopes. I. Pure Thomson scattering envelopes. Astrophys J 461:828. doi:10.1086/177105
Wood K, Bjorkman KS, Bjorkman JE (1997) Deriving the geometry of Be star circumstellar envelopes from continuum spectropolarimetry. I. The case of ζ Tauri. Astrophys J 477:926. doi:10.1086/303747
Woosley SE (1993) Gamma-ray bursts from stellar mass accretion disks around black holes. Astrophys J 405:273–277. doi:10.1086/172359
Woosley SE, Bloom JS (2006) The supernova gamma-ray burst connection. Annu Rev Astron Astrophys 44:507–556. doi:10.1146/annurev.astro.43.072103.150558
Yoon SC, Langer N, Norman C (2006) Single star progenitors of long gamma-ray bursts. I. Model grids and redshift dependent GRB rate. Astron Astrophys 460:199–208. doi:10.1051/0004-6361:20065912
Yudin RV (2001) Statistical analysis of intrinsic polarization, IR excess and projected rotational velocity distributions of classical Be stars. Astron Astrophys 368:912–931. doi:10.1051/0004-6361:20000577
Zaal PA, de Koter A, Waters LBFM, Marlborough JM, Geballe TR, Oliveira JM, Foing BH (1999) On the nature of the HI infrared emission lines of tau Scorpii. Astron Astrophys 349:573–587
Zorec J, Briot D (1997) Critical study of the frequency of Be stars taking into account their outstanding characteristics. Astron Astrophys 318:443–460
Zorec J, Frémat Y (2005) On the frequency of field galactic Be stars. In: Casoli F, Contini T, Hameury JM, Pagani L (eds) SF2A-2005: Semaine de l'Astrophysique Francaise, p 361
Zorec J, Frémat Y, Cidale L (2005) On the evolutionary status of Be stars. I. Field Be stars near the Sun. Astron Astrophys 441:235–248. doi:10.1051/0004-6361:20053051
Zorec J, Arias ML, Cidale L, Ringuelet AE (2007) Be star disc characteristics near the central object. Astron Astrophys 470:239–247. doi:10.1051/0004-6361:20066615